chemistry

MDPI

Review

Magnetic Nanoparticles: Current Advances in Nanomedicine, Drug Delivery and MRI

Cezar Comanescu [1,2,3]

[1] National Institute of Materials Physics, Atomiștilor 405A, 077125 Magurele, Romania; cezar.comanescu@infim.ro
[2] Department of Inorganic Chemistry, Physical Chemistry and Electrochemistry, Faculty of Chemical Engineering and Biotechnologies, University Politehnica of Bucharest, Polizu 1, 011061 Bucharest, Romania
[3] Faculty of Physics, University of Bucharest, Atomiștilor 405, 077125 Magurele, Romania

Abstract: Magnetic nanoparticles (MNPs) have evolved tremendously during recent years, in part due to the rapid expansion of nanotechnology and to their active magnetic core with a high surface-to-volume ratio, while their surface functionalization opened the door to a plethora of drug, gene and bioactive molecule immobilization. Taming the high reactivity of the magnetic core was achieved by various functionalization techniques, producing MNPs tailored for the diagnosis and treatment of cardiovascular or neurological disease, tumors and cancer. Superparamagnetic iron oxide nanoparticles (SPIONs) are established at the core of drug-delivery systems and could act as efficient agents for MFH (magnetic fluid hyperthermia). Depending on the functionalization molecule and intrinsic morphological features, MNPs now cover a broad scope which the current review aims to overview. Considering the exponential expansion of the field, the current review will be limited to roughly the past three years.

Keywords: magnetic nanoparticle; MRI; nanomedicine; drug delivery; contrast agent; SPION; cancer; functionalization; hyperthermia; targeting

Citation: Comanescu, C. Magnetic Nanoparticles: Current Advances in Nanomedicine, Drug Delivery and MRI. *Chemistry* **2022**, *4*, 872–930. https://doi.org/10.3390/chemistry4030063

Academic Editors: Raluca-Ioana Stefan-van Staden and Marcela Mihai

Received: 1 August 2022
Accepted: 24 August 2022
Published: 27 August 2022

1. Introduction

Ever since nanotechnology grew into a reckoned field of its own, the implications in medicine and pharmacology became obvious, and are today exploited commercially on many drug formulations. A busy lifestyle, erratic work schedule and oxidative stress, together with genetic and other risk factors have contributed to a surge in cancer incidence throughout the globe, and current estimates predict about 1.26 million deaths for 2022 in the EU due to cancer alone. Conventional approaches come with unavoidable side effects due to systemic exposure and response and are less effective than directed therapy—a field where MNPs and SPIONs, in particular, have emerged as suitable candidates with more efficient delivery of the anticancer drugs and limited negative effects on neighboring tissues and organs.

Magnetic nanoparticles (MNPs) are at the very core of magnetic delivery systems and they aim to tackle site-specific tumors while ideally affording a controlled-release profile suitable for disease treatment. Their multifunctional dimensionality makes it possible for MNPs to be used in nanomedicine as elective candidates for drug targeting therapy when using an externally applied magnetic field.

With tunable physico-chemical properties and a very high surface-to-volume ratio typical for nanoparticles, MNPs can be engineered into drug-delivery systems with similar sizes to the organism's own antibodies or proteins for improved biocompatibility, while incorporating therapeutic agents that would otherwise be difficult to deliver to the cancer cells. When superparamagnetic nanoparticles (SPIONs) are coated with biologically compatible polymers of fatty acids, systems with improved colloidal stability and reduced tendency of aggregation are obtained. MNPs were also used as contrast agents in magnetic

resonance imaging (MRI). When functionalized with epithelial growth factor receptor antibodies or aptamers, an efficient diagnosis tool is created for many types of cancer or even detection of brain inflammation. MNPs are being used as alternative contrast agents in MR imaging owing to their superparamagnetic properties and high relaxivity, doubled by high biocompatibility upon surface functionalization and low toxicity, unlike the Gd complexes used traditionally as contract agent in MRI, which could potentially release Gd into the bloodstream.

The promise of viable candidates in cancer treatment made research in the field of MNPs flourish and today hundreds of reports are published annually describing new or improved strategies for using MNP systems in disease treatment. Conjugation of IONs (magnetite and maghemite are generally best tolerated) with drugs yields drug-loaded IONs that can be directed using an external magnetic field to the site where the tumor cells reside, and this drug-delivery variant is termed magnetic drug targeting (MDT). The variety of such approaches would make a comprehensive review quite difficult and lengthy, hence why the current review focuses on the most notable advances recorded with MNPs over the past three years.

2. Justification and Design Strategies for Magnetic Nanoplatforms

The current review strategy entailed an examination of search results on specific research topics such as "magnetic nanoparticle" and/or "drug delivery", "nanomedicine", "MR imaging" or "hyperthermia", but is also based on pertinent examples dealing with the above topic without specifically containing the mentioned keywords (for instance, articles dealing with ferrofluids were also included, provided a tentative use in biomedical applications was provided in the original text). Based on the occurrence of research directions found in both original research and review articles published in the past three years (2020–2022), the current table of content was decided and data curation of the 500+ articles identified was carried out around these main topics. Given the exponential expansion of the field, only the last three years were selected, and the inclusion of each article on the reference list was decided upon by reading the abstract and deciding on the suitability of the article for the included review topics.

There are multiple reasons pleading for the use of MNPs as carriers for drug and gene delivery, making nanoparticle platforms superior to the traditional administration of the drug alone. Moreover, theranostics are able to integrate today's MNPs in procedures capable of both diagnosis and disease treatment, which is unachievable via traditional drug administration. Using NPs for drug delivery allows modification of key aspects related to drug solubility, diffusivity, penetration and retention, pharmacokinetics, biodistribution, cytotoxicity, and half-life (controlled- and/or on-demand release).

Considering how time-consuming (~12 years on average) and extremely expensive (up to USD 2 billion) the drug development process can be, it may be surprising to note that, even when an efficient active component is identified, basic hiccups still plague the process, such as a lower grade in the biopharmaceutical system, which assesses the solubility and permeability of a drug. In other words, a highly efficient drug whose development took years of research may never reach the patient in need due to low solubility/permeability in the biological system. This severe shortcoming can be modulated by drug immobilization on magnetic nanocarriers, that are able to transport insoluble drugs to the target site by smart surface modification (for instance, with antibodies that would bind to molecules overexpressed at the tumoral site). Drug formulations employing stable nanoparticle dispersion of the drug can increase absorption, even when using much lower dosages—this advantage alone can make a drug with low bioavailability and poor penetration/absorption when used alone become suitably efficient for drug-delivery systems, with real prospects of reaching the market. Various groups reported that drug molecules conjugated to MNPs can exhibit efficiencies many times higher than using the drug by itself (Figure 1).

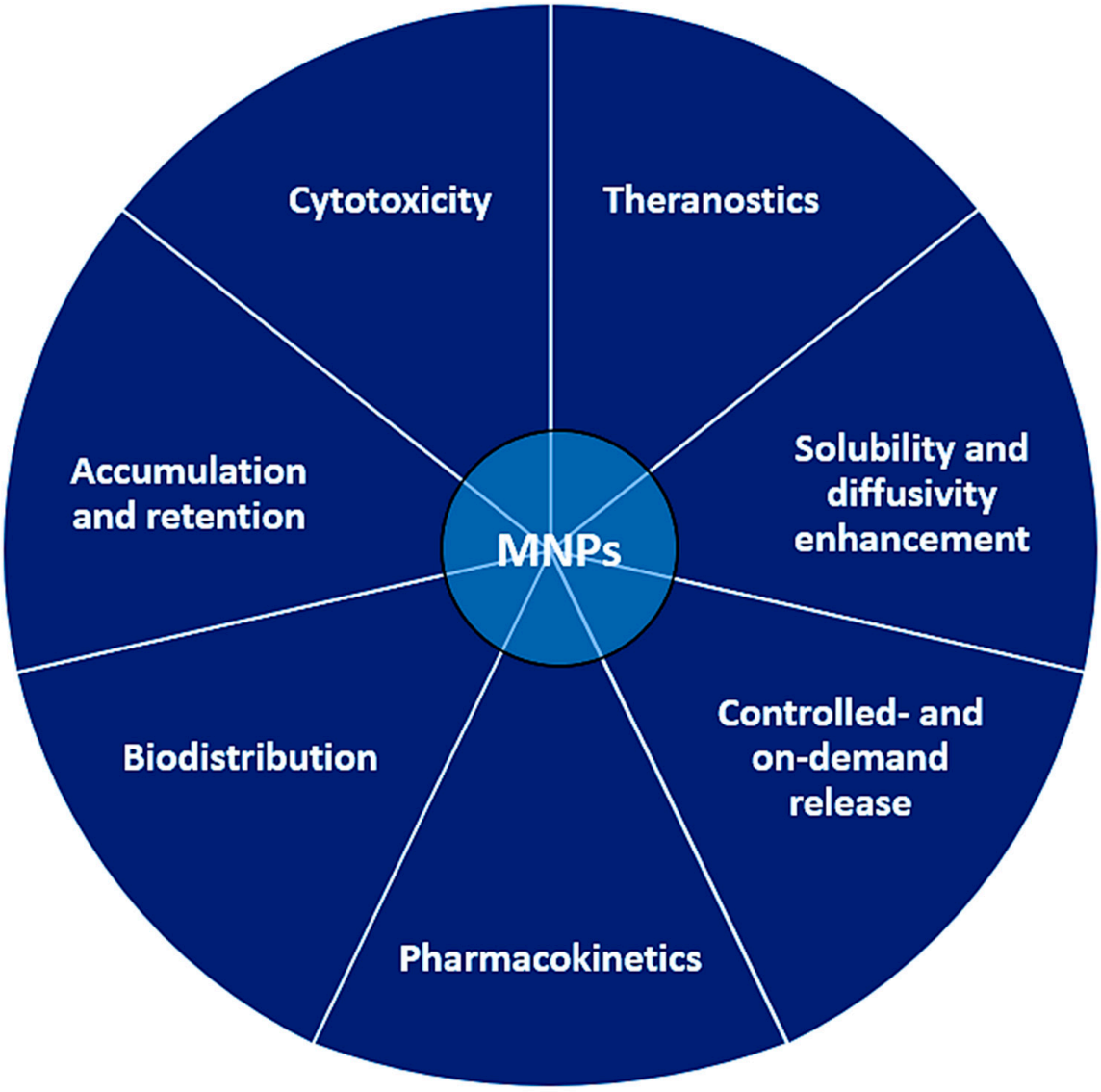

Figure 1. Advantages of using NP-based carrier platforms compared to classical drug administration protocols; improvements are recorded across all presented segments.

Conventional drug administration is typically carried out via oral, parental, pulmonary or transdermal routes, and usually requires several doses for maximum efficiency. However, a controlled release system based on drug-loaded NPs can bypass these shortcomings, by reducing drug quantities and related toxicity, and also the doses required for treatment. In a typical, conventional drug administration, the drug concentration in biological fluids can vary greatly, from subtherapeutic (no effect) to toxic levels; by contrast, the release profile of a drug in a controlled release system is rather constant, and within the limits required for maximal therapeutic effect. Such systems can be regarded as highly beneficial for patients using anti-inflammatory drugs (especially the elders), or diabetic patients; the former will not experience pain due to constant drug concentration in the blood, while the latter will have better glycemic control because insulin would be released on-demand contingent with blood sugar levels. The release can be prolonged to multiple weeks from a single administration, which would be unheard of in the case of traditional administration.

Another key parameter is the enhanced permeability and retention achievable due to specific hypervascularization at the tumor level (with the formation of epithelial pores), which translates into increased permeability to therapeutic drugs when conjugated to polymeric-coated NPs. For efficient drug accumulation, however, the nanoparticle-based

drug formulation must be stable in biological fluids (it should not agglomerate/ precipitate), should be tailored regarding size and concentration for optimal penetration through cellular membrane and cellular uptake.

2.1. Synthetic Strategies and Feedback-Driven Design

Synthetic methods currently utilized for SPION particle synthesis involve the hydrothermal route (with typically mesoporous NPs as the outcome [1–9], as opposed to the classical co-precipitation route, which has a number of disadvantages including reproducibility issues regarding morphological parameters with direct influence over the magnetic properties [10–12] or the well-established sol–gel [13] and (auto)combustion [14] methods. Other synthetic routes focus on natural extracts as bio-inspired routes to MNPs based on iron oxides, with encouraging therapeutic potential [15] and other green synthesis strategies [16]. Other nature-inspired compounds such as magnetic zeolites are also under investigation today [17].

2.2. Physical Characterization

Physical characterization methods were employed for particle size determination, including analysis of magnetization curves [18], cation distribution in ferrites by X-ray absorption [19,20] and Mossbauer spectroscopy [21,22].

Magnetic measurements aim at providing a feedback-driven synthesis route for improving effective magnetic moment [23–25], especially when referring to ferrofluids since these target actual biologic systems [26–28]. Effective quantification of the heating ability of MNPs can be achieved via SAR determination experiments [29] and novel tools such as small-angle scattering can improve the design of functionalized MNPs [30].

2.3. MNPs with Improved Magnetic Properties: Substitution/Doping Effect

Doping strategies have modified the therapeutic potential by altering the paramagnetic behavior of maghemite (γ-Fe_2O_3) [31], metal ferrites [32], as well as Gd^{3+} substitution of magnetite Fe_3O_4 with effect on superparamagnetic NPs [33].

Various strategies for anisotropy enhancement were explored, including layering of MNPs on amorphous substrates with perpendicular anisotropy [34].

Ferrites of spinel structure have been synthesized; $BaFe_2O_4$ [35], Mn–Zn ferrite [36], $CuFe_2O_4$ [37,38], Cu–Ni ferrite [39], Zn, Cu and Co ferrites [40,41], or Ni–Zn–Co ferrites with Gd^{3+} substitution [42].

2.4. Flow Characteristics and Simulated Models for MNPs in Biologic Fluids and High-Performance Ferrofluids

The flow parameters (magnetorheology) were reported recently [43–48], tackling also convection [49], location [50] and sedimentation processes [51,52] or multi-core MNPs [26], proper distribution in form of appropriate matrices such as gels [53], overall tracking efficiency [54], as well as guidance for cell behavior [55], and actual flow through artificial blood [56].

The effect of viscosity of the medium as a means to counteract the sedimentation tendency of MNPs was investigated [57], while the dispersibility of NPs was shown to be an efficient way to obtain stable ferrofluids and magnetic therapeutic fluids [58,59].

Simulation models of MNPs in the actual blood flow were reported very recently [60–62], on the magnetic susceptibility vs. frequency for MNPs [63,64], suitability of poly(vinyl) alcohol PVA coating of MNPs for drug delivery [65] or on the possible replacement of dopamine, the go-to drug used to treat Parkinson's disease, by magnetite Fe_3O_4 NPs [66]. Alzheimer's disease is also among the diseases targeted by functionalized SPIONs when conjugated with NIR dyes [67].

2.5. Morphology—Role of Size and Shape

Size control of MNPs [68] was been recently achieved in a green synthesis, bioinspired strategy by employing lysine in the synthesis of SPION magnetite materials [69]. Studies have shown that, for particle sizes higher than 100 nm, the MNPs are subject to macrophage phagocytosis by the spleen and liver, hence the requirements to design particles below 100 nm.

Size and shape effects on hyperthermia performance were also studied [70–72]. Results point to relatively lower toxicity when spherical nanoparticles are used (such as those obtained by the polyol method), rather than irregular/polyhedral-shaped NPs. I. Craciunescu et al. have investigated hydrophobic (oleic acid coating)/hydrophilic (azelaic acid-coated) magnetite (Fe_3O_4) and ferrites of Mn and Zn (MFe_2O_4), produced by the polyol method, of different shapes: spherical, cubic, hexagonal, octahedral and sizes (10–100 nm) with interesting findings linking shape and size of MNPs to the hyperthermia procedure. MFH (magnetic fluid hyperthermia) is a technique currently investigated which allows MNP-mediated conversion of alternating magnetic field energy into heat; moreover, this heat release event can be doubled by drug release at the tumor site which enhances the therapeutic chances of success in tumor treatment and should respect a maximal exposure criterion $f \times H \leq 5 \times 10^9$ Hz $\times$ A/m for applicability in biological systems [70]. The SAR (specific absorption rate) is a key parameter quantifying the energy conversion process and is dependent on AC magnetic field amplitude, frequency and MNPs relaxation mechanisms. The magnetization at saturation increases to 90 emu/g in the case of cubic shapes and MNPs of 100 nm average size (Fe_3O_4 and $MnFe_2O_4$) and lower values (50–70 emu/g) for zinc ferrite nanoparticles [70]. Large-sized MNPs are expected to transfer heat in hyperthermia applications by means of hysteretic losses due to magnetic wall displacements, hence of prime interest parameters are magnetization at saturation M_S and magnetic susceptibility in low AC magnetic fields—information that can be deduced by analysis of hysteresis loops [70]. Additional information regarding NPs size and size distribution, interparticle interactions and magnetic domain structure can be deduced by analysis of FC–ZFC curves (field-cooled–zero-field-cooled) or Mössbauer spectroscopy (for anisotropy energy determination, KV: K is the magnetic anisotropy constant, and V is the nanoparticle magnetic volume). It is worth noting that among the three types of samples analyzed (Fe_3O_4, $MnFe_2O_4$ and $ZnFe_2O_4$), the highest heating efficiency was that of the soft magnetic $ZnFe_2O_4$@azelaic acid (AZA) with a SAR of 175 W/g, more than double that of Fe_3O_4. AZA (SAR = 85 W/g), although it has the lowest saturation field among them. Increasing the heat efficiency is possible when using MNPs in a magnetically frozen regime at room temperature, which will not allow for the formation of moving magnetic domain walls [70].

Manganese ferrite $MnFe_2O_4$ was investigated extensively due to tunable magnetic properties, high biocompatibility and chemical stability [70,71]. Besides the essential role of hysteresis losses mentioned above (where it was the dominant heat transfer mechanism), two other mechanisms describe the heat transferred by NPs to the surroundings (SPL, specific power losses): Neel and Brownian relaxation [71]. SPL is also strongly influenced by particle size because this parameter alters the shape anisotropy. Chitosan-coated $MnFe_2O_4$ were obtained by co-precipitation of $FeCl_3$ and $MnCl_2.4H_2O$ with NH_4OH, producing stable, functionalized MNPs with potential applications as positive/negative MRI contrast agents in the rat model [71]. A theoretical investigation of various sized Fe_3O_4 NPs (25, 50, 100 and 200 nm) showed that NPs with lower sizes produced a higher heat gradient in the tumor mesh (61, 49, 42 and 41, respectively), while those in the 50–100 nm size ranges were found to be the most promising candidates for hyperthermia and cellular uptake [72]. Considering the heat produced by hysteresis per volume unit $P = \mu_0 f \int H \, dM$, we can expect better results when the alternating magnetic field frequency f is increased, within the biologically safe limit [72,73]. Theoretical simulations for correlating size with potential hyperthermia applications were also reported [73].

2.6. Intra- and Interparticle Interactions: Colloidal Stability and Size Differentiation

Interparticle interaction has long been seen as a possible cause of further aggregation [74]. R. Das et al. have shown the effect of shape (NRs nanorings of 55 nm length vs. NTs nanotubes of 470 nm length) on the MFH performance corresponding to Fe_3O_4 nanoparticles, while also raising the question of inter- and intraparticle interaction [74]. The morphology of NPs was controlled by the amount of $NaH_2PO_4.2H_2O$ used in the first precipitation step (higher concentration leads to NRs, lower concentration favors NTs). The iron oxide nanotubes NTs showed higher effective anisotropy and M_S, but lower SAR value (80 W/g at 400 Oe and 300 Hz) than nanorings NRs featuring weaker intraparticle interactions (110 W/g). It becomes apparent that MFH is positively influenced by using MNPs of lower volume and weaker intraparticle interactions [74].

Colloidal stability is a key parameter to preventing undesired NP accumulation before ever reaching the target organ [75–80]. For instance, optical tracking of iron oxide ferrofluids at 10 T and a 100 T/m gradient has shown that aqueous ferrofluids are best investigated in high fields, which offer a reliable estimation of their behavior under lower, practical fields [75]: 0.25 vol% iron oxide as stabilized dispersion of citrate-coated maghemite nanoparticles (γ-Fe_2O_3), and commercial Fe_4O_4 ferrofluids [75]. Depending on the magnetic field strength (0.3–0.5 T and ~20 T/m for a neodymium magnet, 10 T and 100 T/m for a Bitter magnet), citrate-coated maghemite remains separately dispersed. However, when MNPs of higher polydispersity are used, the largest NPs separate rapidly from the solution while smaller NPs remain dispersed because of their low dipolar coupling energies [75].

V. Pilati et al. synthesized aqueous ferrofluids using the electric double-layer (EDL) strategy to maintain their solution stability [76]. These systems were based on biomagnetic core-shell ZnMn mixed ferrite@ maghemite shell out of which two specific compositions were further investigated, namely $Zn_\delta Mn_{1-\delta}Fe_2O_4$@$\gamma$-$Fe_2O_3$ (δ = 0.2 and 0.5). The surface was further covered by a maghemite layer by exposing the $Zn_\delta Mn_{1-\delta}Fe_2O_4$ core (coprecipitation) to HNO_3 washing followed by hydrothermal treatment with $Fe(NO_3)_3$ 0.5 M. The electrostatically stabilized ferrofluid was achieved by peptization of as-synthesized ferrite NPs in a dialysis bag, using HNO_3 with pH fine tuning (final pH = 2.0) and solution ionic strength adjustment by means of $NaNO_3$ formation [76]. Interestingly, dynamic light scattering (DLS) and small-angle X-ray scattering (SAXS) revealed that changing the NPs concentration from dilute to >25 mg/mL is accompanied by a change in global interaction forces from attractive (diluted) to repulsive (concentrated) [76]. L. L. e Castro et al. extended the applicability of EDL repulsive interactions by using Monte Carlo simulations to surfacted MNPs, where the charge is located typically at the extremities of the surfactant molecule (at the organic functionality, such as amino, carboxyl, etc.). They ran the simulations on spherically shaped magnetic NPs using a model proposed by Schnitzer and Morozov—an improvement over the traditional DLVO model traditionally used for modeling colloid stability [77].

J.C. Riedl et al. used maghemite (γ-Fe_2O_3) NPs dispersed in ionic liquids (ILs) based on ethylmethylimidazolium bistriflimide (EMIM TFSI) in a pursuit to obtain colloids stable from room temperature up to 200 °C; the dispersion of maghemite at concentrations up to 12 vol% was shown to be stable for several days at 200 °C [78]. M. Boskovic et al. synthesized $Fe_{3-x}Gd_xO_4$ (x = 0, 0.1, 0.2) NPs of diameter ~8 nm by the coprecipitation method and by coating with citric acid (CA) with improved colloidal stability; the sample $Fe_{2.80}Gd_{0.20}O_4$@CA embedded in human serum albumin afforded magnetic microspheres (MMS) as suitable carriers for drug-delivery applications [79]. Polymeric coatings of iron oxide nanoparticles such as silica-coated Fe_3O_4 NPs (diblock copolymers obtained by living cationic polymerization, PEO-b-PMAA) are oftentimes used because they lower Gibbs free energy of magnetic nanoparticles in solution, hence maintaining colloidal stability and preventing agglomeration [80].

3. Coating and Surface Functionalization of MNPs: Polymers, Acids, Amines, Siloxanes, Other Coatings

Synthetic routes were implemented using flow reactor design, including surface-coated MNPs with, for instance, PEG [81–89], citric acid functionalization [90], aspartic acid [91], latex [92], pectin [93,94], polycations for A549 cells [95], other acid formulations [96] or polymers [97–99], biopolymers [100,101], PLGA poly(lactic-co-glycolic acid) copolymer [102,103], or poly(L-lactide-co-glycolide) copolymer [104]. Size differentiation was made possible by using chromatography in a simulated bed configuration [105]. The antibacterial properties of various MNP coatings were reported, and even carbohydrates were literally "sugar-coated" on Cu-doped Fe_3O_4 NPs [106,107].

These surface-modified versions of NPs can exhibit enhanced saturation magnetization, offer a better anchor for drug molecules to bind and can sometimes even serve as active catalysts for aromatic compounds synthesis including N-containing heterocycles [108–113], photocatalysis [114–117] and biocatalysis for tumor therapy [118–120]. M. Rajabzadeh et al. reported the innovative use of CuI Immobilized on Tricationic Ionic Liquid Anchored on Functionalized Magnetic Hydrotalcite (Fe_3O_4/HT-TIL-CuI) for Ullman-type C–N coupling reactions between aryl halides and N(H)-heterocycles (benzimidazoles, pyrazoles and triazoles) (no additives, under air atmosphere) in the presence of 2.5 mol% of nanocatalyst [108]. The inorganic–organic hybrid catalyst Fe_3O_4@SiO_2-L-tryptophan (L-tryptophan functionalized silica-coated MNPs) based on Fe_3O_4 synthesized by co-precipitation with NH_4OH from ferric and ferrous chloride salt sources was synthesized and evaluated as a recyclable magnetic nanocatalyst for the synthesis of spiro[indene-2,2′-naphthalene]-4′-carbonitrile derivatives [109]. The choice of L-tryptophan, a chiral α-amino acid was motivated by the presence of both amino (-NH_2) and carboxylic (-COOH) moieties, through which it can partake in various catalytic transformations [109]. Another very recent report focuses on $AlCl_3$@nano Fe_3O_4–SiO_2 multi-layer magnetite nanocatalyst for the one-pot synthesis of spiro[benzochromeno [2,3-d]pyrimidin-indolines] by a three-component condensation in refluxing C_2H_5OH of different naphthols, isatin derivatives, and barbituric acids [110]. Other research efforts made use of coordination, i.e., the binding affinity of polymers containing P-derived functional groups—phosphonic acids R–H_2PO_3, known for strong affinity to metals and multidentate binding ability [111], or participation of MNPs' polymeric coating in further functionalization by activation of esters under mild conditions to form amide bonds, click chemistry consisting of Cu(I)-catalyzed azide-alkyne cycloaddition (CuAAC process), or amine addition to isocyanates, among others [112]. In fact, $CoFe_2O_4$ MNPs recently synthesized by D. Aurélio et al. made use of a hydrothermal process producing cobalt ferrite NPs capped by oleic acid, which was further exchanged with N-containing organic acids such as 11-maleimidoundecanoic acid [113].

The surface functionalization and conjugation with various drugs lead, broadly speaking, to core-shell structures [121,122], including siloxanic coatings of MNPs which are environmentally benign and can be used for biomedical approaches [123–130]. Surface functionalization of SPIONs for biomedical applications by Ar plasma was very recently reported by Asghari et al. [131], or by other chemical methods [132–138]. Detailed experimental parameters are included in Section 5.

4. MR Imaging

MRI is a non-invasive imaging technique that exploits the ability of protons to align and process around B_0 (an applied magnetic field) and to relax when perturbed from B_0 by the application of a transverse radiofrequency. This relaxation process comprises two distinct terms: T1-recovery or longitudinal relaxation (positive contrast enhancement, sensitive to MNPs thickness, hence effective only for thin coatings) and T2-decay or transverse relaxation (favored by MNPs high susceptibility, negative contrast-enhanced, most used for SPIONs). This research direction is also motivated by the need to replace current contrast agents based on Gd^{3+} complexes, which pose worrying health issues and undesired side effects. As valuable MRI contrast agents, SPION nanoparticles have gained increased

attention and popularity, especially iron oxide-based [139–143]. Relaxivity is a direct and quantifiable measure of a contrast agent's efficiency: R1 (1/T1) and R2 (1/T2), and depends on the type of MNPs used, applied field and temperature.

Besenhard et al. have demonstrated a reproducible SPION synthesis in a flow reactor using a co-precipitation method using dextran as the surface coverage agent, followed by quenching (by timely 2–100 s addition of 0.32 M citric acid solution-stops nucleation due to chelation of iron ions) after the formation of the desired iron oxide core, achieving nanoparticles of less than 5 nm (Figure 2) [139].

The longitudinal relaxivity (r_1 = 10.7–12.4 mM^{-1} s^{-1}) and transversal relaxivity achieved (r_2 = 20.5–57.2 mM^{-1} s^{-1}) recommend this synthetic procedure to produce inexpensive SPIONs as efficient MRI T1 contrast agents and replacements for Gd-based ones (of smaller r_1 in commercial Dotarem™ or Gadovist™, 4.2–5.3 mM^{-1} s^{-1}) [139].

Some general introductory reviews covering MRI imaging have emerged in the literature [144,145]. Running the reaction at 60 °C, the salt co-precipitation to form spinel phases (magnetite/maghemite) confirmed by real-time XRD data that intermediate ferrihydrite species transform swiftly into the final spinel. Key aspects that influence the efficiency of iron oxide NPs in MRI include magnetization, size, effective radius, inhomogeneity of surrounding generated magnetic field, crystal phase, coordination number of water, electronic relaxation time, and surface modification [145]. T2 relaxivity for instance can be increased by synthesizing SPIONs with improved M_S and effective radius [145]. However, recently another iron-based compound was investigated as a new agent for enhanced hyperthermia therapy and a T_2 contrast agent for MRI application: iron nitride γ'-Fe_4N nanoparticles, which exhibit three times higher saturation magnetization and could also be properly covered by an oleic acid layer for further functionalization [146].

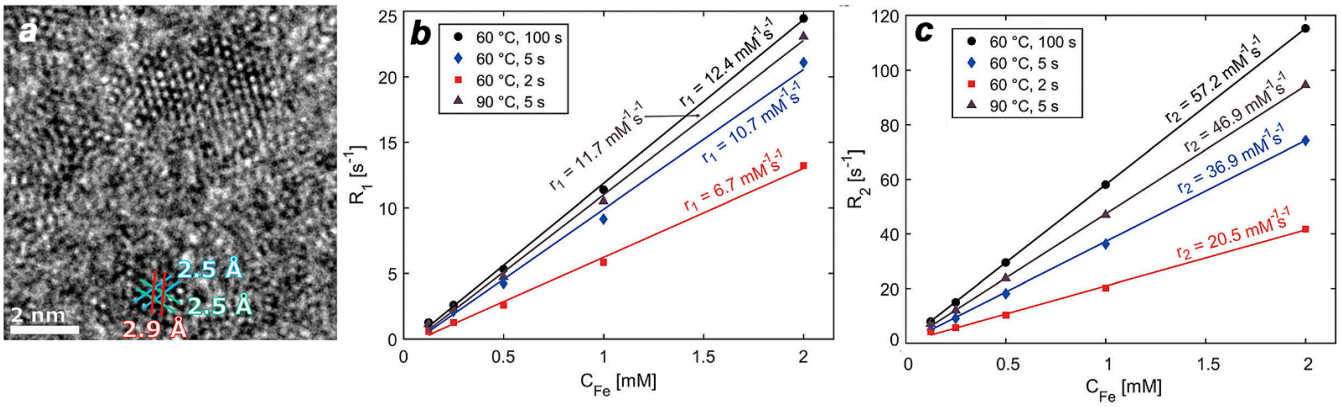

Figure 2. (**a**) HRTEM magnification image of ultra-small IONPs matching the [111] zone axes of magnetite with the two 2.5 Å (113) planes and one 2.9 Å (220) plane (PDF ref. 03-065-3107); (**b**) Relaxation rates R1 (longitudinal) and (**c**) R2 (transversal) vs. iron concentration in the (consecutively diluted) dialyzed samples (CFe) to determine r_1 and r_2 (i.e., the slope) for IONPs synthesized at co-precipitation temperatures and quenching times as indicated. Reprinted/adapted from ref. [139], under a Creative Commons Attribution 3.0 Unported Licence.

SPIONs are particularly efficient at allowing visualization of the cell line uptake (head and neck, for instance) [147], and their use became widespread in both MRI and MPI (magnetic particle imaging). MPI shares many similarities to MRI and is a tracer-based modality providing convenient diagnostic and therapeutic tools featuring important advantages: high sensitivity (0.1 µm), good spatial resolution (<1 mm) and temporal resolution (<1 s) with medium cost associated [141]. It does come with some drawbacks; typically, SPIONs are used as T2 contrast agents, as demonstrated above [139], and in that respect, they obscure adjacent tissue, while also making the resulted contrast unreliable in some particular cases—air-tissue interfaces or hemorrhagic tissue would behave similarly; additionally, there is the potential risk of heating and peripheral nerve stimulation

for patients undergoing the procedure [141]. While some coatings such as Au coatings provide extra stability and corrosion resistance, some critical aspects of Fe_3O_4/Au magnetite/gold core-shell nanostructures pinpoint some clear disadvantages and may be a reason why their current development came to a halt [148], although some scattered reports exist dealing with magnetic plasmonic Co@Au/Ag/Au–Ag core-shell nanoparticles for their biological imaging potential [149], with Fe–Pt@Au core-shell NPs [150] or custom designed for MRI and drug delivery [151–159]. For instance, Iancu et al. have shown that gold-coated magnetite Fe_3O_4@Au NPs can act be used as biocompatible drug carriers (at concentrations $<2 \times 10^{-8}$ mg/cell), while in vivo tests in rats revealed a negative T2 signal at a concentration of 6 mg/100 g body would suffice for obtaining high-quality MRI images [153].

Chelating ligands such as DoS (diblock polymer PDOPA-b-PSar) were shown to bind to Mn^{2+} centers to form novel, uniform micelles Mn^{2+}@PDOPA-b-PSar of 73.4 nm size (low polydispersity index PDI = 0.159) that were investigated as MRI contrast agents with good contrast features in imaging owing to the magnetic manganese core [159]. These micelles showed good results in MRI tests as T1-weighted contrast agents with relaxivity $r_1 = 27.7\ mM^{-1}s^{-1}$, and showed promising results for other biomedical applications such as drug release systems, while in vivo tests performed on rats showed cell survival rates higher than 70% [159].

The opportunity of using MNPs as contrast enhancements in MR imaging proves a current topic of interest, as the results are very detailed and the irradiation impact is reduced to a minimum [76,160–163]. Specific effects of coatings (with amine-carrying molecules) on MNPs' performance in MRI revealed interesting enhancement effects [164], and examples include coating with sodium oleate [165], chitosan [166–175] or organic acids [176], as well as amino moieties-poly(acrylamide) coatings [177].

4.1. Radiolabeling

Radiolabeling strategy (^{18}F, ^{64}Cu, etc) is an excellent tool for tumor imaging [178,179], one that is constantly improving owing, in part, to complementary theoretical computations [180,181].

Metal oxides have made important strides as T1 and/or T2 MRI contrast agents [182–185], either in the form of dysprosium oxide NPs coated with polyacrylic acid [186], gadolinium oxide NPs coated with poly(methyl vinyl ether-alt-maleic acid) [187], paramagnetic gadolinium oxide NPs coated by polyaspartic acid [188], gadolinium NPs coated with sericin—a protein created by silkworms (Bombyx mori) in the production of silk [189], iron oxide-magnetite Fe_3O_4 coated with folic acid [190] or other polymeric coatings [191–195], and colloidally stable Fe NPs [196,197].

4.2. SARS-CoV-2 and MRI with SPIONs

SPIONs' advances were also stimulated by the world pandemic that burst in late 2019, which urged scientists to find new tools to identify and cure the SARS-CoV-2 virus. In this respect, magnetic NPs have shown real promise not only for detection [143,198–200] but also for targeted pulmonary drug release [201,202]. Magnetic particle spectroscopy (MPS) was employed as a viable tool to detect target nucleic acids down to concentrations of 500 pM, without special sample preparation; Bionized NanoFerrite particles with a mean diameter of 80 nm (BNF80), coated with streptavidin were used for this goal, with a Brownian-dominated relaxation mechanism [143]. Most patients infected with the SARS-CoV-2 virus developed respiratory syndromes, therefore the development of microcarriers for targeted drug delivery at the bronchi level became of high interest to the scientific community [201]. Microcarriers of ~2 μm diameter (silica, iron oxide, nickel oxide) were released at the lung level and their adherence to the inner walls of lung branches was studied; interestingly, changing the inlet velocity from constant to pulsatile increased the drug delivery performance to the lungs by ~31% when 10 nm Fe_3O_4 MNPs coated microcarriers were studied in conjunction with a permanent magnet (~$4 \times 4 \times 2$ cm), a

strategy inspired by previous reports by Cai et al. who observed increased drug release efficiency when utilizing cobalt ferrite NPs [201,202].

4.3. Functionalization Agents and Strategies

Additional improvements can be obtained by experimental advances recorded in synthetic methods [203,204]. Surface functionalization [205–207] and polymeric coatings [208,209] are a prerequisite for using MNPs at the core of drug-delivery biocompatible systems. Even the known family of non-ionic block copolymers known under the trade brand Pluronic^{TM} (the surfactant typically used in many 2D and 3D mesoporous silica synthesis)), were used for anti-cancer formulations [210,211]. Polymer coatings have evolved to the usage of nanopolymers [212].

Along with drugs targeting specific diseases, genes can also be loaded onto functionalized MNPs, with PDMAEMA—a water-soluble cationic polymer capable of DNA electrostatic interaction [213] or coated by hyaluronic acid [214].

5. Therapeutic Features

Despite impressive achievements during the 21st century, life expectancy is still low in many countries, and a common and rising leading cause of serious health problems and ultimately death is the occurrence of cancer, which is believed to eventually be responsible for roughly 1.3 million deaths in 2022 in the European Union alone [215]. Various tumors and cancers were triggered by MNP formulations [216–219], and a breakthrough was the transition of MNPs from fundamental research to viable options in oncologic treatment [220], theranostic applications [221,222] and drug-delivery systems [98,223,224] (Figure 3).

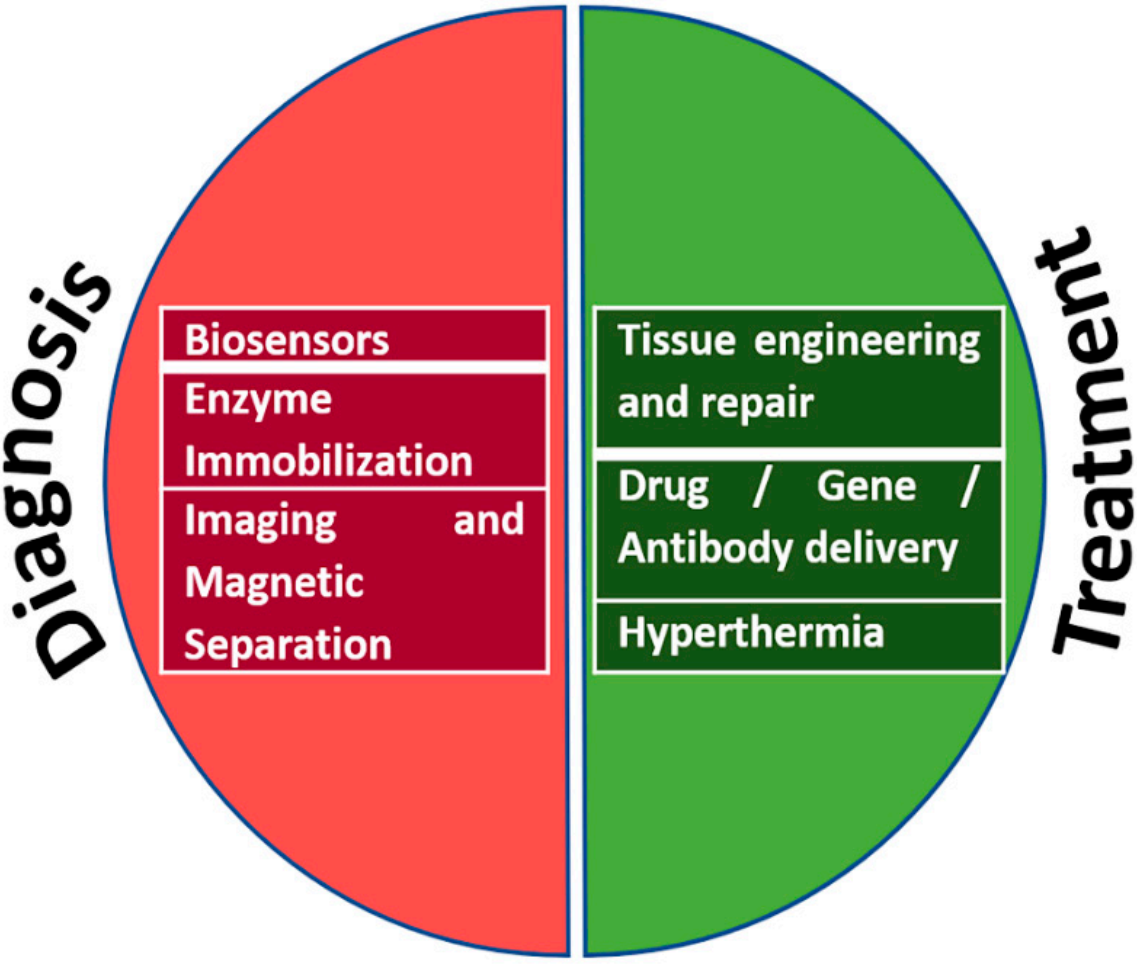

Figure 3. Diagnosis and treatment options provided by MNPs.

Antibody immobilization on MNPs can yield powerful sensing platforms [225]. Many biomedical applications including cancer and tumor cell treatment have been reported [226–231]. Applications of MNPs in medicine and particularly nanomedicine have been reviewed recently in the literature [232–235].

5.1. Drug Delivery

Drug-delivery systems have diversified immensely and today they cover a broad spectrum of both MNPs and targeting drug loadings [236–241], including intraocular delivery via smart microrobot technology [242], or delivery of erythropoietin-hybridized MNPs for treatment of central nervous system injury [243,244]. Magnetic nanoplatforms for delivery of classical platinum-based anticancer medicine (i.e., cis-platin) were investigated [245] and their toxicity in vitro was evaluated [246]. It was shown that shape contribution to cytotoxicity is very important, with spherically-shaped NPs being comparable less toxic than cylindrical or oval-shaped homologous, especially with increased reactive oxygen species (ROS) concentration.

Efficient delivery of drugs by MNP-coated nanocomposites requires a thorough knowledge of the proteic behavior of the drug molecule [247–249]. Pharmacokinetic behavior is of utmost importance since it can lead to better drug administration and by this, to more efficient disease treatment and management [250,251]. Drugs, genes and other biologically relevant molecules can be conjugated with NPs for efficient delivery at the targeted site (MDT, magnetic drug targeting). Drug-delivery applications have gained momentum and many reports have surfaced, dealing with a variety of problematic-to-target-and-cure types of cancer or disease [96,239,252–262]. A summary of the most commonly used anticancer drugs is depicted in Figure 4, with their chemical formulas (where space allowed it) and associated brand-name; the following organs were chosen—brain, stomach, pancreas, liver, breast and lung (Figure 4).

Various types of cancers are currently investigated by means of MNP drug conjugation, targeting lung cancer [263–267], gastric cancer [268–271], pancreatic cancer [272], hepatocellular carcinoma [273], bone cancer—osteosarcoma [274], blood cancer—leukemia [275,276] anemia—decreased number of red blood cells or hemoglobin [277], breast cancer [278] or liver fibrosis [279] either as a theoretical model [280] or actively conveying the chemotherapeutic medication Docetaxel (DTX or DXL, commercially available under the brand name Taxotere) [281,282], Artemisinin (initially anti-malaria drug in 1972)/Tannic acid [283], or folic acid [284]. Various types of tumors have been investigated, including grade IV astrocytoma—Glioblastoma Multiforme (GBM), an aggressive and rapid-growing brain tumor, whose management requires the MNPs to be able to bypass the feared BBB (blood–brain barrier) [285–293]. Brain tumors continue to be a demise sentence, with a 5% patient survival rate 5 years after the first glioblastoma (GBM) diagnosis, as statistics show. One of the many added benefits of utilizing MNPs in a variety of cancer types is the ability to diagnose that specific form of cancer with ease and detect it even in its early stages, which greatly expands the life expectancy of the patients. Smart surface modifications, i.e., coating with a biocompatible layer of tumor/cancer membrane have led for example to important advances in bone cancer treatment. However, MNPs can now address not only cancers but also abnormal levels of sugar or glucose in the blood, hence being potential treatment agents in glycemia; as such, magnetic nanocomposites of α-amylase inhibitors have been designed to this end [294]. Targeted delivery across specific organs was proven feasible by Zhou et al. who used an MNP-robotic capsule to deliver specific drugs at the gastrointestinal level [295] or at the cardiovascular system level [296].

Extending fundamental research to in vitro studies utilizing cell lines revealed important features that iron oxide and other MNPs might present [297–310]. Bionanomaterials are now at the convergence of materials science/nanotechnology and biomedical applications, and the investigation methods have reached a level to match theoretical predictions to in vitro and in vivo behavior of many drug formulations, many of which have become FDA-approved and commercially available to patients in need [311].

Magnetosomes have become important tools to manage cancer growth, and their bacterial biosynthesis is under active development [312–316]. In the final stages of cancer (metastasis), isolation of exosome-active participants in cancer progression and metastasis was shown to be possible when using Fe/Au nanowires [317]. Some of the many important advances recorded in drug delivery over the past three years are summarized in Table 1.

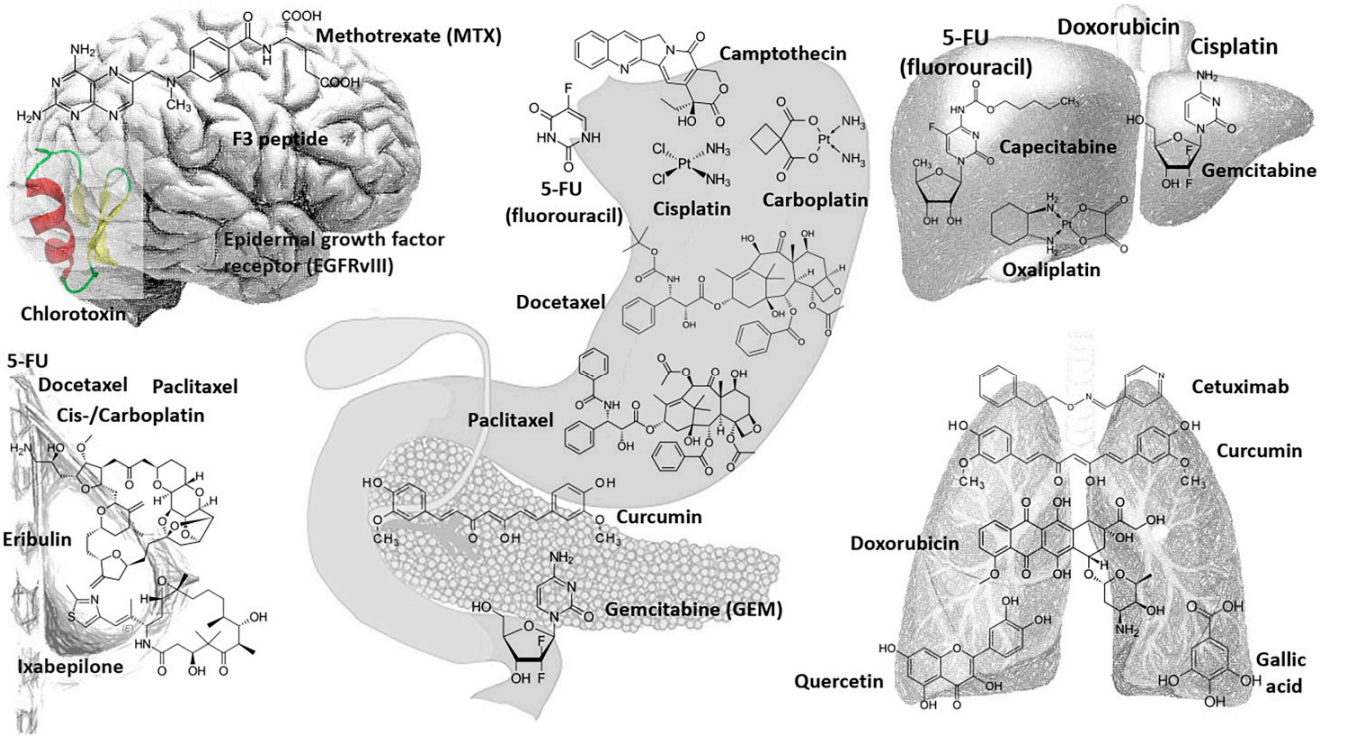

Figure 4. Magnetic NPs with anchored anticancer drugs and chemical formula attached. The drugs have been grouped by target organ, depicted as transparent background (brain, stomach–pancreas, liver, breast, lung).

Table 1. An overview of recent drug-delivery parameters for drug-delivery therapies.

Type of NP	Synthesis of MNPs/Coating	Surface Functionalization	Type of Drug/Molecule	Targeted Disease/Application	Ref.
Fe_3O_4	Tripolyphosphate (TPP) and glutaraldehyde stabilizers	polyvinyl alcohol/collagen	BSA protein	drug release system	[65]
Ni_xCu_{1-x}-silica nanoparticles (x = 0.675)	sol–gel method	SiO_2 silica from tetraethyl-orthosilicate (TEOS, $Si(OC_2H_5)_4$) hydrolysis and condensation	PTX ($C_{13}H_{18}N_4O_3$), BPC ($C_{18}H_{28}N_2O$), PCM ($C_8H_9NO_2$)	Skin cancer-Humanskin fibroblasts (ATCC-CCL-110, Detroit 551)	[126]
Multifunctional Fe_3O_4@SiO_2-APTES-DOTA	sol–gel	SiO_2 with amino-functionality by aminopropyltriethoxysilane (APTES) usage; and 1,4,7,10-Tetraazacyclododecane-1,4,7,10-tetraacetic acid (DOTA)	Teniposide, anticancer drug	brain tumors, acute lymphocytic leukemia (ALL)	[258]
$MnFe_2O_4$ and $Cr_2Fe_6O_{12}$ nanocarriers	combustion/calcination of PVP stabilized metal salt complexes	N/A; curcumin loading by precipitation	curcumin (CUR) release to MCF-7 cells; anti-inflammatory, anti-oxidant, antimicrobial, antispasmodic and antiproliferative activity; (release was pH-dependent)	photosensitizer for photodynamic therapy (PDT); drug delivery	[259]
superparamagnetic iron oxide (Fe_3O_4) nanoparticles (SPIONs)	co-precipitation; Dextran (DEX) stabilization	Folate (FA)-modification by conjugation to MNPs	camptothecin (CPT) action on AT3B-1 cancer cells	prostate cancer	[260]
$ZnFe_2O_4$ zinc ferrite nano-hollowspheres (NHSs)	solvothermal method	Sodium folate ligand modification for biocompatibility (folic acid small molecule vitamin)	Doxorubicin	cancer treatment	[318]
iron oxides (hematite, magnetite); carbonyl iron (due to its low size)	various (precipitation etc.)	polyethylene glycol (PEG); Magnetic liposomes; biodegradable polymers as stabilizers against oxidation (celluloseacetate; hydrogen phthalate)	Paclitaxel; Celecoxib; (Doxorubicin—poor distribution through BBB); Ferrocenyl diphenoltamoxifen; Gadd 153	Glioblastoma Multiforme management	[319]
SPION (magnetite, Fe_3O_4 nanospheres)	emulsion solvent evaporation method; polymer (ethylcellulose) coating	ascorbic acid (Vitamin C) capping	Carboplatin (CPt)	Breast cancer	[320]

Table 1. *Cont.*

Type of NP	Synthesis of MNPs/Coating	Surface Functionalization	Type of Drug/Molecule	Targeted Disease/Application	Ref.
multifunctional mesoporous silica nanoparticles (MSNs)	coating: Polydopamine (PDA) and graphene oxide (GO) double layer	fluorescent conjugates to yield FMSNs	ibuprofen and acetaminophen	Drug release	[321]
Fe_3O_4	dextran, PEG, Hyaluronic acid, Human serum albumin conjugate	polyvinyl alcohol (PVA) and PEG-derivatives/functional ligands: PEG(5)-nitrodopamine, PEG(5)-dopamine, PEG(5)-hydroxipyridine	Cetuximab and doxorubicin, Gallic acid, Erotinib, Actein, Quercetin	Lung cancer	[263]
Fe_3O_4-Dex-MA-g-P(NVI/NVCL) (pH-sensitive multi-functional magnetic nanocomposite)	Dex-MA (dextran modified by Glycidyl methacrylate)	Poly(N-vinylcaprolactam) (PNVCL), a temperature-sensitive biocompatible polymer	5-FLU (5-fluorouracil or 5-Fluoro-2,4-pyrimidinedione)	cancer	[322]
magnetic microspheres (MMS) based on Fe_3O_4	co-precipitation and water-in-oil-in-water ($W_1/O/W_2$) ternary emulsion solvent evaporation process	PLGA (poly-(D, L-lactide-co-glycolic acid)) microspheres; polymer coating tuned for required drug release rate	5-fluorouracil	cancer therapy, drug release	[323]
carbon-coated iron magnetic NPs; USPIOs; magnetite-gold nanocluster Fe_3O_4@AuNCs@ERL nanocomposite	various (precipitation followed by magnetic separation)	carbon coating; Au/polymeric coating	Erlotinib. ERL: N-(3-ethynylphenyl)-6,7-bis(2-methoxyethoxy)-4-quinazolinamine (epidermal growth factor receptor (EGFR) inhibitor)	metastatic non-small cell lung cancer; aggressive pancreatic cancer	[324]
magnetite nanoparticles (MNPs)	modified co-precipitation method (MNPs); glutaraldehyde (GA)/calcium chloride $CaCl_2$ (crosslinker)	sodium alginate (SA)/polyvinylpyrrolidone-co-vinyl acetate (PVP-co-VAc) semi ipn microbeads	curcumin (CUR) (encapsulation by simple ionotropic gelation technique)	cancer treatment	[325]

Table 1. *Cont.*

Type of NP	Synthesis of MNPs/Coating	Surface Functionalization	Type of Drug/Molecule	Targeted Disease/Application	Ref.
SPIONs (Maghemite)	no organic dispersant	linking the keto-enol moiety of CUR with Fe atoms to form SPION@curcumin hybrids	curcumin	photodynamic therapy (PDT): photodynamic action against *S. aureus* using blue LED light.	[326]
iron oxide nanoparticles (bare Fe_3O_4 NPs)	Micellar-assisted aqueous stabilization: micelles ($d_{hydrodynamic}$ =120 nm): sodium dodecyl sulfate (SDS) and aniline hydrochloride (AHC)	-	curcumin	hyperthermia therapy (under AC magnetic field); drug (curcumin) delivery	[327]
multicore magnetic nanoparticles: magnetite (Fe_3O_4) and/or maghemite (γ-Fe_2O_3)	coprecipitation method; coating with SiO_2 silica using TEOS, in a modified Stöber method	SiO_2 coating of MNPs yields MNP@SiO_2 (centrifugation)	Curcuminoids (CC) extracted from turmeric: curcumin (>50%), desmethoxycurcumin, and bisdemethoxycurcumin	theranostic nanoplatform; drug release; hyperthermia candidate	[328]
Fe_3O_4	chemical co-precipitation; folic acid labeling of MNPs	Polyethylenimine-graft-poly (maleic anhydride-alt-1-octadecene) coated, to yield Fe_3O_4@PIMF	curcumin (effect on MCF-7 and Helacells)	Drug delivery, MRI (negative signal enhancement in MRI)	[329]
$NiFe_2O_4$ in $x(NiFe_2O_4)@(100-x)SiO_2$ @HKUST-1 ($10 \leq x \leq 60$ wt.%)	Core-shell strategy; trichloroacetic acid (BTC) as the organic binding for MOF	Silica coating (by TEOS) and MOF functionalization; $NiFe_2O_4@SiO_2$@HKUST-1 as Novel Magnetic Metal-Organic Framework Nanocomposites	Curcumin adsorption in mesoporous host	drug delivery	[330]
Magnetite Fe_3O_4 in PEGylated Fe_3O_4/hydroxyapatite (PMHA) nanocomposite	PEG coating	Hydroxyapatite (shell)	Curcumin (effect on A549, MCF-7, and MRC-5 cells) (1.9 mg/g loading, pH-dependent release)	MRI; drug release	[331]
Yttrium Y^{3+}-Doped Iron Oxide Fe_3O_4 Nanoparticles	Co-precipitation (Fe_3O_4 and $Y^{3+}{}_xFe^{2+}Fe^{3+}{}_{2-x}O_4$)	-	(effect on 4T1 cells-mice mammary gland cancer cells; ATCC CRL2539)	Hyperthermia	[332]

Table 1. *Cont.*

Type of NP	Synthesis of MNPs/Coating	Surface Functionalization	Type of Drug/Molecule	Targeted Disease/Application	Ref.
Mesoporous Fe_3O_4 nanoparticles (SPIONs)	solvothermal method (PEG-diamine, hydrazine; for SPIONs); Folate encapsulation in PEG-diamine grafted NPs	Multifunctional polyethyleneglycol-diamine functionalized; 1-ethyl-3-(3-dimethylaminopropyl) carbodiimide hydrochloride/Nhydroxysuccinimide	doxorubicin (DOX) (effect on breast cancer cells MCF-7); through electrostatic attachment to daunosamine (NH_3^+)	(breast) cancer treatment	[333]
iron oxides maghemite (γ-Fe_2O_3) and magnetite (Fe_3O_4) nanoparticles	ultrasonic irradiation assisted co-precipitation route (providing good dispersion)	-	-	Hyperthermia	[334]
Co/Li/Zn-mixed ferrites: $Co_{0.76}Zn_{0.24}Fe_2O_4$, $Li_{0.375}Zn_{0.25}Fe_{2.375}O_4$ and $ZnFe_2O_4$ mixed-structure ferrite	'dry gel' formed by a sol–gel auto-combustion method	-	-	Magnetic hyperthermia	[335]
FeNiCo ternary alloy nanoparticles	$[FeNi]_{100-x}Co_x$ ($2.5 \leq x \leq 50$) by polyol method	-	-	Hyperthermia	[336]
Co^{2+}-doped magnetite, $Co_xFe_{3-x}O_4$–carboxymethylcellulose conjugate ferrofluids	Co_x-Fe_3O_4; (x = 3, 5, and 10% mol of cobalt)	carboxymethylcellulose (biocompatible macromolecular ligand) ferrofluids	(effect of AC magnetic field on human brain cancer cells U87)	magnetic hyperthermia, cancer therapy	[337]
magnetic hydrogel based on Fe_3O_4 NPs	co-precipitation method; Hydrogel formation	Gelatin formulation; Functionalization with methacrylic anhydride (GelMA), then copolymerization with (2-dimethylaminoethyl) methacrylate (DMAEMA) monomer	Doxorubicin (Dox)	breast cancer, hyperthermia	[338]

Table 1. *Cont.*

Type of NP	Synthesis of MNPs/Coating	Surface Functionalization	Type of Drug/Molecule	Targeted Disease/Application	Ref.
Copper Ferrite Nanoparticles $CuFe_2O_4$ MNPs	Co-precipitation, then magnetic separation; Silica coating (TEOS tetraethyl orthosilicate and CPTMS (3-chloropropyl)-trimethoxysilane)	Aromatic Polyamide Chains by polymerization of diamino-benzenes and -naphtalene with terephthaloyl chloride. Final nanocomposite: $CuFe_2O_4$@SiO_2-poly(p-phenylene Terephthalamide) star-like polymers	-	Hyperthermia evaluation-suitable for mild hyperthermia (ΔT~4 °C)	[339]
$Fe_{3-x}Co_xO_4$ (X = 0–1) spherical nanoparticles (7 nm)	thermal decomposition or organometallic precursors: $Fe(acac)_3$ and $Co(acac)_2$ in 1,2 hexadecanediol, oleic acid, and olylamine (polyol)	hydrophilization of hydrophobic $Fe_{3-x}Co_xO_4$ by TMAH (tetramethyl ammonium hydroxide, caping agent)	-	Hyperthermia (maximum SAR for x = 0.75)	[340]
Fe_3O_4	polyol synthesis to give Fe_3O_4@Au@$Cu_{2-x}S$ dumbbell heterostructures	hydrophobic-to-hydrophilic by two-step procedure (ligand exchange); thiol-polyethylene glycol coordinate Au and $Cu_{2-x}S$ surfaces and polycatechol–polyethylene glycol bind Fe_3O_4 surface; $^{64}CuCl_2$ radiolabeling	-	Photo-Magnetic Hyperthermia and ^{64}Cu Radio-Insertion (Tri-Modal Therapy); suggested efficient for skin cancer treatment	[341]
$Mg_{1-x}Co_xFe_2O_4$ ($0 < x < 1$; $\Delta x = 0.1$)	chemical co-precipitation method	surface-functionalized: chitosan and chitosan-coated MNPs reported biocompatible behavior	(effect on HeLa cells showed no cytotoxicity)	hyperthermia and in vivo MR imaging	[342]
Coated Iron Oxide Nanoparticles (IONPs)	cross-linking with the adsorbed model drug (DOX)	Gelatin-coated (biocompatible natural polymer)	Doxorubicin (DOX); effect on MG-63 osteosarcoma cells	Cancer Treatment; potential hyperthermia effect	[343]
Magnetic nanoparticles (MNPs) Iron oxide (Fe_3O_4)	co-precipitation synthesis of magnetite Fe_3O_4; coated with four types of primary surfactants, polyethylene glycol 2000 (PEG 2000), oleic acid (OA), Tween 20, and Tween 80	-	Doxorubicin (high loading); effect on lung adenocarcinoma A549 cell line	cancer treatment	[344]

Table 1. *Cont.*

Type of NP	Synthesis of MNPs/Coating	Surface Functionalization	Type of Drug/Molecule	Targeted Disease/Application	Ref.
MNPs (Fe^{3+})	Mohr salt $(NH_4)_2Fe(SO_4)_2(H_2O)_6$ alkaline solution with sodium hypophosphite NaH_2PO_2 in the presence of NIPAM; Fe^{2+}/PAA = 1/1	polyacrylic acid (30%), N-isopropylacrylamide (70%) (NIPAM) nanogel of ~150 nm	Doxorubicin (DOX)	anticancer activity	[345]
Magnetite Fe_3O_4	simple ionotropic gelationmethod (Gelatin-Coated)	Sodium Alginate (anionic polysaccharide)/Magnetite Nanoparticle Microbeads, doped with $Mg^{2+}$and Al^{3+} ions	Doxorubicin (DOX)	drug delivery carriers and applications	[346]
MNPs—manganese ferrite $MnFe_2O_4$ nanoparticles	co-precipitation method ($MnFe_2O_4$)	citrate coating yielding Cit-$MnFe_2O_4$	Doxorubicin (effect on 60 male Wistar rats)	kidney injury (in rats); Chronic kidney disease (CKD)	[347]
MNPs (Magnetite Fe_3O_4 NPs)	co-precipitation (product recovery by magnetic decantation);	PEG coating to produce Fe_3O_4@PEG; Fe_3O_4@PEG immersion in Graphene quantum dots solution (by pyrolysis of citric acid, and 24 h still) to yield Fe_3O_4@PEG@GQD dispersed in PBS, then Fe_3O_4@PEG@GQD-DOX (magnetic separation)	Doxorubicin (effect on breast cancer MCF7 cells)	anticancer activity, drug release (in vitro)	[348]
-	unseeded stable cavitation (ultrasound)	-	Doxorubicin (or Adriamycin); effect on 4T1 murine mammary carcinoma	Murine Mammary Tumor Cells	[349]
Magnetite-based magnetic gelatin microspheres	co-precipitation method; using $FeCl_2$ instead of $FeSO_4$ produces higher Ms (61.6 emu/g); gelatin coating	fructose, glucose, genipin (most efficient) and 1-ethyl-3(3-dimethylaminopropyl)carbodiimide (EDC) as crosslinking agents of gelatin	Doxorubicin	drug delivery	[350]

Table 1. *Cont.*

Type of NP	Synthesis of MNPs/Coating	Surface Functionalization	Type of Drug/Molecule	Targeted Disease/Application	Ref.
$MgFe_2O_4$ ferrite MNPs	glycol-thermal method	Chitosan (CHI), polyethylene glycol (PEG) and polyvinyl alcohol (PVA); CHI-MNPs have highest DOX encapsulation (84.28%)	Doxorubicin; effect on human embryonic kidney (HEK293), colorectal adenocarcinoma (Caco-2), and breast adenocarcinoma (SKBR-3) cell lines	(pH controlled) drug release, cancer treatment	[351]
Fe_3O_4@SiO_2@SBA-15	co-precipitation (and magnetic separation); PEG 400 coating	SiO_2 silica coating (TEOS); PEI grafted	Doxorubicin	MCF-7 cell line drug delivery	[352]
MNPs	co-precipitation in alkaline media (NH_4OH) of Fe^{2+}/Fe^{3+}/ethylene diamine (for introduction of -NH_2 functionalization)	carboxymethyl chitosan (CMC) coating to yield MNPs-CMC-DOX	Doxorubicin	drug release	[353]
Superparamagnetic SPIONs (Fe_3O_4)	co-precipitation (using chloride sources); polymer-coated NPs, by polymerization of glycidyl methacrylate (GMA).	SiO_2 and SiO_2-NH_2 functionalization with tetraethoxysilane (TEOS) and 3-(trimethoxysilyl) propyl methacrylate (TMSPM)	carboranes (by 1sopropyl-*o*-carborane immobilization)	boron neutron cancer therapy	[354]
MNPs magnetite Fe_3O_4	co-precipitation; Silica coating	surface-modification with N-(phosphonomethyl) iminodiacetic acid (PMIDA) to Fe_3O_4@SiO_2@PMIDA	anti-CD4 monoclonal antibody (by bioconjugation)	positive selection of peripheral blood T CD4+ lymphocytes	[355]
γ-Fe_2O_3	bio-assisted method/aqueous co-precipitation; 3 morphologies of MNPs: nanospheres (NS), nanograsses (NG) and nanowires (NW)	green route: biosurfactant Furostanol Saponin (FS) from Fenugreek seeds extract	dopamine (DA) and uricacid (UA)	biosensors (molecular recognition platform for simultaneous detection of biomarkers)	[356]

Table 1. *Cont.*

Type of NP	Synthesis of MNPs/Coating	Surface Functionalization	Type of Drug/Molecule	Targeted Disease/Application	Ref.
Iron oxide MNPs	precipitation (under N_2); coating and conjugation to yield Gem-PHB-MNPs hybrids	polyhydroxybutyrate coated	gemcitabine (effect on cell proliferation assay using SKBR-3 and MCF-7 breast cancer cell lines)	targeted drug delivery; treatment of breast cancer	[357]
SPION-type, reduced graphene oxide GO—Fe_3O_4	co-precipitation; In situ surface functionalization; coating with Pluronic F-127 (PF) to reduce cytotoxicity	delivery via an oriental fungus-type Ganoderma lucidum(provides stabilization); after drug Que loading: rGO-Fe_3O_4-GL-PF	Quercetin (Que), natural polyphenolic flavonoid with anti-cancer properties	cancer therapy; targeted drug delivery	[358]
Magnetite Fe_3O_4	precipitation in aqueous media with NH_4OH of precursors, then oleic acid coating	PLGA–mPEG star-like block copolymers using biodegradable poly(lactic-co-glycolic acid) (PLGA) and methoxy poly(ethylene glycol) (mPEG)	Quercetin (conjugation to MNPs by dialysis method)	anticancer; nanocarrier for hydrophobic drugs	[359]
Magnetite Fe_3O_4	microemulsion-assisted co-precipitation method (for MNPs)	PEG-ylation (coating) to PMNPs	gallic acid	cancer treatment	[360]
Paramagnetic Fe_3O_4 nanoparticles	Monte Carlo simulated annealing scheme; molecular dynamics (MD)	PEG-ylation	5-fluorouracil	cancer treatment; drug delivery	[361]
MNPs (DEAE-FluidMAG; 5 mg, 200 nm, Chemicell^{TM})	enzyme encapsulation stable at 37 °C	-	CLytA-DAAO Chimeric Enzyme; effect against Hs766T, IMIM-PC-2 and RWP-1 pancreatic carcinoma cells, HT-29, SW-480and SW-620 colorectal carcinoma cell lines	cancer therapy (pancreatic and colorectal carcinoma and glioblastoma)	[362]
iron oxide nanoparticle	Quantum chemical analysis (B3LYP/6-31G(d,p) in aqueous solution; M06-2X dispersion correction)	-	5-aminolevulinic acid (anticancer drug); drug binding via advanced hydrogen bonding	cancer treatment	[363]

Table 1. *Cont.*

Type of NP	Synthesis of MNPs/Coating	Surface Functionalization	Type of Drug/Molecule	Targeted Disease/Application	Ref.
self-assembled magnetic nanospheres (MNS)	solvothermal method (MNS); Nintedanib (NTD) conjugated with MNS-APTES through the acid liable imine bond	Aminopropyltriethoxysilane (APTES) monolayer coating and functionalization	Nintedanib (NTD); targets human lung cancer cells L-132	anticancer	[364]
iron oxide (IO)	wet chemical co-precipitation (with enriched KNO_3 content of $FeSO_4$ solution prior to KOH precipitation)	APTES-Modified Nanohydroxyapatite (nHAp); Nanohydroxyapatite–Iron Oxide Composite (nHAp/IO) produces after APTES surface modification: nHAp/IO@APTES	effect on murine osteoblast precursor cell line (MC3T3-E1) and murine monocyte–macrophage cell line (RAW 264.7)	Early Osteogenesis, Reduces Inflammation and Inhibits Osteoclast Activity	[365]
Magnetic nanoparticles Fe_3O_4	co-precipitation method (using chloride iron sources); drug was loaded on MNP-CS through an amide bond between -NH_2 groups (chitosan) and -COOH groups (TEL)	Chitosan coating; their solutions shaken gently for 2 h at 25 °C to obtain chitosan coated MNPs (MNP-CS)	Telmisartan (TEL), a water-soluble anticancer drug	cancer treatment	[366]
Fe_3O_4 in superparamagnetic graphene oxide (SPMGO) nanocomposite	chemical precipitation method, graphene oxide/magnetite nanocomposite	cyanuric chloride (CC), used as linker; final nanocarriers: SPMGO and SPMGO/CC, to yield SPMGO/MTX and SPMGO/CC/MTX	methotrexate (MTX); tested against Caov-4, HeLa and MCF-7 cell lines	cancer treatment	[367]
$Mn_{0.5}Zn_{0.5}Dy_xFe_{2-x}O_4$ ($x \leq 0.1$) NPs	ultrasonic irradiation method	sonication in LB (Luria Bertaini) to achieve the suspended broth-drug solution	tested against Escherchia coli ATCC35218 as Gram-negative and Staphlyloccocus aureus ATCC29213, as Gram-positive bacteria; and Human colorectal or colon carcinoma cells (HCT-116)	anticancer; antifungal activity (vs. Candida albicans ATCC 14053, yeast)	[368]

Table 1. *Cont.*

Type of NP	Synthesis of MNPs/Coating	Surface Functionalization	Type of Drug/Molecule	Targeted Disease/Application	Ref.
magnetic silk nanoparticles	microfluidic device using silk fibroin and MNPs	Peptide-functionalization of magnetic silk NPs, with Antitumor peptide G3-a cationic amphiphilic anticancer peptide, $G(IIKK)_3I\text{-}NH_2$	Dimethylcurcumin (ASC-J9), androgen receptor inhibitor; tested against HCT 116 colorectal cancer cells	anticancer	[369]
metal ferrite NPs, $MnFe_2O_4$, $CuFe_2O_4$	one-pot solvothermal method (270 °C, polyol method, in situ CD formation, ethanolamine 1-amino-2-hydroxy-ethane as source)	oleyl amine surface coating and functionalization; carbon dots-metal ferrite hybrids, CDs-MNPs: CDs@$MnFe_2O_4$, CDs@$CuFe_2O_4$	(tested on HeLa cancer cells)	multipurpose marker agent of HeLa cancer cells	[370]
magnetic graphene oxide hybrid, based on $MnFe_2O_4$ magnetic core	nanocomposite (mGG3F) of graphene, $MnFe_2O_4$ NPs, poly(amidoamine) dendrons and folic acid	poly(amidoamine) dendron-functionalization	Pd(II) complex synthesized using Naphcon as a model drug, with entrapment efficiency (EE) 73.9% ± 0.08	cancer therapy	[371]
SPIONs (Fe_3O_4)	superparamagnetic iron oxide nanoparticles	polyamidoamine PAMAM-modified mesoporous silica-coating of SPIONS	folic acid (effect on MCF-7 cells); Indocyanine green (ICG) a near-infrared dye was loaded in M-MSN-PAMAM nanocarriers	cancer (photodynamic) therapy	[372]
Methionine Magnetic Nanoparticles $Ni_{1-x}Co_xFe_2O_4$ @Methionine@PEG NPs	$Ni_{1-x}Co_xFe_2O_4$ NP coated with methionine using the reflux method (under N_2); 1 mg of $Ni_{1-x}Co_xFe_2O_4$ @Methionine@PEG NPs could load 0.51 mg naproxen	PEG-coating by 30 min vigorously stirring PEG-6000 powder in a phosphate-buffered saline (PBS) with $Ni_{1-x}Co_xFe_2O_4$@Methionine	Naproxen (most potent COX-1 and COX-2 inhibitors)	cancer growth inhibition; controlled drug release	[373]

Table 1. *Cont.*

Type of NP	Synthesis of MNPs/Coating	Surface Functionalization	Type of Drug/Molecule	Targeted Disease/Application	Ref.
iron oxide nanocubes (IONCs)	one pot synthesis, from $Fe(acac)_3$, decanoic acid and dibenzylether (DBE) in squalene (SQ) at 310 °C, then magnetic separation and centrifugation yield IONCs (15 nm ± 1 nm and 23 nm ± 5 nm edge length)	polycaprolactone fibers (electrospinning process)	doxorubicin; tested against Mouse embryonic fibroblast cell line (NIH 3 T3 cells), DOXOsensitive HeLa-WT cervical cancer cells and the DOXO-resistant MCF7 breast cancer cells	hyperthermia and cancer treatment	[374]
Iron Oxide nanocomposites with Fe_2O_3 core	commercial	Polyurethane diol/Polycaprolactone to yield PUD/PCL-Fe_2O_3 nanocomposites	-	catalytic effect (potential alternative use in fuel cells)	[375]
Iron Oxide (Fe_3O_4)	Two-Step LASER Ablation in Aqueous Media; TiO_2 (core-shell), in both Fe_3O_4 and TiO_2 pressed into pellets (commercial sources)	organic binder material	cytotoxicity against lung cancer cell lines (A549), *Escherichia coli* and *Staphylococcus aureus*	Antimicrobial and Anticancer	[376]
Iron MNPs	Co-precipitation method (MNPs); Polymer coatings were synthesized by two-stage melt polycondensation using BD:ADA:TBT as catalyst (molar ratio of 1:1:0.1), under N_2.	biofunctionalized with poly(butylene adipate-co-terephthalate) (PBAT), and poly(butylene adipate) (PBA).	Absorption of DOPh and DBPh from aqueous medium	Phthalate absorption	[377]
SPIONs	dextran-coated PEG-COOH functionalized super-paramagnetic ironoxide nanoparticles, SPIONs (micromod Partikeltechnologie, GmbH); carbodiimide chemistry producing FGF2-SPIONs	dextran-coated PEG-COOH functionalized super-paramagnetic ironoxide nanoparticles, SPIONs (micromod Partikeltechnologie, GmbH, Rostock, Germany)	Fibroblast growth factor 2 (FGF2); effect studied on normal and cirrhotic human livers, Human hepatic stellate cells (LX2 cells)	treatment of acute liver injury (in vivo)	[378]

Table 1. *Cont.*

Type of NP	Synthesis of MNPs/Coating	Surface Functionalization	Type of Drug/Molecule	Targeted Disease/Application	Ref.
Manganese ferrite $MnFe_2O_4$ magnetic core	Microwave Driven Solvothermal Synthesis	Functionalization by oxidation polymerization process to yield polyrhodanine manganese ferrite PRHD@$MnFe_2O_4$ binary hybrids	effect against specific cell lines: macrophages (RAW 264.7), osteosarcoma cells line (UMR-106), and stromal progenitor cells of adipose tissue (ASCs); Antimicrobial activity against *Escherichia coli* and *Staphylococcus aureus*.	protection against Fenton's reactions, and generation of highly toxic radicals; antimicrobial therapy	[379]
Zn^{2+}Doped Magnetite Fe_3O_4 Nanoparticles	low-cost method oleic acid/alcohol/water system to synthesize $Zn_{0.4}Fe_{2.6}O_4$ NPs; dimercaptosuccinic acid coated Zn^{2+} doped magnetite nanoparticles (DMSA-$Zn_{0.4}Fe_{2.6}O_4$)	dimercaptosuccinic coating providing -SH functionalization	Spleen accumulation through translocation of oral medicine; in vivo study (rats)	(oral) drug delivery, MRI; evidence of drug translocation from oral to organ (liver, spleen) in non-toxic forms	[380]
magnetic microspheres with γ-Fe_2O_3 magnetic core	core-shell synthesis; doping with Tb^{3+} ions could sensitize the fluorescence of Enr	silica coating with -NH_2 grafted functionality, and MOF and CMC- sodium carboxymethyl cellulose functionalization; γ-Fe_2O_3@SiO_2-NH_2-CMC/MOF5 and γ-Fe_2O_3@SiO_2-NH_2-CMC/IRMOF3 magnetic MOF nanoparticles	Enrofloxacin Enr (fluoroquinolone antibiotic, brand name: Baytril®); best results for γ-Fe_2O_3@SiO_2-NH_2-CMC/IRMOF3	treatment of bacterial infections	[381]
$Ni_{(1-x)}Co_xFe_2O_4$ NPs	reflux process (modified co-precipitation with NaOH under N_2, reflux, then amino-acid addition)	Methionine (amino acid) coating during MNPs synthesis	Tetracycline (drug loading 0.33 mg in 1 mg of carrier); tested on Melanoma cancer cell line (A375) and HFF normal cell, *Staphylococcus aureus*, *Escherichia coli*.	drug delivery	[382]

Table 1. *Cont.*

Type of NP	Synthesis of MNPs/Coating	Surface Functionalization	Type of Drug/Molecule	Targeted Disease/Application	Ref.
MNPs Fe_3O_4	co-precipitation	SH functionalization via (3-Mercaptopropyl) and trimethoxysilane	Coenzyme Q_0 (CoQ0, 2,3-dimethoxy-5-methyl-1,4-benzo-quinone); effect on Saos, MCF7 and Hela cell lines	antitumoral effect; anti-inflammatory, anticancer, and antioxidant	[383]
MNPs Fe_3O_4	coprecipitation of iron sulfate salts in basic media; 2-step strategy for nanohybrid	APTES linker between MNPs and the stearyl moiety (amide bond)	(R)-9-Acetoxystearic Acid (9-HSA);	biomedical (antiproliferative agent active against different cancer cells)	[384]
iron oxide NPs	co-precipitation of Fe(III) and Fe(II) in alkaline medium (MNPs); ceftriaxone (CFT)-loaded N′-methacryloylisonicotinohydrazide (MIH)-functionalized magnetic nanoparticles(CFT-MIH-MNPs)	high functionalization degree	ceftriaxone (oral administration, brand name Rocephin, a third-generation cephalosporin antibiotic) in vitro stability using simulated gastrointestinal tract (GIT) fluids	treatment of bacterial infections; high drug entrapment, gradual drug release; enhanced oral delivery of CFT.	[385]
α -Fe_2O_3/Gadofullerene (GdF) Hybrid	simple chemical precipitation method	chitosan	chitosan-α-Fe_2O_3/GdF hybrid composites-antibacterial resistance against *Escherichia coli*, *Pseudomonas aeruginosa*, *Bacilus subtilis*, and *Staphylococcus aereus*, and *P. aeruginosa* (inducing pneumonia)	Treatment of Antibiotic-Resistant Bacterial Pneumonia	[386]
α-Fe_2O_3	chemical precipitation method	chitosan	Chitosan/α-Fe_2O_3 nanocomposite; antibacterial activity against *Staphylococcus aureus* and *Escherichia coli*.	antibacterial treatment	[387]
SPION Fe_3O_4	co-precipitation with sonication in thermostatic bath (under Ar)	chitosan coating, collagen functionalization	-	biomedical and technological applications, scaffolds for tissue regeneration	[388]

Table 1. *Cont.*

Type of NP	Synthesis of MNPs/Coating	Surface Functionalization	Type of Drug/Molecule	Targeted Disease/Application	Ref.
Fe_2O_3	chitosan coating	Fe_2O_3/chitosan/montmorillonite (MMT, polymer layered silicate); after encapsulation, QC release is pH-dependent and follows Weibullkinetic model.	Quercetin (QC) delivery (potential adjuvant in COVID-19 medication); Fe_2O_3/CS/MMT NPs tested against MCF-7 cells	drug delivery; cancer treatment	[389]
Fe_3O_4@PAA@MIL-100(Cr) metal-organic framework	50 wt% drug CIP encapsulation in Fe_3O_4@PAA@MIL-100(Cr)@CIP	PAA@MIL-100(Cr)	ciprofloxacin (CIP)(fluoroquinolone antibiotic); tested by disk diffusion method against *Escherichia coli* and *Staphylococcus aureus*	antibacterial	[390]
Ag-coated MNPs; Fe_3O_4/Ag and Fe_3O_4@SiO_2/Ag (33.2–35.1 nm)	chemical reduction method (co-precipitation)	Ag coating; -NH_2 functionalization via APTES	trimethoprim (antibiotic); sulfamethoxazole; effect on *Escherichia coli* and *Staphylococcus aureus*	antibiotic treatment; drug release	[391]
$CoFe_2O_4$–$BaTiO_3$, $CoFe_2O_4$–$Bi_4Ti_3O_{12}$ and Fe_3O_4–$BaTiO_3$ core-shell magnetoelectric nanoparticles	core-shell type magnetoelectric nanoparticles	PNIPAm. -functionalized	methotrexate MTX (model drug; its adsorption best described by Freundlich model)	drug delivery	[392]
magnetic nanoparticles MNPs	Co-precipitation of Fe^{2+}/Fe^{3+} = 1/2, with NH_4OH	Tryptophan (amino acid involved in metabolic functions); 99mTc labeling afforded evaluation of the biodistribution and the blood kinetics	indoleamine 2,3 dioxygenase (IDO) and L-type amino acid transporter (effect on cell lines A-549, MCF-7)	tumor treatment; cancer treatment (ovarian, lung, colorectal)	[393]
Maghemite (γ-Fe_2O_3)	core-shell magnetic nanoparticles;	γ-Fe_2O_3@SiO_2, γ-Fe_2O_3@SiO_2-NH_2 and γ-Fe_2O_3@SiO_2-NH_2-COOH MNPs via TEOS, APTMS and glutaric anhydride (GA). Further functionalization: Core-Shell package of Tb-BDC-NH_2 and Tb-BDC, with ligands 2-aminoterephthalic acid (H_2BDC-NH_2) and terephthalic acid (H_2BDC).	norfloxacin (Nor); via coordination between γ-Fe_2O_3@SiO_2-NH_2-COOH/Tb-BDC and Nor	antibiotic	[394]

Table 1. *Cont.*

Type of NP	Synthesis of MNPs/Coating	Surface Functionalization	Type of Drug/Molecule	Targeted Disease/Application	Ref.
MNPs (Fe)	For C-coating, Fe is more biocompatible and less toxic than Fe_3O_4	Graphene-encapsulated to produce Fe@C (biocompatible graphene shell)	ferulic acid (pharmaceutical ingredient found in the traditional Chinese herb *Angelica sinensis*)	diabet (mice); (controlled) drug release	[395]
Ionic magnetic Fe_2O_3 core-shell nanoparticles	coprecipitation of Fe^{3+} and Fe^{2+} ions at a molar ratio of 2:1. with NH_4OH. Oxidation occurs due to air exposure (24 h)	silica shell and functionalized with alkylimidazolium organic halide: Guerbet imidazoles (to yield NpFeSi MNPs)	DNA extraction and stabilization against fragmentation	promising platform for therapeutic delivery; DNA extraction	[396]
superparamagnetic iron oxide nanoparticles Fe_3O_4 (APTMS@SPIONs)	co-precipitation method from iron salts Fe^{3+}/Fe^{2+}: 2/1 (mol ratio) using NH_4OH in presence of APTMS at 85 °C (Ar flow)	3-aminopropylsilane coating (APTMS) for cationic APTMS@SPIONs; after ICG encapsulation, hydrodynamic size increased from 18 to 35 nm for ICG-APTMS@SPIONs	indocyanine green (ICG) (25 μg mL^{-1}); effect evaluated on planktonic cells and biofilms of Gram-negative (*E. coli*, *K. pneumoniae*, *P. aeruginosa*) and Gram-positive (*S. epidermis*) bacteria	Antimicrobial photodynamic therapy (aPDT) and antimicrobial photothermal therapy (aPTT)	[397]
MNPs (Fe_3O_4) as Fe_3O_4@SIO_2/SH/NH_2	Chemical co-precipitation for core-shell MNPs (under N_2)	Silica-thiol coating; -NH_2 functionalization via hydrolysis/condensation of APTES solution, CPTES and MPTES.	methotrexate (MTX) and cysteine (Cys); up to 65% drug absorption	drug release (tested at 37° and 25 °C)	[398]
Magnetite Fe_3O_4	(commercial powder, from Sigma-Aldrich Ltd., ≥97% trace metal basis, particle size 50–100 nm.)	chemical-free, pulsed laser ablation (PLAL) to give ibuprofen:magnetite composites 4:1, 3:1 and 2:1 (wt)	ibuprofen	inflammation and pain management; targeted drugdelivery	[399]
MNPs $Fe_6(OH)_{18}(H_2O)_6$	quantum chemical study (using GAUSSIAN 09 and LANL2DZ basis set)	drug approaches TPZ via NH_2 (MNP/TPZ1), NO (MNP/TPZ2-3) and intraring N-atom (MNP/TP4) functional groups/-NH2 mechanism leads to the thermodynamically- stable product via reaction to surface -OH groups (MNPs)	Tirapazamine (TPZ), experimental anticancer drug activated to a toxic radical only at hypoxia (low [O_2])	cancer treatment	[400]

Table 1. *Cont.*

Type of NP	Synthesis of MNPs/Coating	Surface Functionalization	Type of Drug/Molecule	Targeted Disease/Application	Ref.
core-shell magnetic nanoparticles (NPs): Fe_3O_4@SiO_2/NH_2 and Fe_3O_4@CS	co-precipitation under Ar atmosphere; chitosan coating	silica coating and -NH_2 functionalization using APTES (3-(triethoxysilyl)-propylamine)	goat anti-HBsAg antibody (with $NaIO_4$ activation procedure)	antibody immobilization; sensing nanoplatforms (detection of HBsAg)	[401]
iron oxide nanoparticles (Magnetite Fe_3O_4 with hydroxyl endings)	standard co-precipitation technique (MNPs); silane coating with APTES by silanization reaction; Galactosylated coating	lactobionic acid (LBA)-functionalized: MNP-LBA	ceftriaxone (CFT)	controlled drug release for the oral delivery of CFT	[402]
bare iron oxide NPs (IONs): magnetite (cubic)	-	-	lasioglossin III (short cationic peptide) from bee venom	drug delivery (*Escherichia coli* tests show higher antimicrobial activity of bound lasioglossin)	[403]

As one may observe from Table 1, many MNPs have a core derived from either Fe_3O_4 (magnetite) or from Fe_2O_3 (maghemite). After successful drug loading, the release parameters are essential for the evaluation of efficient therapeutic drug levels in biological systems. Various release mechanisms have been proposed in the literature, and research data suggest some are more appropriate than others. For instance, when ibuprofen or acetaminophen was conjugated to multifunctional mesoporous silica nanoparticles (MSNs) containing APTMS and PDA/GO double layer functionalization, the drug loading was facilitated by π–π stacking interactions (Figure 5).

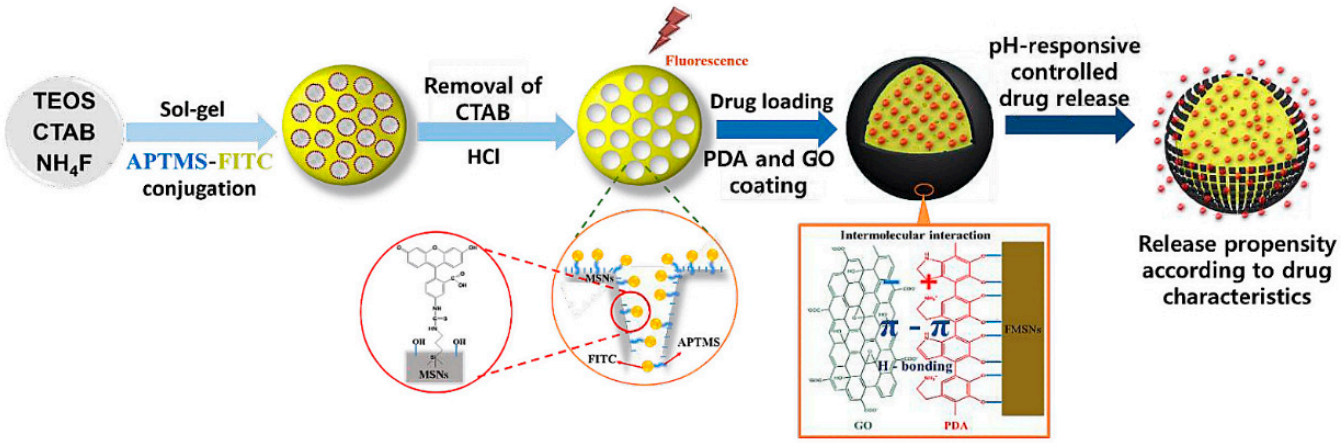

Figure 5. Schematic snapshots illustrating the fabrication process of MSNs grafted with APTMS-FITC conjugates, followed by coating of the PDA and GO double layer, and their controlled drug release mechanism. Reprinted/adapted from ref. [321] with permission from RSC—Royal Society of Chemistry, 2020.

The drug release profiles seemed pH-dependent, and this consideration is typically valid for a plethora of drugs; the release ability under slightly acidic pH (4–6) seems to be considerably higher than under near-neutral or slightly basic pH values (pH > 7.4). However, the latter is more important since the biological pH usually is maintained by living organisms at around 7.4, with coma or convulsions whenever the pH deviates by more than 0.3 pH units from this value. Therefore, ongoing efforts concentrate on enhancing kinetic release profiles under this biologically relevant value. Analysis of ibuprofen or acetaminophen from NPs (FMSNs) bearing a single-layer coating of PDA (FMSNs@PDA) or a double-layered coating of PDA and GO (FMSNs@PDA@GO) revealed that the most relevant release mechanisms are Fickian, Kp and Higuchi models (Figure 6), as illustrated the goodness of fit (GoF) parameter [321]. The results can serve as reference data for nanoparticulate systems that bear similar surface coating and functionalization to MNPs; their behavior in drug-release systems reveals many similarities [321,322].

The drug transport can show concomitant effects from both swellings of the polymer chain and diffusion of the drug from the matrix. Since typically polymeric coatings can be protonated under acidic pH if their functional groups allow it (such as imidazole, for instance), the enhanced drug release is dominated under acidic conditions (pH < 7) by swelling of the polymer [322]. This aspect is important, and evaluation of drug release under acidic pH is useful since tumors usually feature an acidic microenvironment that can trigger further invasion of organs and metastasis through many possible mechanisms (intracellular pH_i = 7.0–7.2, while extracellular pH_e = 6.4–7.0 or even lower). As such, when magnetite MNPs (Fe_3O_4) coated with glycidyl methacrylate, dextran and then N-vinylcaprolactam and N-vinylimidazole monomers (used for inducing temperature and pH sensitivity, respectively) were conjugated with 5 FU drug in Fe_3O_4-Dex-MA-g-P(NVI/NVCL), the release profile confirms a much better release under acidic pH values (pH = 5) rather than near-neutral conditions (pH = 7.4) when just ~20% of the drug was being eliminated by 62 h mark (Figure 7) [322].

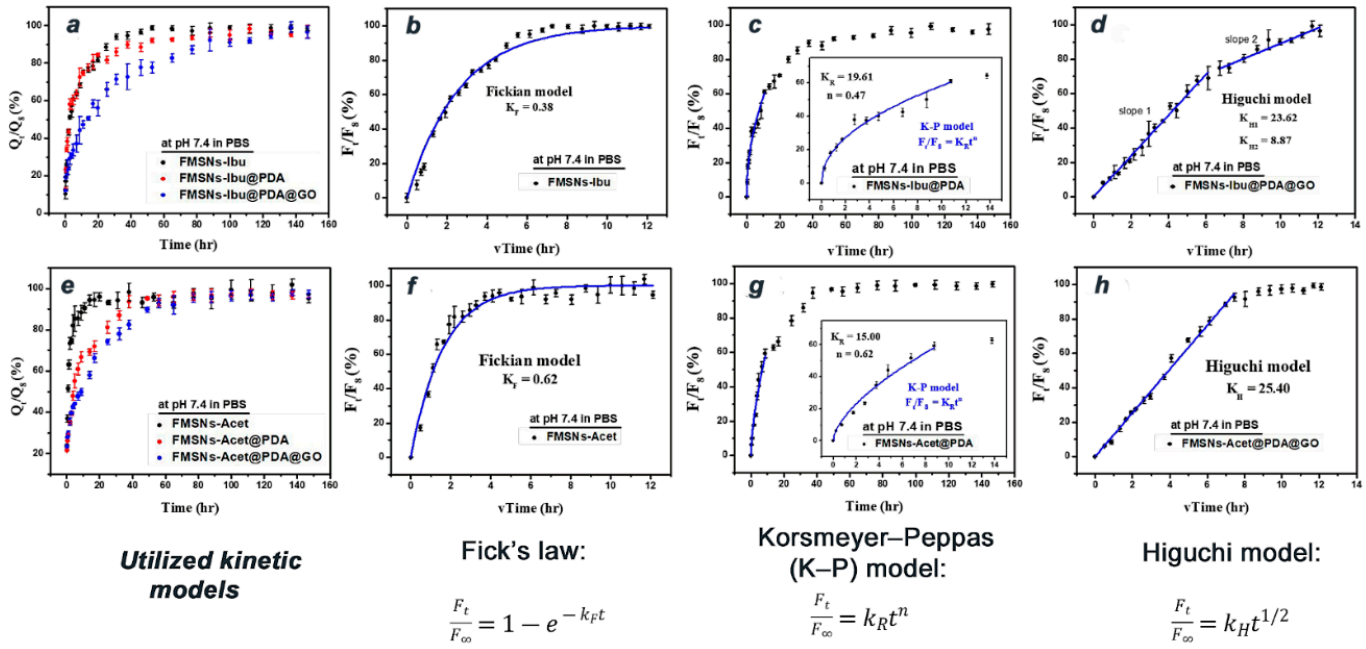

Figure 6. Release profiles of FMSNs, FMSNs@PDA, and FMSNs@PDA@GO when (**a**–**d**) ibuprofen and (**e**–**h**) acetaminophen were loaded in PBS (pH 7.4) at 37 °C. Model fits of ibuprofen and acetaminophen release from FMSNs-Drug, FMSNs-Drug@PDA, and FMSNs-Drug@PDA@GO by the Fickian exponential or Higuchi model versus cumulative time or square root time, and Kp model versus cumulative time. Reprinted/adapted from ref. [321] with permission from RSC—Royal Society of Chemistry, 2020.

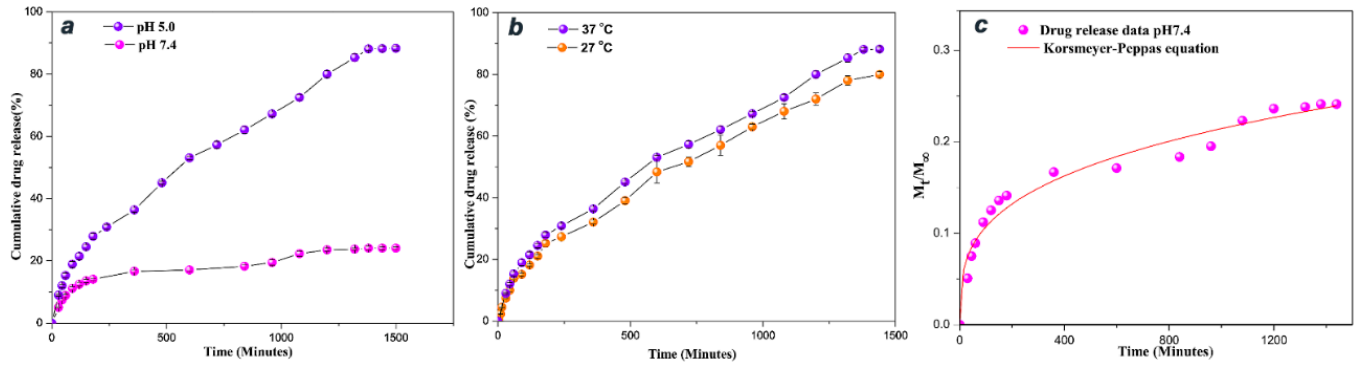

Figure 7. (**a**) pH responsive 5 FU release profile of 5 FU-loaded Fe_3O_4-Dex-MA-g-P(NVI/NVCL) at 37 °C at pH of 5.0 and 7.4. Data are presented as mean ± SD (n = 3); (**b**) In vitro 5 FU release of profile of 5 FU-loaded Fe_3O_4-Dex-MA-g-P(NVI/NVCL) at pH 5.0, temperatures 27 and 37 °C. Data are presented as mean ± SD (n = 3); (**c**) Korsmeyer–Peppas fit for 5 FU release from 5 FU-loaded Fe_3O_4-Dex-MAg-P(NVI/NVCL) at pH 7.4. Reprinted/adapted from ref. [322] with permission from Elsevier, 2020.

Notably, due to the immobilization of a water-soluble drug, 5-fluorouracil (5 FU), the drug release may occur also due to a chemical potential gradient [322]. A typical release profile such as those in Figure 5 or Figure 6 exhibits an initial burst release due to drug diffusion at the solid–liquid interface. The Korsmeyer–Peppas fit of drug release ($\frac{M_t}{M_\infty} = kt^n$) bears important mechanistic significance, especially when referring to the value of "n". Under acidic conditions, which are indicative of tumoral site behavior, n = 0.585 (R^2 = 0.997), pointing to both swelling and diffusion mechanisms when reaching the acidic tumoral environment, but the value of "n" is much lower for release under bloodstream conditions (pH = 7.4), n = 0.302, so only minute amounts of drug will be released during

blood circulation [322]. This divergent behavior of drug-loaded microcarriers will be beneficial for reaching maximum target efficiency.

Other release models under consideration are the 0th (constant amount of drug released per unit time, irrespective of drug concentration) and 1st order ($c = c_0 e^{-kt}$) kinetics, linear equation (y = ax + b), Weibull ($\frac{M_t}{M_\infty} = 1 - e^{-at^b}$), Michaelis–Menten ($\nu = \frac{V_{max}[S]}{K_m + [S]}$) or Hill equation ($y = \frac{y_{max} x^\alpha}{c^\alpha + x^\alpha}$) [329].

An interesting functionalization process is depicted in Figure 8. The magnetite NPs obtained from the co-precipitation method are covered by hydroxyl groups (from either NH_4OH or MOH, where M = Na, K), and this provides chemical anchors for $Si(OEt)_4$ (tetraethoxysilane), forming a silica-coated MNPs as a result (product 1, Figure 8). Then, there is a further reaction with 3-(trimethoxysilyl) propyl methacrylate (TMSPM) to produce Fe_3O_4/TEOS/TMSPM hybrids containing C=C bonds for grafting subsequent functional polymers. Subsequently, polymerization of Fe_3O_4/TEOS/TMSPM with glycidyl methacrylate (GMA) initiated by benzoyl peroxide occurs, and a reactive suspension of Fe_3O_4/TEOS/TMSPM/GMA is obtained, that reacts with isopropyl-*o*-carborane to produce Fe_3O_4/TEOS/TMSPM/GMA/Carborane (product 4, Figure 8). The cytotoxicity of these nanohybrids was assessed towards tumoral cell lines: HeLa (cervical cancer), BxPC-3 (pancreatic cancer) and MCF-7 (breast cancer) with promising results motivating a shift to boron cancer therapy. Interestingly, Mossbauer spectra of starting Fe_3O_4 differ significantly from that of Fe_3O_4/TEOS pointing to a change in phase composition upon coating and further functionalization. Nevertheless, the saturation magnetization registered a decrease upon siloxanic coating, from 65.2 emu/g (Fe_3O_4) to 48.6 emu/g in final nanocomposite Fe_3O_4/TEOS/TMSPM/GMA/Carborane [354].

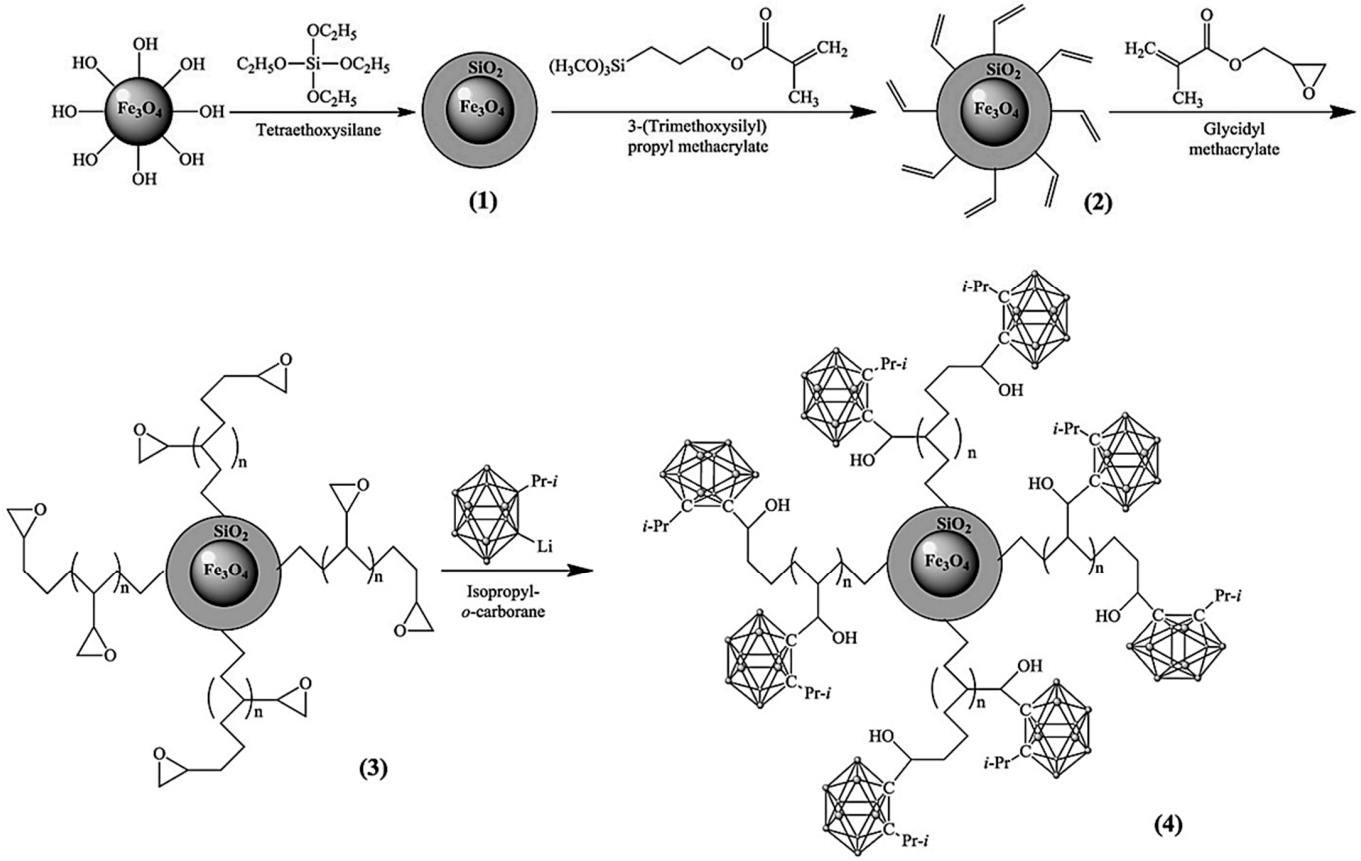

Figure 8. Functionalization scheme for Fe_3O_4 MNPs with carborane immobilization. Reprinted from ref. [354], with permission from Elsevier, 2020.

Another typical example depicting MNPs formation is coating with biocompatible chitosan (MNP-CS) and further binding Telmisartan (an anticancer drug that is water-soluble and contains carboxyl -COOH moieties) (Figure 9).

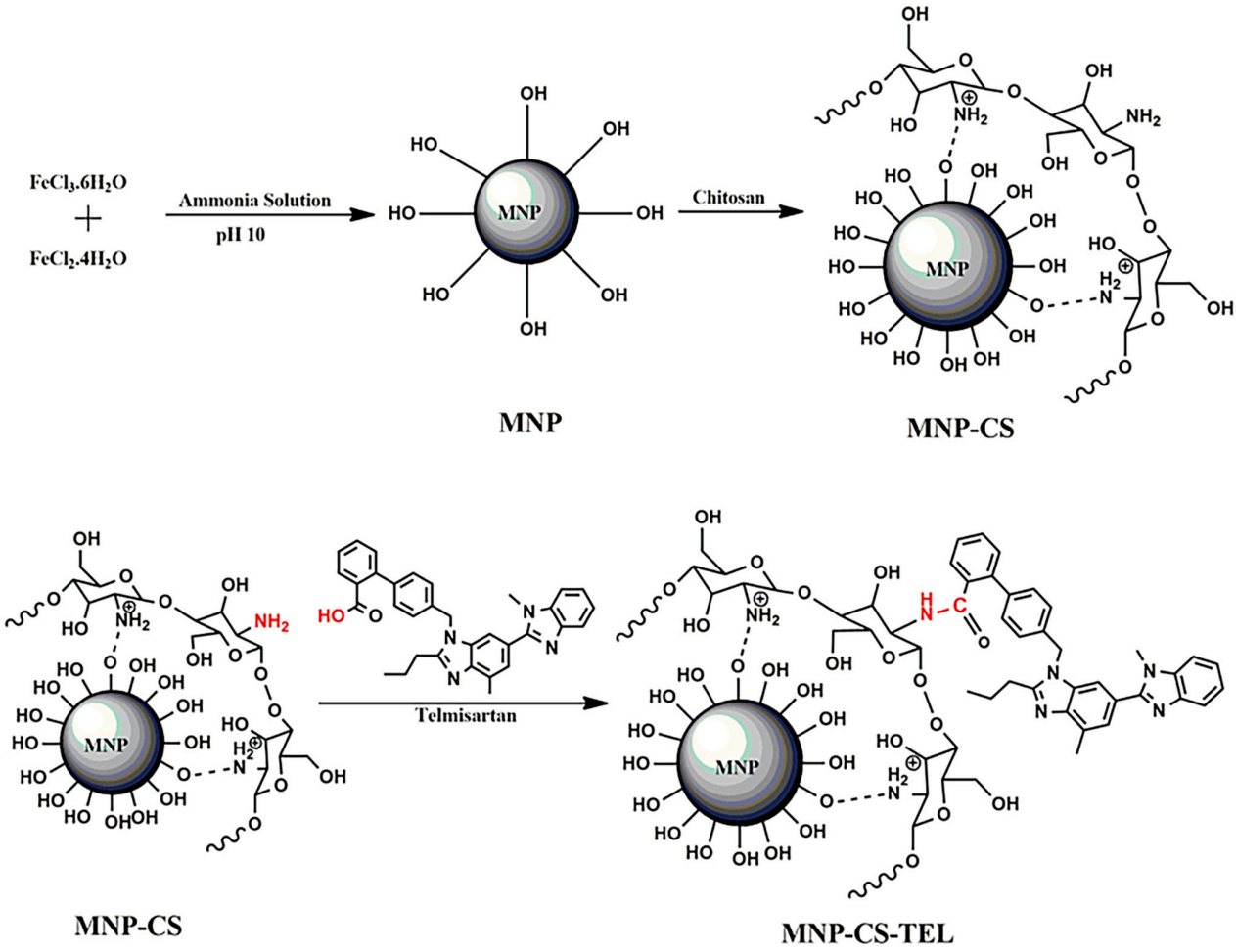

Figure 9. Synthesis of drug-loaded, chitosan-coated magnetite NPs. Reprinted from ref. [366], with permission from Elsevier, 2021.

The chitosan is loaded by gently shaking the as-prepared Fe_3O_4 MNPs (by co-precipitation from chloride iron sources) with an acylated chitosan solution (chitosan reaction with CH_3COOH). The obtained hybrid, MNP-CS, was magnetically separated from the reaction mixture. The actual loading of Telmisartan by a classical condensation reaction between an amine and an acid, produces an amidic bond -NH-C(=O)- when kept in an incubator shaker for 24 h at 100 rpm, at room temperature [366].

In this case, the magnetization curves of MNPs and MNP-CS show a close resemblance, and, more importantly, the M_S is only slightly reduced by coating from 59 emu/g (Fe_3O_4) to 50 emu/g (Fe_3O_4@chitosan) (Figure 10a). The magnetization curves show no coercivity, indicative of the superparamagnetic behavior of Fe_3O_4. The reduction of magnetic response and M_S is potentially problematic in polymeric coatings of MNPs since this coating procedure leads to a decrease in M_S. Ideally, the coating agent should have a thin coverage such that the magnetic behavior would remain largely unchanged [366].

An example of cytotoxicity assessment involved testing on PC-3 human prostate cancer cell line. The cell viability showed dependence on pH (drug release occurring at acidic pH) and dose administered (Figure 10b). The coating/functionalization techniques described in Figures 8 and 9 represent a strategy with wide applicability for the conjugation of many other drugs (Table 1).

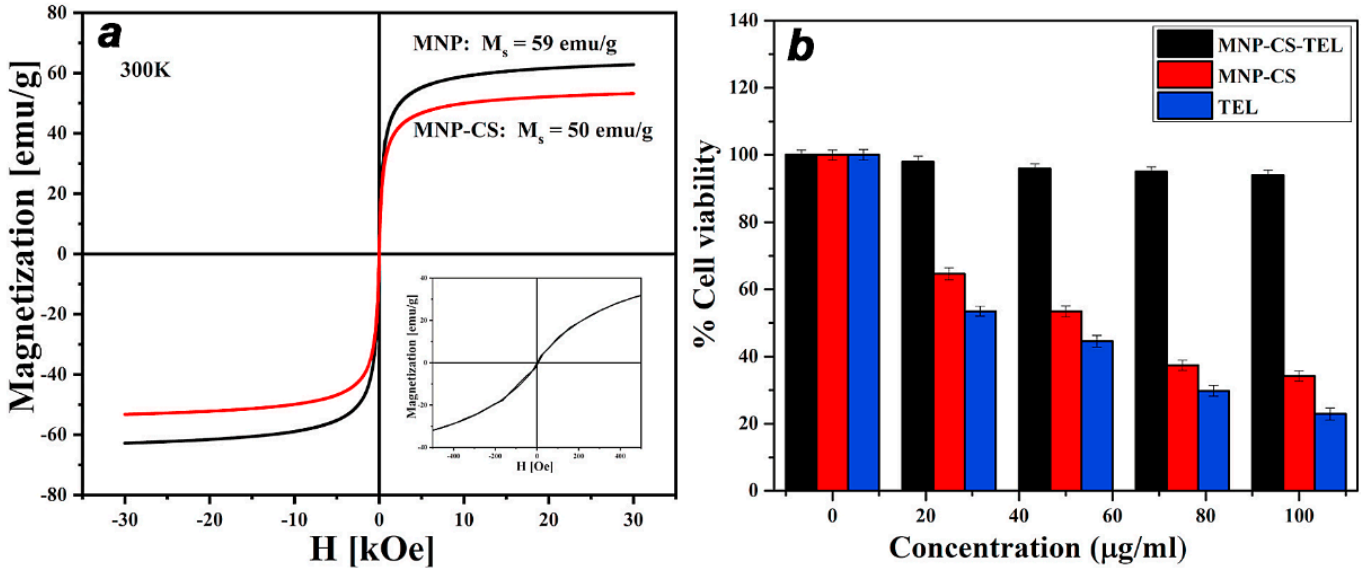

Figure 10. (**a**) Room temperature magnetization curves of MNPs and MNP-CS. (**b**) In vitro cytotoxicity assay of MNP-CS, MNP–CS–TEL, and TEL on PC-3 human prostate cancer cell line by MTT assay. Reprinted from ref. [366], with permission from Elsevier, 2021.

5.2. Cell Drug Uptake

The porous structure containing mesopores (D_p = 2–50 nm) enhances remarkably the efficiency of MNPs to uptake different biologically active molecules, such as paclitaxel (PTX), better known under its commercial name of Taxol, a chemotherapy medication for the treatment of many types of cancer [404], among others. There is a fine line delimiting cell uptake and accumulation, and MNPs should only accumulate at the target site where cancer or tumor cells lie [405].

Other in situ/operando characterization methods have been employed to better visualize the uptake process of NPs by cancer cells and Raman spectroscopy has served recently this purpose when cancer cells were subjected to Co-NPs [406,407]. Improvements in cell uptake were recorded when using biomimetic MNPs, attesting once again that the key to overcoming biologic barriers is to use other bio-inspired mechanisms [408].

5.3. Hyperthermia

Magnetic nanoparticles investigated for biomedical and hyperthermia applications have been reviewed recently [409–412]. Of particular interest are hyperthermia applications, since they can offer new horizons in cancer treatment and disease detection, management and treatment [70,335,413–428]. Many critical aspects have been investigated regarding the use of ferrofluid media and critical heat transfer issues [429,430]. At the core of MFH interpretation lies the proper establishment of the magnetic state of the examined NPs, and the main parameter is the blocking temperature (T_B), the vast majority of SPIONs being found in a superparamagnetic state at room temperature: $T_B = \frac{K_{eff}V}{k_B ln\left(\frac{\tau}{\tau_0}\right)}$, with V as the mean NP volume, and t as the measurement time, typically ~10^{-6} s, K_{eff} the anisotropy constant and k_B the Boltzmann's constant 1.38 × 10^{-23} J K^{-1} [76]. In order for MNPs based on biomagnetic core-shell $Zn_\delta Mn_{1-\delta}Fe_2O_4$@γ-$Fe_2O_3$ composition (δ = 0.2 and 0.5) to exhibit a blocking temperature near room temperature (T_B = 300 K), their size was estimated to be 32–25 nm; hence, the actual MNPs synthesized with sizes 7.2–9.2 nm were all in superparamagnetic state at 300 K [76].

Aiming for a more effective hyperthermia procedure to combat tumors would imply a synergic effect of drug delivery (tuned for the specific disease), corroborated with the

hyperthermia effect itself providing an efficient tool to locally increase the temperature to a range where cancer/tumor cells are most sensitive to and eventually die (41–46 °C) [431,432].

DFT modeling using the Monte Carlo model is also available for clinical hyperthermia applications [433] or magnetic gel behavior under magnetic guidance simulation [434]. Mechanistic studies on the effect and interplay of the essential heat release mechanisms have been presented in detail [23,435,436], as well as the effect of Ti atoms on Néel relaxation of MNPs [437], the drug-release modeling such as the 0th order, 1st order, Higuchi model or Korsmeyer–Peppas kinetic models [438], the magnetization reduction essential in sustainable hyperthermia [439], or others [440].

Theoretical simulations have revealed interesting features of MNPs related to their performance in hyperthermia experiments, and some of these investigations pointed to an optimal aspect ratio for maximum heating effect [441]. Closing the loop in the heating process, the temperature reduction mechanism was shown to greatly depend on the heating rate of a core-shell magnetite NP system [442].

5.4. Hypoxia

Hypoxia is a medical condition where the oxygen levels in body tissues are low and represents a turning point in cancer treatment that is resistant to traditional or targeted therapies. Oxygen binds to hemoglobin to form oxyhemoglobin and deoxyhemoglobin, and these two forms experience concentration modifications that can be visualized by functional MRI (fMRI) technique: BOLD (blood oxygenation-dependent imaging) MRI [144]. Biodegradable Fe-based nanohybrids have been used for hypoxia-modulated tumor treatment when H-MnFe(OH)$_x$ hydroxide nanocapsules were designed with high loading capacity, for instance using a chemotherapeutic drug, doxorubicin (DOX) with in vitro and in vivo proof-of-concept anticancer synergy [443,444].

5.5. MDT: Magnetic Drug Targeting

Targeting cancer and tumors with an effective treatment therapy is at the forefront of biomedical research and diagnosis [24,141,208,445–464]. This is the result of traditional chemotherapy treatments being non-specific, and by this, the healthy tissues could also be harmed by the aggressive anticancer drugs. MNPs respond to an externally applied magnetic field, offering the means to guide the transport and delivery of cytotoxic drug-loaded magnetic nanocarriers at the target organ/tissue. Many variables complicate this process, including blood flow velocity, drug immobilization strategy on MNP carriers, poor diffusion control after intravenous injection, geometry and depth of affected organ among others. Moreover, in order to beat the odds, early diagnosis is an essential moment—vital for the life of affected patients, especially when the drug formulation has to target specific organs/tissue [261,465–495].

The flow behavior in MDT was studied by several groups [496–500], as well as their ability to penetrate different types of tissues, including eye tissue [501]. The modeling of flow behavior is even more important when the targeted disease is localized at the arterial segment (atherosclerosis), where control of NP aggregation is vital and is addressed by numerical solving of vorticity stream-function formulation [497]. Other research groups studied the potential removal of MNP-tagged cytokine during cardiopulmonary bypass, by employing simulation methods based on Navier–Stokes equations [498], or the feasibility study of introducing multicore MNPs of ~50 nm through the eye tissue using a magnetic field gradient of 20 T m^{-1} [501]. Many of the research groups concluded that the best results in MDT can be obtained only when affected tissues are close to the body surface, hence the depth factor of the tumor seems to be prevalent. Moreover, the behavior of MNPs in the coronary circulatory system is of vital importance to understand and optimize the drug-delivery nanovehicles [502].

5.6. On-Demand Drug Release

Nano-engineered hybrid formulations can release the loaded molecule on-demand [378,503–513], but also leach divalent cations from ferrite composites [514]. The leaching test mentioned is an important piece of evidence regarding magnetic core integrity on its passage through the biological system, and ideally, it should retain its integrity, as some data in the literature has shown.

5.7. Apoptosis

The process of programmed cell death (apoptosis) is another important achievement of utilizing SPIONs; HT-29 cells have shown apoptosis by stimulative oxidative stress by iron oxide SPIONs [515–517].

6. Biocompatibility and Toxicity

Biocompatibility and toxicity features of anti-cancer formulations are nowadays treated with equal care and thoroughly investigated [518,519]. Oftentimes, endocytosis is not an easy task because various immune responses from the cells can decompose the nanocarrier before entering the cell membrane. Biomimetics was exploited as a tool to ease the incorporation of MNPs into living tissue [450,520,521].

Liposomes resemble the structure of cell membranes and are spherical vesicles composed of multiple phospholipid bilayers, and the incorporation of MNPs or SPIONs into such vesicles can ease the design and efficiency of drug-delivery systems since both hydrophilic and lipophilic drugs can be encapsulated [522,523]. Liposome use was expanded to vaccine formulation and stabilization [524]. This bio-inspired strategy typically affords swift entry of the drug by endocytosis with no to minimal damage.

6.1. Cytotoxicity

Oftentimes, the therapeutic effect was the main concern of the clinician; however, the toxicity that MNPs can have towards neighboring tissue or during its magnetically-guided path to the tumor site is less investigated, yet is just as important. The non-magnetic shell typically covering MNPs was shown to be essential to the reduced overall toxicity of polymer-coated metal oxide-based MNPs [525–527], drug-loaded nanoparticles [528] or that of bare MNPs [529,530] and derived ferrofluids with biological administration relevance [531]. The antioxidant effect was assessed by recent reviews in relation to the potential toxicity issues of MNPs [532].

The effect of $CoFe_2O_4$ cobalt ferrite on Channel catfish ovary cells was reported in 2022 by Srikanth et al. [533]. However, magnetite Fe_3O_4 can reduce $CdCl_2$-induced toxicity by oxidative stress as shown in a test on small intestine cells of mice, while orally-administered nano-Fe_3O_4 showed no toxicity at all [534]. The biodistribution and cytotoxicity of oral iron supplements, which are particularly relevant for patients suffering from iron-deficiency-induced anemia, have been investigated [535], and the effect on the human adipose tissue-derived stromal cell system of very small SPIONs [536,537] or targeting Parkinson's disease [538]. Other coatings of magnetite showed no gene toxicity, making them suitable candidates for biomedical applications when guar gum-coated Fe_3O_4 MNPs obtained by co-precipitation (Fe_3O_4-GG nanocomposites) were used on Drosophila melanogaster (fruit fly), a leading invertebrate model system used in aging research [539]. Regarding anemia treatment options, MNPs are now available in a commercially, FDA-approved drug formulation, ferumoxytol (Feraheme as brand name), with intravenous administration.

6.2. NPs Accumulation in Tissue: The Fate of MNPs in Biological Systems

Accumulation of MNPs is an issue for MDT practices, as well as understanding the complete picture of MNP fate in the biological systems [540]. It was also found that the injection rate can affect the efficiency of MNPs accumulation [541–543]. However, the natural evolution in the treatment of cancerous cells would be to increase localized

MNPs concentration, a theme tackled by various groups [544], as well as investigating its suitability to stimulate the activation of a targeted immune response [545].

Other research directions use model fish systems such as the common carp (Cyprinus carpio) to evaluate the accumulation of SPIONs in tissue and subsequent antioxidant and immune responses to iron oxides [546,547], or the effect of $KFeO_2$ nanoparticles on MCF-7 cell lines [548]. General toxicology studies have been also performed [526]. Other metal ferrites such as $NiFe_2O_4$ NPs have been investigated regarding histopathological mediated toxicity and the oxidative stress induced in rabbits [549]. The final fate of MNPs introduced in biological systems is complex and still not completely understood but it constitutes a theme of great practical significance [550–553].

7. Conclusions and Outlook

Various types of MNP platforms exist today and they are under rapid development. The MNPs can be tailored for detection (MR imaging contrast agents) and treatment therapies of various diseases, including early-stage and advanced forms of cancer. Surface manipulation (silica, gold or biocompatible polymers such as PEG or dextran) can yield stable MNP systems with minimal aggregation or opsonization, providing minimal systemic response and a high likelihood of passage through biological barriers (reticuloendothelial, vascular endothelium or blood–brain barrier). Achieving enhanced biocompatibility, precise targeting and increased accumulation of target cells for proper biological response remain the main goals. Multifunctional MNPs can offer diverse therapeutic strategies for healthcare providers.

Improvements to MNP formulations are still possible, and they tackle enhanced magnetic features of the magnetic core, new bio-inspired coatings and/or multifunctional drug loading. When a suitable system is identified, it will undergo scrutiny from quality, reproducibility, efficacy and stability criteria—all necessary prerequisites for scaling up processes and further pre-clinical implementation and testing. However, a number of unknowns still linger on: the uncertain fate of the MNPs after reaching the biological system, or the interaction mechanism of MNPs in vivo, an insight to further enhance the great opportunities that MNPs could provide, namely detection and treatment of various diseases, including cancer. Recent years have witnessed advances in drug-delivery systems being optimized and expanded by incorporating new functionalization agents for multifunctional MNPs synthesis and applications, as well as expanding the scope of therapeutic choices by employing highly-effective drugs that would be otherwise hard to deliver at the tumoral site due to many possible shortcomings, solubility issues being one example.

Moreover, a recent research direction aims to use magnetic (nano)particle imaging (MPI) in diagnostic imaging and guided treatment therapy, effectively linking image contrast and quality to relaxation mechanisms while emphasizing a safety administration profile. With no depth attenuation, MPI based on magnetic nano tracers—usually SPIONs—could provide excellent imaging contrast, spatial and temporal resolution and excellent signal-to-noise ratio. At its core, the emerging field of MPI relies heavily on the successful implementation of magnetic tracers, and this endeavor can take advantage of current development in MNPs used for drug-delivery applications.

Funding: This work was supported by the Romanian Ministry of Research and Innovation through Project PN-III-P1-1.1-TE-2021-1657 (TE 84/2022), TE 91/2022 and Core Program PN19-03 (contract no. PN21N/2019).

Institutional Review Board Statement: Not applicable.

Informed Consent Statement: Not applicable.

Data Availability Statement: Not applicable.

Conflicts of Interest: The authors declare no conflict of interest. The funders had no role in the design of the study; in the collection, analyses, or interpretation of data; in the writing of the manuscript; or in the decision to publish the results.

References

1. Fadli, A.; Amri, A.; Sari, E.O.; Sukoco, S.; Saprudin, D. Superparamagnetic nanoparticles with mesoporous structure prepared through hydrothermal technique. *Mater. Sci. Forum* **2020**, *1000*, 203–209. [CrossRef]
2. Ghaemi, A.; Mohave, F.; Farhadi, A.; Takassi, M.A.; Tavakkoli, H. Hydrothermal synthesis of mesoporous cobalt ferrite by ionic liquid-assisted process; catalytic performance, morphology, and magnetic studies. *J. Aust. Ceram. Soc.* **2021**, *57*, 1321–1330. [CrossRef]
3. Tombuloglu, H.; Khan, F.A.; Almessiere, M.A.; Aldakheel, S.; Baykal, A. Synthesis of niobium substituted cobalt-nickel nanoferrite ($Co_{0.5}Ni_{0.5}Nb_xFe_{2-x}O_4$ ($x \leq 0.1$) by hydrothermal approach show strong anti-colon cancer activities. *J. Biomol. Struct. Dyn.* **2021**, *39*, 2257–2265. [CrossRef] [PubMed]
4. Panda, J.; Das, S.; Kumar, S.; Tudu, B.; Sarkar, R. Investigation of antibacterial, antioxidant, and anticancer properties of hydrothermally synthesized cobalt ferrite nanoparticles. *Appl. Phys. A Mater. Sci. Process.* **2022**, *128*, 562. [CrossRef]
5. Albornoz, C.A.; Paulin, M.A.; Cristóbal, A.A.; Vega, D.R.; Leyva, A.G.; Ramos, C.P. Microwave-assisted hydrothermal nanoarchitectonics of polyethyleneimine-coated iron oxide nanoparticles. *Appl. Phys. A Mater. Sci. Process.* **2022**, *128*, 68. [CrossRef]
6. Fayazzadeh, S.; Khodaei, M.; Arani, M.; Mahdavi, S.R.; Nizamov, T.; Majouga, A. Magnetic Properties and Magnetic Hyperthermia of Cobalt Ferrite Nanoparticles Synthesized by Hydrothermal Method. *J. Supercond. Nov. Magn.* **2020**, *33*, 2227–2233. [CrossRef]
7. Park, Y.; Yoon, H.J.; Lee, S.E.; Lee, L.P. Multifunctional Cellular Targeting, Molecular Delivery, and Imaging by Integrated Mesoporous-Silica with Optical Nanocrescent Antenna: MONA. *ACS Nano* **2022**, *16*, 2013–2023. [CrossRef]
8. Wang, F.; Qi, X.; Geng, J.; Liu, X.; Li, D.; Zhang, H.; Zhang, P.; He, X.; Li, B.; Li, Z.; et al. Template-free construction of hollow mesoporous Fe_3O_4 nanospheres as controlled drug delivery with enhanced drug loading capacity. *J. Mol. Liq.* **2022**, *347*, 118000. [CrossRef]
9. Gao, Y.; Shi, X.; Shen, M. Intelligent Design of Ultrasmall Iron Oxide Nanoparticle-Based Theranostics. *ACS Appl. Mater. Interfaces* **2021**, *13*, 45119–45129. [CrossRef]
10. Saputra, O.A.; Wibowo, F.R.; Lestari, W.W.; Handayani, M. Highly monodisperse and colloidal stable of L-serine capped magnetite nanoparticles synthesized via sonochemistry assisted co-precipitation method. *Adv. Nat. Sci. Nanosci. Nanotechnol.* **2020**, *11*, 025012. [CrossRef]
11. Kafi-Ahmadi, L.; Khademinia, S.; Nansa, M.N.; Alemi, A.A.L.I.; Mahdavi, M.; Marjani, A.P. Co-precipitation synthesis, characterization of $CoFe_2O_4$ nanomaterial and evaluation of its toxicity behavior on human leukemia cancer K562 cell line. *J. Chil. Chem. Soc.* **2020**, *65*, 4845–4848. [CrossRef]
12. Tadic, M.; Lazovic, J.; Panjan, M.; Kralj, S. Hierarchical iron oxide nanocomposite: Bundle-like morphology, magnetic properties and potential biomedical application. *Ceram. Int.* **2022**, *48*, 16015–16022. [CrossRef]
13. Porrawatkul, P.; Nuengmatcha, P.; Tangwatanakul, W.; Chanthai, S. Effect of Zn, Ni, and Mn doping ions on magnetic properties of MFe_2O_4 (M = Mn, Zn, and Ni) nanoparticles synthesized via sol–gel autocombustion using PVA/sago starch blend as a chelating agent. *J. Korean Ceram. Soc.* **2020**, *57*, 676–683. [CrossRef]
14. Qayoom, M.; Bhat, R.; Shah, K.A.; Pandit, A.H.; Firdous, A.; Dar, G.N. Modified Solution Combustion Synthesis of Nickel-Doped Magnetite Nanoparticles and the Influence of Annealing on Their Optical, Electrical, and Magnetic Properties. *J. Electron. Mater.* **2020**, *49*, 1215–1229. [CrossRef]
15. Haydar, M.S.; Das, D.; Ghosh, S.; Mandal, P. Implementation of mature tea leaves extract in bioinspired synthesis of iron oxide nanoparticles: Preparation, process optimization, characterization, and assessment of therapeutic potential. *Chem. Pap.* **2022**, *76*, 491–514. [CrossRef]
16. Mangamma, J.L.; Devi, D.R.; Sagar, P.S.R.V.; Babu, M.R.; Basavaiah, K. Review on Plant Mediated Green Synthesis of Magnetite Nanoparticles for Pollution Abatement, Biomedical and Electronic Applications. *Asian J. Chem.* **2022**, *34*, 1047–1054. [CrossRef]
17. Loiola, A.R.; Bessa, R.A.; Oliveira, C.P.; Freitas, A.D.L.; Soares, S.A.; Bohn, F.; Pergher, S.B.C. Magnetic zeolite composites: Classification, synthesis routes, and technological applications. *J. Magn. Magn. Mater.* **2022**, *560*, 169651. [CrossRef]
18. Bertran, A.; Sandoval, S.; Oro-Sole, J.; Sanchez, A.; Tobias, G. Particle size determination from magnetization curves in reduced graphene oxide decorated with monodispersed superparamagnetic iron oxide nanoparticles. *J. Colloid Interface Sci.* **2020**, *566*, 107–119. [CrossRef]
19. Harada, M.; Kuwa, M.; Sato, R.; Teranishi, T.; Takahashi, M.; Maenosono, S. Cation Distribution in Monodispersed MFe_2O_4 (M = Mn, Fe, Co, Ni, and Zn) Nanoparticles Investigated by X-ray Absorption Fine Structure Spectroscopy: Implications for Magnetic Data Storage, Catalysts, Sensors, and Ferrofluids. *ACS Appl. Nano Mater.* **2020**, *3*, 8389–8402. [CrossRef]
20. Wahba, A.M.; Mohamed, M.B. Correlating cation distribution with the structural and magnetic properties of $Co_{0.5}Zn_{0.5}Al_xFe_{2-x}O_4$ nanoferrites. *Appl. Phys. A Mater. Sci. Process.* **2020**, *126*, 488. [CrossRef]
21. Palade, P.; Comanescu, C.; Kuncser, A.; Berger, D.; Matei, C.; Iacob, N.; Kuncser, V. Mesoporous Cobalt Ferrite Nanosystems Obtained by Surfactant-Assisted Hydrothermal Method: Tuning Morpho-structural and Magnetic Properties via pH-Variation. *Nanomaterials* **2020**, *10*, 476. [CrossRef] [PubMed]

22. Orozco-Henao, J.M.; Muraca, D.; Sánchez, F.H.; Mendoza Zélis, P. Determination of the effective anisotropy of magnetite/maghemite nanoparticles from Mössbauer effect spectra. *J. Phys. D Appl. Phys.* **2022**, *55*, 335302. [CrossRef]
23. Kahmann, T.; Ludwig, F. Magnetic field dependence of the effective magnetic moment of multi-core nanoparticles. *J. Appl. Phys.* **2020**, *127*, 233901. [CrossRef]
24. Wang, S.; Xu, J.; Li, W.; Sun, S.; Gao, S.; Hou, Y. Magnetic Nanostructures: Rational Design and Fabrication Strategies toward Diverse Applications. *Chem. Rev.* **2022**, *122*, 5411–5475. [CrossRef] [PubMed]
25. Pyatakov, A.; Pyatakova, Z.; Tishin, A.M. Short history overview of magnetism and magnetic technologies for medical applications. In *Materials and Technologies for Medical Applications*; Woodhead Publishing: Cambridge, UK, 2022; pp. 3–21. [CrossRef]
26. Krasia-Christoforou, T.; Socoliuc, V.; Knudsen, K.D.; Tombácz, E.; Turcu, R.; Vekas, L. From single-core nanoparticles in ferrofluids to multi-core magnetic nanocomposites: Assembly strategies, structure and magnetic behavior. *Nanomaterials* **2020**, *10*, 2178. [CrossRef]
27. Scanone, A.C.; Gsponer, N.S.; Alvarez, M.G.; Heredia, D.A.; Durantini, A.M.; Durantini, E.N. Magnetic Nanoplatforms for in Situ Modification of Macromolecules: Synthesis, Characterization, and Photoinactivating Power of Cationic Nanoiman–Porphyrin Conjugates. *ACS Appl. Bio Mater.* **2020**, *3*, 5930–5940. [CrossRef]
28. Shi, Y.; Jyoti, D.; Gordon-Wylie, S.W.; Weaver, J.B. Quantification of magnetic nanoparticles by compensating for multiple environment changes simultaneously. *Nanoscale* **2020**, *12*, 195–200. [CrossRef]
29. Papadopoulos, C.; Efthimiadou, E.K.; Pissas, M.; Fuentes, D.; Boukos, N.; Psycharis, V.; Kordas, G.; Loukopoulos, V.C.; Kagadis, G.C. Magnetic fluid hyperthermia simulations in evaluation of SAR calculation methods. *Phys. Med.* **2020**, *71*, 39–52. [CrossRef] [PubMed]
30. Honecker, D.; Bersweiler, M.; Erokhin, S.; Berkov, D.; Chesnel, K.; Venero, D.A.; Qdemat, A.; Disch, S.; Jochum, J.K.; Michels, A.; et al. Using small-angle scattering to guide functional magnetic nanoparticle design. *Nanoscale Adv.* **2022**, *4*, 1026–1059. [CrossRef]
31. Priyadarshi, H.; Gaur, U. Paramagnetism-enhanced doped maghemite nanoparticles for targeted drug delivery. *Mater. Today Proc.* **2021**, *43*, 3030–3033. [CrossRef]
32. Pardo, A.; Pelaz, B.; Gallo, J.; Bañobre-López, M.; Parak, W.J.; Barbosa, S.; Del Pino, P.; Taboada, P. Synthesis, Characterization, and Evaluation of Superparamagnetic Doped Ferrites as Potential Therapeutic Nanotools. *Chem. Mater.* **2020**, *32*, 2220–2231. [CrossRef]
33. Dhillon, G.; Kumar, N.; Chitkara, M.; Sandhu, I.S. Effect of Gd^{3+} substitution on physicochemical properties of superparamagnetic Fe_3O_4 nanoparticles. *J. Mater. Sci. Mater. Electron.* **2021**, *32*, 22387–22397. [CrossRef]
34. Saini, A.; Borchers, J.A.; George, S.; Maranville, B.B.; Krycka, K.L.; Dura, J.A.; Theis-Bröhl, K.; Wolff, M. Layering of Magnetic Nanoparticles at Amorphous Magnetic Templates with Perpendicular Anisotropy. *Soft Matter* **2020**, *16*, 7676. [CrossRef] [PubMed]
35. Zhao, P.; Zhao, J.; Deng, Y.; Zeng, G.; Jiang, Y.; Liao, L.; Zhang, S.; Tao, Q.; Liu, Z.; Tang, X.; et al. Application of iron/barium ferrite/carbon-coated iron nanocrystal composites in transcatheter arterial chemoembolization of hepatocellular carcinoma. *J. Colloid Interface Sci.* **2021**, *601*, 30–41. [CrossRef]
36. Hölscher, J.; Petrecca, M.; Albino, M.; Garbus, P.G.; Saura-Múzquiz, M.; Sangregorio, C.; Christensen, M. Magnetic Property Enhancement of Spinel Mn-Zn Ferrite through Atomic Structure Control. *Inorg. Chem.* **2020**, *59*, 11184–11192. [CrossRef]
37. Riaz, H.; Hashmi, R.; Abid, S.; Shareef, N.; Faqir, A.; Amir, A.; Shahzad, M.S.; Shakeel, M.; Akhtar, S.; Ashiq, M.N.; et al. Intraperitoneal injections of copper ferrite nanoparticles disturb blood, plasma, and antioxidant parameters of Wistar rats in a sex-specific manner. *Naunyn-Schmiedeberg's Arch. Pharmacol.* **2020**, *393*, 2019–2028. [CrossRef]
38. Sarkar, B.J.; Bandyopadhyay, A. Studies of magnetic behavior of chemically synthesized interacting superparamagnetic copper ferrite nanoparticles. *J. Mater. Sci. Mater. Electron.* **2021**, *32*, 1491–1505. [CrossRef]
39. Manju, B.G.; Raji, P. Green synthesis, characterization, and antibacterial activity of lime-juice-mediated copper–nickel mixed ferrite nanoparticles. *Appl. Phys. A Mater. Sci. Process.* **2020**, *126*, 156. [CrossRef]
40. Althubayti, M.M.; Hjiri, M.; Alonizan, N.H.; Lemine, O.M.; Aida, M.S. Influence of divalent metals (Zn, Cu and Co) on the synthesis and magnetic properties of spinel ferrite nanopowders. *J. Mater. Sci. Mater. Electron.* **2020**, *31*, 8194–8205. [CrossRef]
41. Silvestri, N.; Gavilán, H.; Guardia, P.; Brescia, R.; Fernandes, S.; Samia, A.C.S.; Teran, F.J.; Pellegrino, T. Di- and tri-component spinel ferrite nanocubes: Synthesis and their comparative characterization for theranostic applications. *Nanoscale* **2021**, *13*, 13665–13680. [CrossRef]
42. Hossain, M.D.; Khan, M.N.I.; Nahar, A.; Ali, M.A.; Matin, M.A.; Hoque, S.M.; Hakim, M.A.; Jamil, A.T.M.K. Tailoring the properties of Ni-Zn-Co ferrites by Gd^{3+} substitution. *J. Magn. Magn. Mater.* **2020**, *497*, 165978. [CrossRef]
43. Vangijzegem, T.; Stanicki, D.; Panepinto, A.; Socoliuc, V.; Vekas, L.; Muller, R.N.; Laurent, S. Influence of Experimental Parameters of a Continuous Flow Process on the Properties of Very Small Iron Oxide Nanoparticles (VSION) Designed for T1-Weighted Magnetic Resonance Imaging (MRI). *Nanomaterials* **2020**, *10*, 757. [CrossRef] [PubMed]
44. Morillas, J.R.; de Vicente, J. Magnetorheology: A review. *Soft Matter* **2020**, *16*, 9614–9642. [CrossRef] [PubMed]
45. Zablotsky, D.; Kralj, S.; Maiorov, M.M. Features of magnetorheology of biocompatible chain-forming ferrofluids with multi-core magnetic nanoparticles: Experiment and simulation. *Colloids Surf. A* **2020**, *603*, 125079. [CrossRef]
46. Craciunescu, I.; Chiţanu, E.; Codescu, M.M.; Iacob, N.; Kuncser, A.; Kuncser, V.; Socoliuc, V.; Susan-Resiga, D.; Bălănean, F.; Ispas, G.; et al. High performance magnetorheological fluids: Very high magnetization FeCo-Fe_3O_4 nanoclusters in ferrofluid carrier. *Soft Matter* **2022**, *18*, 626–639. [CrossRef]

47. Lu, Q.; Choi, K.; Nam, J.-D.; Choi, H.J. Magnetic Polymer Composite Particles: Design and Magnetorheology. *Polymers* **2021**, *13*, 512. [CrossRef]
48. Willis, A.J.; Pernal, S.P.; Gaertner, Z.A.; Lakka, S.S.; Sabo, M.E.; Creighton, F.M.; Engelhard, H.H. Rotating magnetic nanoparticle clusters as microdevices for drug delivery. *Int. J. Nanomed.* **2020**, *15*, 4105–4123. [CrossRef]
49. Esfe, M.H.; Afrand, M.; Esfandeh, S. Investigation of the effects of various parameters on the natural convection of nanofluids in various cavities exposed to magnetic fields: A comprehensive review. *J. Therm. Anal. Calorim.* **2020**, *140*, 2055–2075. [CrossRef]
50. Ma, W.; Xu, M.; Zhong, Z.; Li, X.; Huan, Z. Closed-Loop Control for Trajectory Tracking of a Microparticle Based on Input-to-State Stability Through an Electromagnetic Manipulation System. *IEEE Access* **2020**, *8*, 46537–46545. [CrossRef]
51. van Silfhout, A.M.; Engelkamp, H.; Erné, B.H. Magnetic Sedimentation Velocities and Equilibria in Dilute Aqueous Ferrofluids. *J. Phys. Chem. B* **2020**, *124*, 7989–7998. [CrossRef]
52. Socoliuc, V.; Turcu, R. Large scale aggregation in magnetic colloids induced by high frequency magnetic fields. *J. Magn. Magn. Mater.* **2020**, *500*, 166348. [CrossRef]
53. Ganguly, S.; Margel, S. Review: Remotely controlled magneto-regulation of therapeutics from magnetoelastic gel matrices. *Biotechnol. Adv.* **2020**, *44*, 107611. [CrossRef] [PubMed]
54. Podoliak, N.; Richardson, G. Correctly computing targeting efficiency in magnetically targeted delivery from particle tracking models. *J. Magn. Magn. Mater.* **2022**, *549*, 168960. [CrossRef]
55. Russo, T.; Peluso, V.; Gloria, A.; Oliviero, O.; Rinaldi, L.; Improta, G.; de Santis, R.; D'Antò, V. Combination Design of Time-Dependent Magnetic Field and Magnetic Nanocomposites to Guide Cell Behavior. *Nanomaterials* **2020**, *10*, 577. [CrossRef]
56. Bhatt, A.; Sakai, K.; Madhyastha, R.; Murayama, M.; Madhyastha, H.; Rath, S.N. Biosynthesis and characterization of nano magnetic hydroxyapatite (nMHAp): An accelerated approach using simulated body fluid for biomedical applications. *Ceram. Int.* **2020**, *46*, 27866–27876. [CrossRef]
57. Vijayakanth, V.; Chintagumpala, K. A review on an effect of dispersant type and medium viscosity on magnetic hyperthermia of nanoparticles. *Polym. Bull.* **2022**. [CrossRef]
58. Zuluaga-Parra, J.D.; Sánchez-Valdés, S.; Ramos-deValle, L.F.; Beltrán-Ramírez, F.I.; da-Silva, L.; Ramírez-Vargas, E.; Vázquez-Rodríguez, S.; Flores-Gallardo, S.; Méndez-Nonell, J.; Valera-Zaragoza, M.; et al. A novel method for the modification of magnetite nanoparticles for the enhancement of its dispersibility in hydrophobic media. *J. Magn. Magn. Mater.* **2020**, *514*, 167169. [CrossRef]
59. Park, Y.; Cho, H. Improvement in the dispersion stability of iron oxide nanoparticles in highly concentrated brine solution using encapsulation with polymer-polymer crosslinked shells. *Adv. Powder Technol.* **2020**, *31*, 4743–4750. [CrossRef]
60. Roa-Barrantes, L.M.; Patarroyo, D.J.R. Magnetic Field Effect on the Magnetic Nanoparticles Trajectories in Pulsating Blood Flow: A Computational Model. *BioNanoScience* **2022**, *12*, 571–581. [CrossRef]
61. Salem, S.F.; Tuchin, V.V. Numerical simulation of magnetic nanoparticles in the blood stream. In Proceedings of the Saratov Fall Meeting 2019: Optical and Nano-Technologies for Biology and Medicine, Saratov, Russia, 23–27 September 2019; Volume 11457, p. 114571N. [CrossRef]
62. Badfar, H.; Motlagh, S.Y.; Sharifi, A. Numerical Simulation of Magnetic Drug Targeting to the Stenosis Vessel Using Fe_3O_4 Magnetic Nanoparticles Under the Effect of Magnetic Field of Wire. *Cardiovasc. Eng. Technol.* **2020**, *11*, 162–175. [CrossRef]
63. Kreissl, P.; Holm, C.; Weeber, R. Frequency-dependent magnetic susceptibility of magnetic nanoparticles in a polymer solution: A simulation study. *Soft Matter* **2021**, *17*, 174–183. [CrossRef] [PubMed]
64. Chen, H.-H.; Hsu, M.-H.; Lee, K.-H.; Chen, W.-Y.; Yang, S.-Y. Real-time changes in the AC magnetic susceptibility of reagents during immunomagnetic reduction assays. *AIP Adv.* **2022**, *12*, 065220. [CrossRef]
65. Labbafzadeh, M.R.; Vakili, M.H. Application of magnetic electrospun polyvinyl alcohol/collagen nanofibres for drug delivery systems. *Mol. Simul.* **2022**, *48*, 1–7. [CrossRef]
66. Harris, R.A. Simulation study on the physicochemical properties of Fe_3O_4 nanoparticles as drug delivery vehicles for dopamine replacement therapy of Parkinson's disease. *Mater. Today Commun.* **2022**, *31*, 103829. [CrossRef]
67. Cai, J.; Dao, P.; Chen, H.; Yan, L.; Li, Y.L.; Zhang, W.; Li, L.; Du, Z.; Dong, C.-Z.; Meunier, B. Ultrasmall superparamagnetic iron oxide nanoparticles-bound NIR dyes: Novel theranostic agents for Alzheimer's disease. *Dye Pigment.* **2020**, *173*, 107968. [CrossRef]
68. Sadeghi-Goughari, M.; Jeon, S.; Kwon, H.-J. Magnetic nanoparticles-enhanced focused ultrasound heating: Size effect, mechanism, and performance analysis. *Nanotechnology* **2020**, *31*, 245101. [CrossRef]
69. Contreras-Montoya, R.; Jabalera, Y.; Blanco, V.; Cuerva, J.M.; Jimenez-Lopez, C.; Alvarez De Cienfuegos, L. Lysine as Size-Control Additive in a Bioinspired Synthesis of Pure Superparamagnetic Magnetite Nanoparticles. *Cryst. Growth Des.* **2020**, *20*, 533–542. [CrossRef]
70. Craciunescu, I.; Palade, P.; Iacob, N.; Ispas, G.M.; Stanciu, A.E.; Kuncser, V.; Turcu, R.P. High Performance Functionalized Magnetic Nanoparticles with Tailored Sizes and Shapes for Localized Hyperthermia Applications. *J. Phys. Chem. C* **2021**, *125*, 11132–11146. [CrossRef]
71. Islam, K.; Haque, M.; Kumar, A.; Hoq, A.; Hyder, F.; Hoque, S.M. Manganese ferrite nanoparticles ($MnFe_2O_4$): Size dependence for hyperthermia and negative/positive contrast enhancement in MRI. *Nanomaterials* **2020**, *10*, 2297. [CrossRef]
72. Malekie, S.; Rajabi, A. Study on Fe_3O_4 Magnetic Nanoparticles Size Effect on Temperature Distribution of Tumor in Hyperthermia: A Finite Element Method. *Int. J. Nanosci. Nanotechnol.* **2020**, *16*, 181–188.

73. Bilmez, B.; Toker, M.Ö.; Toker, O.; İçelli, O. Monte Carlo study on size-dependent radiation enhancement effects of spinel ferrite nanoparticles. *Radiat. Phys. Chem.* **2022**, *199*, 110364. [CrossRef]
74. Das, R.; Masa, J.; Kalappattil, V.; Nemati, Z.; Rodrigo, I.; Garaio, E.; García, J.; Phan, M.-H.; Srikanth, H. Iron Oxide Nanorings and Nanotubes for Magnetic Hyperthermia: The Problem of Intraparticle Interactions. *Nanomaterials* **2021**, *11*, 1380. [CrossRef] [PubMed]
75. van Silfhout, A.M.; Engelkamp, H.; Erné, B.H. Colloidal Stability of Aqueous Ferrofluids at 10 T. *J. Phys. Chem. Lett.* **2020**, *11*, 5908–5912. [CrossRef] [PubMed]
76. Pilati, V.; Gomide, G.; Gomes, R.C.; Goya, G.F.; Depeyrot, J. Colloidal Stability and Concentration Effects on Nanoparticle Heat Delivery for Magnetic Fluid Hyperthermia. *Langmuir* **2021**, *37*, 1129–1140. [CrossRef] [PubMed]
77. Castro, L.L.; Amorim, C.C.C.; Miranda, J.P.V.; Cassiano, T.S.A.; Paula, F.L.O. The role of small separation interactions in ferrofluid structure. *Colloids Surf. A* **2022**, *635*, 128082. [CrossRef]
78. Riedl, J.C.; Sarkar, M.; Fiuza, T.; Cousin, F.; Depeyrot, J.; Dubois, E.; Mériguet, G.; Perzynski, R.; Peyre, V. Design of concentrated colloidal dispersions of iron oxide nanoparticles in ionic liquids: Structure and thermal stability from 25 to 200 °C. *J. Colloid Interface Sci.* **2022**, *607*, 584–594. [CrossRef]
79. Boskovic, M.; Fabián, M.; Vranjes-Djuric, S.; Antic, B. Magnetic nano- and micro-particles based on Gd-substituted magnetite with improved colloidal stability. *Appl. Phys. A Mater. Sci. Process.* **2021**, *127*, 372. [CrossRef]
80. Aguilar, N.M.; Perez-Aguilar, J.M.; González-Coronel, V.J.; Moro, J.G.S.; Sanchez-Gaytan, B.L. Polymers as Versatile Players in the Stabilization, Capping, and Design of Inorganic Nanostructures. *ACS Omega* **2021**, *6*, 35196–35203. [CrossRef]
81. Mahin, J.; Franck, C.O.; Fanslau, L.; Patra, H.K.; Mantle, M.D.; Fruk, L.; Torrente-Murciano, L. Green, scalable, low cost and reproducible flow synthesis of biocompatible PEG-functionalized iron oxide nanoparticles. *React. Chem. Eng.* **2021**, *6*, 1961–1973. [CrossRef]
82. Parham, N.; Panahi, H.A.; Feizbakhsh, A.; Moniri, E. Synthesis of PEGylated superparamagnetic dendrimers and their applications as a drug delivery system. *Polym. Adv. Technol.* **2021**, *32*, 1568–1578. [CrossRef]
83. Taghizadeh, A.; Pesyan, N.N.; Alamgholiloo, H.; Sheykhaghaei, G. Immobilization of Nickel on Kryptofix 222 Modified Fe_3O_4 @PEG Core-Shell Nanosphere for the Clean Synthesis of 2-Aryl-2,3-dihydroquinazolin-4(1 *H*)-ones. *Appl. Organomet. Chem.* **2022**, e6787. [CrossRef]
84. Da, X.; Li, R.; Li, X.; Lu, Y.; Gu, F.; Liu, Y. Synthesis and characterization of PEG coated hollow Fe_3O_4 magnetic nanoparticles as a drug carrier. *Mater. Lett.* **2022**, *309*, 131357. [CrossRef]
85. Shi, D.; Beasock, D.; Fessler, A.; Szebeni, J.; Ljubimova, J.Y.; Afonin, K.A.; Dobrovolskaia, M.A. To PEGylate or not to PEGylate: Immunological properties of nanomedicine's most popular component, polyethylene glycol and its alternatives. *Adv. Drug Deliv. Rev.* **2022**, *180*, 114079. [CrossRef] [PubMed]
86. Karaagac, O.; Köçkar, H. Improvement of the saturation magnetization of PEG coated superparamagnetic iron oxide nanoparticles. *J. Magn. Magn. Mater.* **2022**, *551*, 169140. [CrossRef]
87. Mohammadi, M.A.; Asghari, S.; Aslibeiki, B. Surface modified Fe_3O_4 nanoparticles: A cross-linked polyethylene glycol coating using plasma treatment. *Surf. Interfaces* **2021**, *25*, 101271. [CrossRef]
88. Suciu, M.; Mirescu, C.; Crăciunescu, I.; Macavei, S.G.; Leoștean, C.; Ştefan, R.; Olar, L.E.; Tripon, S.-C.; Ciorîță, A.; Barbu-Tudoran, L. In vivo distribution of poly(Ethylene glycol) functionalized iron oxide nanoclusters: An ultrastructural study. *Nanomaterials* **2021**, *11*, 2184. [CrossRef]
89. Chroni, A.; Forys, A.; Trzebicka, B.; Alemayehu, A.; Tyrpekl, V.; Pispas, S. Poly[oligo(ethylene glycol) methacrylate]-bpoly[(vinyl benzyl trimethylammonium chloride)] based multifunctional hybrid nanostructures encapsulating magnetic nanoparticles and DNA. *Polymers* **2020**, *12*, 1283. [CrossRef] [PubMed]
90. Akkurt, N.; Altan, C.L.; Sarac, M.F. Continuous Flow–Assisted Polyol Synthesis of Citric Acid Functionalized Iron Oxide Nanoparticles. *J. Supercond. Nov. Magn.* **2022**, *35*, 615–623. [CrossRef]
91. Răcuciu, M.; Tecucianu, A.; Oancea, S. Impact of Magnetite Nanoparticles Coated with Aspartic Acid on the Growth, Antioxidant Enzymes Activity and Chlorophyll Content of Maize. *Antioxidants* **2022**, *11*, 1193. [CrossRef]
92. Li, K.; Dugas, P.-Y.; Lansalot, M.; Bourgeat-Lami, E. Synthesis of Iron Oxide-Armored Latex Particles by Pickering Emulsion Polymerization Using 2-Acrylamido-2-methyl-1-propane Sulfonic Acid as an Auxiliary Comonomer. *Macromolecules* **2022**, *55*, 4284–4296. [CrossRef]
93. Sood, A.; Arora, V.; Kumari, S.; Sarkar, A.; Kumaran, S.S.; Chaturvedi, S.; Jain, T.K.; Agrawal, G. Imaging application and radiosensitivity enhancement of pectin decorated multifunctional magnetic nanoparticles in cancer therapy. *Int. J. Biol. Macromol.* **2021**, *189*, 443. [CrossRef] [PubMed]
94. Viratchaiboott, N.; Sakunpongpitiporn, P.; Niamlang, S.; Sirivat, A. Release of 5-FU loaded pectin/Fe_3O_4 from porous PBSA matrix under magnetic and electric fields. *J. Alloys Compd.* **2022**, *906*, 164239. [CrossRef]
95. Rozhina, E.; Danilushkina, A.; Akhatova, F.; Fakhrullin, R.; Rozhin, A.; Batasheva, S. Biocompatibility of magnetic nanoparticles coating with polycations using A549 cells. *J. Biotechnol.* **2021**, *325*, 25–34. [CrossRef] [PubMed]
96. Nowak-Jary, J.; Defort, A.; Kozioł, J.J. Modified Physicochemical Properties of Acidic Model Drugs Immobilized on Fe_3O_4Magnetic Iron Oxide Nanoparticles. *Pharm. Chem. J.* **2020**, *53*, 1025–1035. [CrossRef]
97. Bealer, E.J.; Kavetsky, K.; Dutko, S.; Lofland, S.; Hu, X. Protein and polysaccharide-based magnetic composite materials for medical applications. *Int. J. Mol. Sci.* **2020**, *21*, 186. [CrossRef] [PubMed]

98. Sharifianjazi, F.; Irani, M.; Esmaeilkhanian, A.; Bazli, L.; Asl, M.S.; Jang, H.W.; Kim, S.Y.; Ramakrishna, S.; Shokouhimehr, M.; Varma, R.S. Polymer incorporated magnetic nanoparticles: Applications for magnetoresponsive targeted drug delivery. *Mater. Sci. Eng. B Solid-State Mater. Adv. Technol.* **2021**, *272*, 115358. [CrossRef]
99. Sang-Mook, Y.; Jin-Sung, P.; Ke, L.; Ki-Baek, J.; Joy, A.H.; Young-Rok, K. Modulation of the peroxidase-like activity of iron oxide nanoparticles by surface functionalization with polysaccharides and its application for the detection of glutathione. *Carbohydr. Polym.* **2021**, *267*, 118164.
100. Guzmán-Rocha, D.A.; Córdova-Fraga, T.; Bernal-Alvarado, J.J.; López, Z.; Cholico, F.A.; Quintero, L.H.; Paz, J.A.; Cano, M.E. A Ferrofluid with High Specific Absorption Rate Prepared in a Single Step Using a Biopolymer. *Materials* **2022**, *15*, 788. [CrossRef]
101. Laborie, E.; Le-Minh, V.; Mai, T.D.; Ammar, M.; Taverna, M.; Smadja, C. Analytical methods of antibody surface coverage and orientation on bio-functionalized magnetic beads: Application to immunocapture of TNF-α. *Anal. Bioanal. Chem.* **2021**, *413*, 6425. [CrossRef]
102. Zhou, Y.; Que, K.-T.; Tang, H.-M.; Zhang, P.; Fu, Q.-M.; Liu, Z.-J. Anti CD206 antibody conjugated Fe_3O_4 based PLGA nanoparticles selectively promote tumor associated macrophages to polarize to the pro inflammatory subtype. *Oncol. Lett.* **2020**, *20*, 12161. [CrossRef]
103. He, C.; Zeng, W.; Su, Y.; Sun, R.; Xiao, Y.; Zhang, B.; Liu, W.; Wang, R.; Zhang, X.; Chen, C. Microfluidic-based fabrication and characterization of drug-loaded PLGA magnetic microspheres with tunable shell thickness. *Drug Deliv.* **2021**, *28*, 692–699. [CrossRef] [PubMed]
104. Zumaya, A.L.V.; Martynek, D.; Bautkinová, T.; Šoóš, M.; Ulbrich, P.; Raquez, J.-M.; Dendisová, M.; Merna, J.; Vilčáková, J.; Kopecký, D.; et al. Self-assembly of poly(L-lactide-co-glycolide) and magnetic nanoparticles into nanoclusters for controlled drug delivery. *Eur. Polym. J.* **2020**, *133*, 109795. [CrossRef]
105. Kuger, L.; Arlt, C.-R.; Franzreb, M. Magnetic/flow controlled continuous size fractionation of magnetic nanoparticles using simulated moving bed chromatography. *Talanta* **2022**, *240*, 123160. [CrossRef] [PubMed]
106. Aghazadeh, M.; Ganjali, M.R.; Morad, M.M.; Gharailou, D. Saccharide-capped superparamagnetic copper cations-doped magnetite nanoparticles for biomedical applications: A novel and simple synthesis procedure, in-situ surface engineering and characterization. *Curr. Nanosci.* **2020**, *16*, 770–778. [CrossRef]
107. Metaxa, A.-F.; Vrontaki, E.; Efthimiadou, E.K.; Mavromoustakos, T. Drug Delivery Systems Based on Modified Polysaccharides: Synthesis and Characterization. *Methods Mol. Biol.* **2021**, *2207*, 151–161. [CrossRef]
108. Rajabzadeh, M.; Najdi, N.; Zarei, Z.; Khalifeh, R. CuI Immobilized on Tricationic Ionic Liquid Anchored on Functionalized Magnetic Hydrotalcite (Fe_3O_4/HT-TIL-CuI) as a Novel, Magnetic and Efficient Nanocatalyst for Ullmann-Type C–N Coupling Reaction. *J. Inorg. Organomet. Polym. Mater.* **2022**, *32*, 2696–2711. [CrossRef]
109. Ghasemi-Ghahsareh, A.; Safaei-Ghomi, J.; Oboudatian, H.S. Supported l-tryptophan on Fe_3O_4@SiO_2 as an efficient and magnetically separable catalyst for one-pot construction of spiro[indene-2,2′-naphthalene]-4′-carbonitrile derivatives. *RSC Adv.* **2022**, *12*, 1319–1330. [CrossRef] [PubMed]
110. Nikoofar, K.; Arian, Z.; Djahaniani, H. Novel $AlCl_3$@nano Fe_3O_4-SiO_2: A benign multi-layer magnetite nanocatalyst for the three-component one-pot synthesis of spiro[benzochromeno [2,3-d]pyrimidin-indolines]. *Inorg. Nano-Met. Chem.* **2022**, *52*, 365–374. [CrossRef]
111. Berret, J.-F.; Graillot, A. Versatile Coating Platform for Metal Oxide Nanoparticles: Applications to Materials and Biological Science. *Langmuir* **2022**, *18*, 5323–5338. [CrossRef]
112. Pinelli, F.; Perale, G.; Rossi, F. Coating and functionalization strategies for nanogels and nanoparticles for selective drug delivery. *Gels* **2020**, *6*, 6. [CrossRef]
113. Aurélio, D.; Mikšátko, J.; Veverka, M.; Michlová, M.; Kalbáč, M.; Vejpravová, J. Thermal traits of MNPs under high-frequency magnetic fields: Disentangling the effect of size and coating. *Nanomaterials* **2021**, *11*, 797. [CrossRef] [PubMed]
114. Gupta, P.; Tomar, R.; Sahni, M.; Chauhan, S. Cobalt, nickel and copper doped non-stoichiometric cadmium gallate as a prominent magnetic and photocatalytic material. *Chem. Phys.* **2022**, *554*, 111419. [CrossRef]
115. Hezam, F.A.; Rajeh, A.; Nur, O.; Mustafa, M.A. Synthesis and physical properties of spinel ferrites/MWCNTs hybrids nanocomposites for energy storage and photocatalytic applications. *Phys. B Condens. Matter.* **2020**, *596*, 412389. [CrossRef]
116. Lei, Y.; Zhang, X.; Meng, X.; Wang, Z. The preparation of core–shell Fe_3O_4@SiO_2 magnetic nanoparticles with different surface carboxyl densities and their application in the removal of methylene blue. *Inorg. Chem. Commun.* **2022**, *139*, 109381. [CrossRef]
117. Mubarak, M.F.; Selim, H.; Elshypany, R. Hybrid magnetic core–shell TiO_2@$CoFe_3O_4$ composite towards visible light-driven photodegradation of Methylene blue dye and the heavy metal adsorption: Isotherm and kinetic study. *J. Environ. Heal. Sci. Eng.* **2022**, *20*, 265–280. [CrossRef]
118. Li, M.; Zhang, H.; Hou, Y.; Wang, X.; Xue, C.; Li, W.; Cai, K.; Zhao, Y.; Luo, Z. State-of-the-art iron-based nanozymes for biocatalytic tumor therapy. *Nanoscale Horiz.* **2020**, *5*, 202–217. [CrossRef]
119. da Silva, N.M.; Bajgiran, K.R.; Melvin, A.T.; Dooley, K.M.; Dorman, J.A. Direct Probing of Fe_3O_4 Nanoparticle Surface Temperatures during Magnetic Heating: Implications for Induction Catalysis. *ACS Appl. Nano Mater.* **2021**, *4*, 13778–13787. [CrossRef]
120. da Silva, R.T.P.; de Barros, H.R.; Sandrini, D.M.F.; de Torresi, S.I.C. Stimuli-Responsive Regulation of Biocatalysis through Metallic Nanoparticle Interaction. *Bioconjugate Chem.* **2021**, *33*, 53–66. [CrossRef]
121. Kumar, R.; Mondal, K.; Panda, P.K.; Kaushik, A.; Abolhassani, R.; Ahuja, R.; Rubahn, H.-G.; Mishra, Y.K. Core-shell nanostructures: Perspectives towards drug delivery applications. *J. Mater. Chem. B* **2020**, *8*, 8992–9027. [CrossRef]

122. Wankar, J.; Kotla, N.G.; Gera, S.; Rasala, S.; Pandit, A.; Rochev, Y.A. Recent Advances in Host–Guest Self-Assembled Cyclodextrin Carriers: Implications for Responsive Drug Delivery and Biomedical Engineering. *Adv. Funct. Mater.* **2020**, *30*, 1909049. [CrossRef]
123. Fatimah, I.; Fadillah, G.; Purwiandono, G.; Sahroni, I.; Purwaningsih, D.; Riantana, H.; Avif, A.N.; Sagadevan, S. Magnetic-silica nanocomposites and the functionalized forms for environment and medical applications: A review. *Inorg. Chem. Commun.* **2022**, *137*, 109213. [CrossRef]
124. Mehta, S.; Suresh, A.; Nayak, Y.; Narayan, R.; Nayak, U.Y. Hybrid nanostructures: Versatile systems for biomedical applications. *Coord. Chem. Rev.* **2022**, *460*, 214482. [CrossRef]
125. Taheri-Ledari, R.; Rahimi, J.; Maleki, A. Method screening for conjugation of the small molecules onto the vinyl-coated Fe_3O_4/silica nanoparticles: Highlighting the efficiency of ultrasonication. *Mater. Res. Express* **2020**, *7*, 015067. [CrossRef]
126. Stergar, J.; Maver, U.; Bele, M.; Gradišnik, L.; Kristl, M.; Ban, I. NiCu-silica nanoparticles as a potential drug delivery system. *J. Sol-Gel Sci. Technol.* **2022**, *101*, 493–504. [CrossRef]
127. Ali, T.H.; Mandal, A.M.; Heidelberg, T.; Hussen, R.S.D. Sugar based cationic magnetic core-shell silica nanoparticles for nucleic acid extraction. *RSC Adv.* **2022**, *12*, 13566–13579. [CrossRef]
128. Demirdogen, R.E.; Emen, F.M.; Karaçolak, A.I.; Kılıç, D.; Kutlu, E.; Meral, O. Preparation of novel $CaMoO_4$:Eu^{3+}-MCM-41 nanocomposites and their applications and monitoring as drug release systems. *J. Drug Deliv. Sci. Technol.* **2021**, *66*, 102792. [CrossRef]
129. Goderski, S.; Kanno, S.; Yoshihara, K.; Komiya, H.; Goto, K.; Tanaka, T.; Kawaguchi, S.; Ishii, A.; Shimoyama, J.-I.; Hasegawa, M.; et al. Lanthanide Luminescence Enhancement of Core-Shell Magnetite-SiO_2Nanoparticles Covered with Chain-Structured Helical Eu/Tb Complexes. *ACS Omega* **2020**, *5*, 32930–32938. [CrossRef]
130. Sanoh, N.C.; Salazar, G.M.; Penaloza, D.P. Magnetic biopolymeric hydrogel composite material with self-healing attribute. *Biointerface Res. Appl. Chem.* **2021**, *11*, 14881–14888. [CrossRef]
131. Asghari, S.; Mohammadi, M.A.; Julaei, R.; Taheri, R.A. Surface Modification of Superparamagnetic Iron Oxide Nanoparticles by Argon Plasma for Medical Applications. *J. Appl. Biotechnol. Rep.* **2022**, *9*, 563–568. [CrossRef]
132. Ahmad, F.; Salem-Bekhit, M.M.; Khan, F.; Alshehri, S.; Khan, A.; Ghoneim, M.M.; Wu, H.-F.; Taha, E.I.; Elbagory, I. Unique Properties of Surface-Functionalized Nanoparticles for Bio-Application: Functionalization Mechanisms and Importance in Application. *Nanomaterials* **2022**, *12*, 1333. [CrossRef]
133. Hupfeld, T.; Salamon, S.; Landers, J.; Sommereyns, A.; Doñate-Buendía, C.; Schmidt, J.; Wende, H.; Schmidt, M.; Barcikowski, S.; Gökce, B. 3D printing of magnetic parts by laser powder bed fusion of iron oxide nanoparticle functionalized polyamide powders. *J. Mater. Chem. C* **2020**, *8*, 12204–12217. [CrossRef]
134. Pavón-Hernández, A.I.; Rodríguez-Velázquez, E.; Alatorre-Meda, M.; Elizalde Galindo, J.T.; Paraguay-Delgado, F.; Tirado-Guízar, A.; Pina-Luis, G. Magnetic nanocomposite with fluorescence enhancement effect based on amino acid coated-Fe_3O_4 functionalized with quantum dots. *Mater. Chem. Phys.* **2020**, *251*, 123082. [CrossRef]
135. Jambhulkar, S.; Xu, W.; Ravichandran, D.; Prakash, J.; Kannan, A.N.M.; Song, K. Scalable Alignment and Selective Deposition of Nanoparticles for Multifunctional Sensor Applications. *Nano Lett.* **2020**, *20*, 3199–3206. [CrossRef]
136. Russo, T.; De Santis, R.; Peluso, V.; Gloria, A. Multifunctional Bioactive Magnetic Scaffolds with Tailored Features for Bone Tissue Engineering. In *Magnetic Nanoparticles in Human Health and Medicine*; Wiley: Hoboken, NJ, USA, 2021; pp. 87–112. [CrossRef]
137. Aslam, H.; Shukrullah, S.; Naz, M.Y.; Fatima, H.; Ullah, S.; Al-Sehemi, A.G. Multifunctional Magnetic Nanomedicine Drug Delivery and Imaging-Based Diagnostic Systems. *Part. Part. Syst. Charact.* **2021**, *38*, 2100179. [CrossRef]
138. Al-Terke, H.H.; Latikka, M.; Timonen, J.V.I.; Vékás, L.; Paananen, A.; Joensuu, J.; Ras, R.H.A. Functional Magnetic Microdroplets for Antibody Extraction. *Adv. Mater. Interfaces* **2022**, *9*, 2101317.
139. Besenhard, M.O.; Panariello, L.; Kiefer, C.; LaGrow, A.P.; Storozhuk, L.; Perton, F.; Begin, S.; Mertz, D.; Thanh, N.T.K.; Gavriilidis, A. Small iron oxide nanoparticles as MRI T1 contrast agent: Scalable inexpensive water-based synthesis using a flow reactor. *Nanoscale* **2021**, *13*, 8795–8805.
140. Gradinaru, L.M.; Mandru, M.B.; Drobota, M.; Aflori, M.; Butnaru, M.; Spiridon, M.; Doroftei, F.; Aradoaei, M.; Ciobanu, R.C.; Vlad, S. Composite materials based on iron oxide nanoparticles and polyurethane for improving the quality of mri. *Polymers* **2021**, *13*, 4316. [CrossRef]
141. Harvell-Smith, S.; Tung, L.D.; Thanh, N.T.K. Magnetic particle imaging: Tracer development and the biomedical applications of a radiation-free, sensitive, and quantitative imaging modality. *Nanoscale* **2021**, *14*, 3658–3697. [CrossRef]
142. Svenskaya, Y.; Garello, F.; Lengert, E.; Kozlova, A.; Verkhovskii, R.; Bitonto, V.; Ruggiero, M.R.; German, S.; Gorin, D.; Terreno, E. Biodegradable polyelectrolyte/magnetite capsules for MR imaging and magnetic targeting of tumors. *Nanotheranostics* **2021**, *5*, 362–377. [CrossRef] [PubMed]
143. Rosch, E.L.; Zhong, J.; Lak, A.; Liu, Z.; Etzkorn, M.; Schilling, M.; Ludwig, F.; Viereck, T.; Lalkens, B. Point-of-need detection of pathogen-specific nucleic acid targets using magnetic particle spectroscopy. *Biosens. Bioelectron.* **2021**, *192*, 113536.
144. Bruno, F.; Granata, V.; Bellisari, F.C.; Sgalambro, F.; Tommasino, E.; Palumbo, P.; Arrigoni, F.; Cozzi, D.; Grassi, F.; Brunese, M.C.; et al. Advanced Magnetic Resonance Imaging (MRI) Techniques: Technical Principles and Applications in Nanomedicine. *Cancers* **2022**, *14*, 1626. [CrossRef]
145. Zhao, Z.; Li, M.; Zeng, J.; Huo, L.; Liu, K.; Wei, R.; Ni, K.; Gao, J. Recent advances in engineering iron oxide nanoparticles for effective magnetic resonance imaging. *Bioact. Mater.* **2022**, *12*, 214–245. [CrossRef]

146. Wu, K.; Liu, J.; Saha, R.; Ma, B.; Su, D.; Peng, C.; Sun, J.; Wang, J.-P. Irregularly Shaped Iron Nitride Nanoparticles as a Potential Candidate for Biomedical Applications: From Synthesis to Characterization. *ACS Omega* **2020**, *5*, 11756–11767. [CrossRef]
147. Balk, M.; Haus, T.; Band, J.; Unterweger, H.; Schreiber, E.; Friedrich, R.P.; Alexiou, C.; Gostian, A.-O. Cellular spion uptake and toxicity in various head and neck cancer cell lines. *Nanomaterials* **2021**, *11*, 726. [CrossRef]
148. Sokolov, A.E.; Ivanova, O.S.; Fedorov, A.S.; Kovaleva, E.A.; Vysotin, M.A.; Lin, C.-R.; Ovchinnikov, S.G. Why the Magnetite–Gold Core–Shell Nanoparticles Are Not Quite Good and How to Improve Them. *Phys. Solid State* **2021**, *63*, 1536–1540. [CrossRef]
149. Bhatia, P.; Verma, S.S.; Sinha, M.M. Magneto-plasmonic Co@M (M = Au/Ag/Au-Ag) core-shell nanoparticles for biological imaging and therapeutics. *J. Quant. Spectrosc. Radiat. Transf.* **2020**, *251*, 107095. [CrossRef]
150. Wei, D.-H.; Lin, T.-K.; Liang, Y.-C.; Chang, H.-W. Formation and Application of Core–Shell of FePt-Au Magnetic–Plasmonic Nanoparticles. *Front. Chem.* **2021**, *9*, 653718. [CrossRef]
151. Mohajer, F.; Ziarani, G.M.; Badiei, A. New advances on Au-magnetic organic hybrid core-shells in MRI, CT imaging, and drug delivery. *RSC Adv.* **2021**, *11*, 6517–6525. [CrossRef] [PubMed]
152. Kuhn, J.; Papanastasiou, G.; Tai, C.-W.; Moran, C.M.; Jansen, M.A.; Tavares, A.A.S.; Lennen, R.J.; Corral, C.A.; Wang, C.; Thomson, A.J.W.; et al. Tri-modal imaging of gold-dotted magnetic nanoparticles for magnetic resonance imaging, computed tomography and intravascular ultrasound: An in vitro study. *Nanomedicine* **2020**, *15*, 2433–2445. [CrossRef]
153. Iancu, S.D.; Albu, C.; Chiriac, L.; Moldovan, R.; Stefancu, A.; Moisoiu, V.; Coman, V.; Szabo, L.; Leopold, N.; Bálint, Z. Assessment of gold-coated iron oxide nanoparticles as negative T2 contrast agent in small animal MRI studies. *Int. J. Nanomed.* **2020**, *15*, 4811–4824. [CrossRef]
154. Dheyab, M.A.; Aziz, A.A.; Jameel, M.S.; Noqta, O.A.; Mehrdel, B. Synthesis and coating methods of biocompatible iron oxide/gold nanoparticle and nanocomposite for biomedical applications. *Chin. J. Phys.* **2020**, *64*, 305–325. [CrossRef]
155. Schwaminger, S.P.; Bauer, D.; Fraga-García, P. Gold-iron oxide nanohybrids: Insights into colloidal stability and surface-enhanced Raman detection. *Nanoscale Adv.* **2021**, *3*, 6438. [CrossRef]
156. Chaturvedi, A.; Pranjali, P.; Meher, M.K.; Raj, R.; Basak, M.; Singh, R.K.; Poluri, K.M.; Kumar, D.; Guleria, A. In vitro and ex vivo relaxometric properties of ethylene glycol coated gadolinium oxide nanoparticles for potential use as contrast agents in magnetic resonance imaging. *J. Appl. Phys.* **2020**, *128*, 034903. [CrossRef]
157. Forte, E.; Fiorenza, D.; Torino, E.; Di Polidoro, A.C.; Cavaliere, C.; Netti, P.A.; Salvatore, M.; Aiello, M. Radiolabeled PET/MRI nanoparticles for tumor imaging. *J. Clin. Med.* **2020**, *9*, 89. [CrossRef]
158. Belderbos, S.; González-Gómez, M.A.; Cleeren, F.; Wouters, J.; Piñeiro, Y.; Deroose, C.M.; Coosemans, A.; Gsell, W.; Bormans, G.; Rivas, J.; et al. Simultaneous in vivo PET/MRI using fluorine-18 labeled Fe_3O_4@$Al(OH)_3$ nanoparticles: Comparison of nanoparticle and nanoparticle-labeled stem cell distribution. *EJNMMI Res.* **2020**, *10*, 73. [CrossRef]
159. Yan, Q.; Dong, X.; Xie, R.; Xu, X.; Wang, X.; Zhang, K.; Xia, J.; Ling, J.; Zhou, F.; Sun, J. Preparation of Mn^{2+}@PolyDOPA-b-polysarcosine micelle as MRI contrast agent with high longitudinal relaxivity. *J. Macromol. Sci. Part A Pure Appl. Chem.* **2021**, *58*, 175–181. [CrossRef]
160. Ramazanov, M.; Karimova, A.; Shirinova, H. Magnetism for drug delivery, mri and hyperthermia applications: A review. *Biointerface Res. Appl. Chem.* **2021**, *11*, 8654–8668. [CrossRef]
161. Varghese, R.; Vijay, N.; Dalvi, Y.B. Magnetic Nanoparticles for Image-Guided Drug Delivery. In *Magnetic Nanoparticles*; Springer: Singapore, 2021; pp. 45–71. [CrossRef]
162. Basina, G.; Diamantopoulos, G.; Devlin, E.; Psycharis, V.; Alhassan, S.M.; Pissas, M.; Hadjipanayis, G.; Tomou, A.; Bouras, A.; Hadjipanayis, C.; et al. LAPONITE®nanodisk-"decorated" Fe_3O_4 nanoparticles: A biocompatible nano-hybrid with ultrafast magnetic hyperthermia and MRI contrast agent ability. *J. Mater. Chem. B* **2022**, *10*, 4935. [CrossRef]
163. Salunkhe, A.B.; Khot, V.M.; Patil, S.I.; Tofail, S.A.M.; Bauer, J.; Thorat, N.D. MRI Guided Magneto-chemotherapy with High-Magnetic-Moment Iron Oxide Nanoparticles for Cancer Theranostics. *ACS Appl. Bio Mater.* **2020**, *3*, 2305–2313. [CrossRef]
164. Antal, I.; Strbak, O.; Khmara, I.; Koneracka, M.; Kubovcikova, M.; Zavisova, V.; Kmetova, M.; Baranovicova, E.; Dobrota, D. MRI relaxivity changes of the magnetic nanoparticles induced by different amino acid coatings. *Nanomaterials* **2020**, *10*, 394. [CrossRef]
165. Nagornyi, A.V.; Shlapa, Y.; Avdeev, M.V.; Solopan, S.O.; Belous, A.G.; Shulenina, A.V.; Ivankov, O.I.; Bulavin, L.A. Structural characterization of aqueous magnetic fluids with nanomagnetite of different origin stabilized by sodium oleate. *J. Mol. Liq.* **2020**, *312*, 113430. [CrossRef]
166. Shaumbwa, V.R.; Liu, D.; Archer, B.; Li, J.; Su, F. Preparation and application of magnetic chitosan in environmental remediation and other fields: A review. *J. Appl. Polym. Sci.* **2021**, *138*, 51241. [CrossRef]
167. Arias, L.S.; Pessan, J.P.; de Souza, F.N.N.; Lima, B.H.R.; de Camargo, E.R.; Ramage, G.; Delbem, A.C.B.; Monteiro, D.R. Novel nanocarrier of miconazole based on chitosan-coated iron oxide nanoparticles as a nanotherapy to fight Candida biofilms. *Colloids Surf. B Biointerfaces* **2020**, *192*, 111080. [CrossRef] [PubMed]
168. Bindu, V.U.; Mohanan, P.V. Thermal deactivation of α-amylase immobilized magnetic chitosan and its modified forms: A kinetic and thermodynamic study. *Carbohydr. Res.* **2020**, *498*, 108185. [CrossRef]
169. Balan, V.; Malihin, S.; Verestiuc, L. Chitosan-based systems for theranostic applications. In *Functional Chitosan: Drug Delivery and Biomedical Applications*; Springer: Singapore, 2020; pp. 343–384. [CrossRef]
170. Lawai, V.; Ngaini, Z. Chitosan magnetic nanocomposites for gene delivery. In *Polysaccharide-Based Nanocomposites for Gene Delivery and Tissue Engineering*; Woodhead Publishing: Cambridge, UK, 2021; pp. 279–294. [CrossRef]

171. Pop, N.L.; Nan, A.; Urda-Cimpean, A.E.; Florea, A.; Toma, V.A.; Moldovan, R.; Decea, N.; Mitrea, D.R.; Orasan, R. Chitosan functionalized magnetic nanoparticles to provide neural regeneration and recovery after experimental model induced peripheral nerve injury. *Biomolecules* **2021**, *11*, 676. [CrossRef]
172. Mohammad Gholiha, H.; Ehsani, M.; Saeidi, A.; Ghadami, A.; Alizadeh, N. Magnetic dual-responsive semi-IPN nanogels based on chitosan/PNVCL and study on BSA release behavior. *Prog. Biomater.* **2021**, *10*, 173–183. [CrossRef]
173. Borges, M.M.C.; Pires, B.C.; Vieira, S.S.; Borges, K.B.; Guimarães, L.G.D.L. Magnetic and pH responsive composite hydrogel-based on poly(2-(diethylamino)ethyl methacrylate)/chitosan for fipronil removal from aqueous medium. *React. Funct. Polym.* **2021**, *168*, 105050. [CrossRef]
174. González-Martínez, E.; Pérez, A.G.; González-Martínez, D.A.; Águila, C.R.D.; Urbina, E.C.; Ramírez, D.U.; Yee-Madeira, H. Chitosan-coated magnetic nanoparticles; exploring their potentialities for DNA and Cu(II) recovery. *Inorg. Nano-Met. Chem.* **2021**, *51*, 1098–1107. [CrossRef]
175. Vaewbundit, S.; Siriphannon, P. Soft solution growth of magnetite-maghemite nanocrystals in crosslinked chitosan templates and their superparamagnetic properties. *Nanocomposites* **2022**, *8*, 142–154. [CrossRef]
176. Bianchetti, E.; Di Valentin, C. Mechanism of spin ordering in Fe_3O_4 nanoparticles by surface coating with organic acids. *Mater. Today Nano* **2022**, *17*, 100169. [CrossRef]
177. Yıldırım, E.; Arıkan, B.; Yücel, O.; Çakır, O.; Kara, N.T.; İyim, T.B.; Gürdağ, G.; Emik, S. Synthesis and characterization of amino functional poly(acrylamide) coated Fe_3O_4 nanoparticles and investigation of their potential usage in DNA isolation. *Chem. Pap.* **2022**, *76*, 5747–5759. [CrossRef]
178. Yan, Y.-Q.; Wang, H.; Zhao, Y. Radiolabeled peptide probe for tumor imaging. *Chin. Chem. Lett.* **2022**, *33*, 3361–3370. [CrossRef]
179. Yilmaz, S.; Ichedef, C.; Karatay, K.B.; Teksöz, S. Polymer coated iron nanoparticles: Radiolabeling & in vitro studies. *Curr. Radiopharm.* **2021**, *14*, 37–45. [CrossRef]
180. Shi, S.; Chen, Y.; Yao, X. In Vivo Computing Strategies for Tumor Sensitization and Targeting. *IEEE Trans. Cybern.* **2022**, *52*, 4970–4980. [CrossRef]
181. Zhang, Y.; Cao, J.; Yuan, Z. Strategies and challenges to improve the performance of tumor-associated active targeting. *J. Mater. Chem. B* **2020**, *8*, 3959–3971. [CrossRef] [PubMed]
182. Qi, S.; Wang, X.; Chang, K.; Shen, W.; Yu, G.; Du, J. The bright future of nanotechnology in lymphatic system imaging and imaging-guided surgery. *J. Nanobiotechnol.* **2022**, *20*, 24. [CrossRef]
183. Kubelick, K.P.; Mehrmohammadi, M. Magnetic particles in motion: Magneto-motive imaging and sensing. *Theranostics* **2022**, *12*, 1783–1799. [CrossRef] [PubMed]
184. Grudzinski, I.P.; Bystrzejewski, M.; Bogorodzki, P.; Cieszanowski, A.; Szeszkowski, W.; Poplawska, M.; Bamburowicz-Klimkowska, M. Comprehensive magnetic resonance characteristics of carbon-encapsulated iron nanoparticles: A new frontier for the core-shell–type contrast agents. *J. Nanoparticle Res.* **2020**, *22*, 82. [CrossRef]
185. Zhao, W.; Yu, X.; Peng, S.; Luo, Y.; Li, J.; Lu, L. Construction of nanomaterials as contrast agents or probes for glioma imaging. *J. Nanobiotechnol.* **2021**, *19*, 125. [CrossRef]
186. Marasini, S.; Yue, H.; Ho, S.L.; Cha, H.; Park, J.A.; Jung, K.-H.; Ghazanfari, A.; Ahmad, M.Y.; Liu, S.; Chae, K.-S.; et al. A Novel Paramagnetic Nanoparticle T2 Magnetic Resonance Imaging Contrast Agent with High Colloidal Stability: Polyacrylic Acid-Coated Ultrafine Dysprosium Oxide Nanoparticles. *Bull. Korean Chem. Soc.* **2020**, *41*, 829–836. [CrossRef]
187. Ahmad, M.Y.; Ahmad, M.W.; Yue, H.; Ho, S.L.; Park, J.A.; Jung, K.-H.; Cha, H.; Marasini, S.; Ghazanfari, A.; Liu, S.; et al. In vivo positive magnetic resonance imaging applications of poly(methyl vinyl ether-alt-maleic acid)-coated ultra-small paramagnetic gadolinium oxide nanoparticles. *Molecules* **2020**, *25*, 1159. [CrossRef] [PubMed]
188. Marasini, S.; Yue, H.; Ghazanfari, A.; Ho, S.L.; Park, J.A.; Kim, S.; Cha, H.; Liu, S.; Tegafaw, T.; Ahmad, M.Y.; et al. Polyaspartic acid-coated paramagnetic gadolinium oxide nanoparticles as a dual-modal t1 and t2 magnetic resonance imaging contrast agent. *Appl. Sci.* **2021**, *11*, 8222. [CrossRef]
189. Huang, Z.; Wang, Y.; Wu, M.; Li, W.; Zuo, H.; Xiao, B.; Zhang, X.; Wu, J.; He, H.; Xia, Q. Sericin-based gadolinium nanoparticles as synergistically enhancing contrast agents for pH-responsive and tumor targeting magnetic resonance imaging. *Mater. Des.* **2021**, *203*, 109600. [CrossRef]
190. Fei, M.-Y.; Song, M.-M.; Wang, P.; Pang, G.-Z.; Chen, J.; Lu, D.-P.; Liu, R.; Zhang, G.-Y.; Zhao, T.-T.; Shen, Y.-X.; et al. Folic acid modified Fe3O4 nanoclusters by a one-step ultrasonic technique for drug delivery and MR imaging. *RSC Adv.* **2020**, *10*, 5294–5303. [CrossRef]
191. Rodriguez, G.G.; Erro, E.M. Fast iron oxide-induced low-field magnetic resonance imaging. *J. Phys. D Appl. Phys.* **2021**, *54*, 025003. [CrossRef]
192. Creţu, B.E.-B.; Dodi, G.; Shavandi, A.; Gardikiotis, I.; Şerban, I.L.; Balan, V. Imaging constructs: The rise of iron oxide nanoparticles. *Molecules* **2021**, *26*, 3437. [CrossRef] [PubMed]
193. Almijalli, M.; Saad, A.; Alhussaini, K.; Aleid, A.; Alwasel, A. Towards drug delivery control using iron oxide nanoparticles in three-dimensional magnetic resonance imaging. *Nanomaterials* **2021**, *11*, 1876. [CrossRef]
194. Billings, C.; Langley, M.; Warrington, G.; Mashali, F.; Johnson, J.A. Magnetic particle imaging: Current and future applications, magnetic nanoparticle synthesis methods and safety measures. *Int. J. Mol. Sci.* **2021**, *22*, 7651. [CrossRef]

195. Chow, J.C.L. Magnetic nanoparticles as contrast agents in magnetic resonance imaging and radiosensitizers in radiotherapy. In *Fundamentals and Industrial Applications of Magnetic Nanoparticles*; Woodhead Publishing: Cambridge, UK, 2022; pp. 291–316. [CrossRef]
196. Dash, A.; Blasiak, B.; Tomanek, B.; Banerjee, A.; Trudel, S.; Latta, P.; Van Veggel, F.C.J.M. Colloidally Stable Monodisperse Fe Nanoparticles as T2Contrast Agents for High-Field Clinical and Preclinical Magnetic Resonance Imaging. *ACS Appl. Nano Mater.* **2021**, *4*, 1235–1242. [CrossRef]
197. Liu, X.; Tian, Y.; Jiang, L. Manipulating Dispersions of Magnetic Nanoparticles. *Nano Lett.* **2021**, *21*, 2699–2708. [CrossRef]
198. Mair, L.O.; Hale, O.; Jafari, S.; Chen, C.; Udalov, O.; Probst, R.; Baum, I.; Hevaganinge, A.; Wang, E.Y.; Rodriguez, O.C.; et al. Magnetic Microdevices for MRI-Based Detection of SARS-CoV-2 Viruses. *IEEE Open J. Eng. Med. Biol.* **2020**, *1*, 265–267. [CrossRef] [PubMed]
199. Wu, K.; Saha, R.; Su, D.; Krishna, V.D.; Liu, J.; Cheeran, M.C.-J.; Wang, J.-P. Magnetic-Nanosensor-Based Virus and Pathogen Detection Strategies before and during COVID-19. *ACS Appl. Nano Mater.* **2020**, *3*, 9560–9580. [CrossRef]
200. Medhi, R.; Srinoi, P.; Ngo, N.; Tran, H.-V.; Lee, T.R. Nanoparticle-Based Strategies to Combat COVID-19. *ACS Appl. Nano Mater.* **2020**, *3*, 8557–8580. [CrossRef]
201. Ebrahimi, S.; Shamloo, A.; Alishiri, M.; Mofrad, Y.M.; Akherati, F. Targeted pulmonary drug delivery in coronavirus disease (COVID-19) therapy: A patient-specific in silico study based on magnetic nanoparticles-coated microcarriers adhesion. *Int. J. Pharm.* **2021**, *609*, 121133. [CrossRef]
202. Wang, W.; Huang, Z.; Huang, Y.; Zhang, X.; Huang, J.; Cui, Y.; Yue, X.; Ma, C.; Fu, F.; Wang, W.; et al. Pulmonary delivery nanomedicines towards circumventing physiological barriers: Strategies and characterization approaches. *Adv. Drug Deliv. Rev.* **2022**, *185*, 114309. [CrossRef]
203. Chelluri, L.K.; Mohanram, Y.; Jain, R.; Mallarpu, C.S.; Ponnana, M.; Kumar, D.; Krishna Venuganti, V.V.; Kancherla, R.; Papineni, R.V.; Towner, R.; et al. Effect of engineered superparamagnetic iron oxide nanoparticles in targeted cardiac precursor cell delivery by MRI. *Biochem. Biophys. Res. Commun.* **2021**, *541*, 15–21. [CrossRef]
204. Marasini, R.; Rayamajhi, S.; Moreno-Sanchez, A.; Aryal, S. Iron(iii) chelated paramagnetic polymeric nanoparticle formulation as a next-generation: T 1-weighted MRI contrast agent. *RSC Adv.* **2021**, *11*, 32216–32226. [CrossRef]
205. Hou, Z.; Liu, Y.; Xu, J.; Zhu, J. Surface Engineering of Magnetic Iron Oxide Nanoparticles by Polymer Grafting: Synthesis Progress and Biomedical Applications. *Nanoscale* **2020**, *12*, 14957. [CrossRef]
206. Qin, M.; Xu, M.; Niu, L.; Cheng, Y.; Niu, X.; Kong, J.; Zhang, X.; Wei, Y.; Huang, D. Multifunctional modification of Fe_3O_4 nanoparticles for diagnosis and treatment of diseases: A review. *Front. Mater. Sci.* **2021**, *15*, 36–53. [CrossRef]
207. Díez-Pascual, A.M. Surface Engineering of Nanomaterials with Polymers, Biomolecules, and Small Ligands for Nanomedicine. *Materials* **2022**, *15*, 3251. [CrossRef]
208. Li, Y.; Wang, N.; Huang, X.; Li, F.; Davis, T.P.; Qiao, R.; Ling, D. Polymer-Assisted Magnetic Nanoparticle Assemblies for Biomedical Applications. *ACS Appl. Biol. Mater.* **2020**, *3*, 121–142. [CrossRef] [PubMed]
209. Sanadgol, N.; Wackerlig, J. Developments of smart drug-delivery systems based on magnetic molecularly imprinted polymers for targeted cancer therapy: A short review. *Pharmaceutics* **2020**, *12*, 831. [CrossRef]
210. Jarak, I.; Varela, C.L.; da Silva, E.T.; Roleira, F.F.M.; Veiga, F.; Figueiras, A. Pluronic-based nanovehicles: Recent advances in anticancer therapeutic applications. *Eur. J. Med. Chem.* **2020**, *206*, 112526. [CrossRef] [PubMed]
211. Singla, P.; Garg, S.; McClements, J.; Jamieson, O.; Peeters, M.; Mahajan, R.K. Advances in the therapeutic delivery and applications of functionalized Pluronics: A critical review. *Adv. Colloid Interface Sci.* **2022**, *299*, 102563. [CrossRef] [PubMed]
212. Mostarac, D.; Xiong, Y.; Gang, O.; Kantorovich, S.S. Nanopolymers for magnetic applications: How to choose the architecture? *Nanoscale* **2022**, *14*, 11139–11151. [CrossRef] [PubMed]
213. Saengruengrit, C.; Rodponthukwaji, K.; Sucharitakul, J.; Tummamunkong, P.; Palaga, T.; Ritprajak, P.; Insin, N. Effective gene delivery into primary dendritic cells using synthesized PDMAEMA-iron oxide nanocubes. *Mater. Today Chem.* **2021**, *20*, 100481. [CrossRef]
214. Samim, M. Aarzoo Hyaluronic acid-magnetic nanocomposites for gene delivery. In *Polysaccharide-Based Nanocomposites for Gene Delivery and Tissue Engineering*; Woodhead Publishing: Cambridge, UK, 2021; pp. 311–323. [CrossRef]
215. Dalmartello, M.; La Vecchia, C.; Bertuccio, P.; Boffetta, P.; Levi, F.; Negri, E.; Malvezzi, M. European cancer mortality predictions for the year 2022 with focus on ovarian cancer. *Ann. Oncol.* **2022**, *33*, 330–339. [CrossRef]
216. Low, L.E.; Wu, J.; Lee, J.; Tey, B.T.; Goh, B.; Gao, J.; Li, F.; Ling, D. Tumor-responsive dynamic nanoassemblies for targeted imaging, therapy and microenvironment manipulation. *J. Control. Release* **2020**, *324*, 69–103. [CrossRef]
217. Gauger, A.; Hershberger, K.K.; Bronstein, L.M. Theranostics Based on Magnetic Nanoparticles and Polymers: Intelligent Design for Efficient Diagnostics and Therapy. *Front. Chem.* **2020**, *8*, 561. [CrossRef]
218. Wang, W.; Huang, Z.; Huang, Y.; Pan, X.; Wu, C. Updates on the applications of iron-based nanoplatforms in tumor theranostics. *Int. J. Pharm.* **2020**, *589*, 119815. [CrossRef] [PubMed]
219. Koksharov, Y.A.; Gubin, S.P.; Taranov, I.V.; Khomutov, G.B.; Gulyaev, Y.V. Magnetic Nanoparticles in Medicine: Progress, Problems, and Advances. *J. Commun. Technol. Electron.* **2022**, *67*, 101–116. [CrossRef]
220. Manescu, V.; Paltanea, G.; Antoniac, I.; Vasilescu, M. Magnetic nanoparticles used in oncology. *Materials* **2021**, *14*, 5948. [CrossRef] [PubMed]

221. Cotin, G.; Blanco-Andujar, C.; Perton, F.; Asin, L.; de la Fuente, J.M.; Reichardt, W.; Schaffner, D.; Nguyen, D.; Mertz, D.; Kiefer, C.; et al. Unveiling the role of surface, size, shape and defects for theranostic applications of iron oxide nanoparticles. *Nanoscale* **2021**, *13*, 14552–14571.
222. Khizar, S.; Ahmad, N.M.; Zine, N.; Jaffrezic-Renault, N.; Errachid-el-salhi, A.; Elaissari, A. Magnetic Nanoparticles: From Synthesis to Theranostic Applications. *ACS Appl. Nano Mater.* **2021**, *4*, 4284–4306. [CrossRef]
223. Stueber, D.D.; Villanova, J.; Aponte, I.; Xiao, Z.; Colvin, V.L. Magnetic nanoparticles in biology and medicine: Past, present, and future trends. *Pharmaceutics* **2021**, *13*, 943. [CrossRef]
224. Singh, S.; Chawla, H.; Chandra, A.; Garg, S. Magnetic hybrid nanoparticles for drug delivery. In *Magnetic Nanoparticle-Based Hybrid Materials: Fundamentals and Applications*; Woodhead Publishing: Cambridge, UK, 2021; pp. 319–342. [CrossRef]
225. Gao, S.; Guisán, J.M.; Rocha-Martin, J. Oriented immobilization of antibodies onto sensing platforms—A critical review. *Anal. Chim. Acta* **2022**, *1189*, 338907. [CrossRef]
226. Shabatina, T.I.; Vernaya, O.I.; Shabatin, V.P.; Melnikov, M.Y. Magnetic nanoparticles for biomedical purposes: Modern trends and prospects. *Magnetochemistry* **2020**, *6*, 30. [CrossRef]
227. Abdelgawad, M.A.; Elkanzi, N.A.A.; Nayl, A.A.; Musa, A.; Alotaibi, N.H.; Arafa, W.A.A.; Gomha, S.M.; Bakr, R.B. Targeting tumor cells with pyrazolo[3,4-d]pyrimidine scaffold: A literature review on synthetic approaches, structure activity relationship, structural and target-based mechanisms. *Arab. J. Chem.* **2022**, *15*, 103781. [CrossRef]
228. Ignatovich, Z.; Novik, K.; Abakshonok, A.; Koroleva, E.; Beklemisheva, A.; Panina, L.; Kaniukov, E.; Anisovich, M.; Shumskaya, A. One-step synthesis of magnetic nanocomposite with embedded biologically active substance. *Molecules* **2021**, *26*, 937. [CrossRef]
229. Teimouri, K.; Tavakoli, M.R.; Ghafari, A.; Kim, K.C. Effect of plaque geometry on targeted delivery of stem cells containing magnetic particles in a rigid and elastic curved artery with stenosis. *J. Magn. Magn. Mater.* **2022**, *542*, 168580. [CrossRef]
230. Sanz-Ortega, L.; Rojas, J.M.; Barber, D.F. Improving tumor retention of effector cells in adoptive cell transfer therapies by magnetic targeting. *Pharmaceutics* **2020**, *12*, 812. [CrossRef] [PubMed]
231. Wang, J.T.-W.; Martino, U.; Khan, R.; Bazzar, M.; Southern, P.; Tuncel, D.; Al-Jamal, K.T. Engineering red-emitting multi-functional nanocapsules for magnetic tumour targeting and imaging. *Biomater. Sci.* **2020**, *8*, 2590–2599. [CrossRef]
232. Shasha, C.; Krishnan, K.M. Nonequilibrium Dynamics of Magnetic Nanoparticles with Applications in Biomedicine. *Adv. Mater.* **2020**, *33*, 23. Available online: https://onlinelibrary.wiley.com/doi/10.1002/adma.201904131 (accessed on 30 June 2022). [CrossRef]
233. Yang, X.; Shao, G.; Zhang, Y.; Wang, W.; Qi, Y.; Han, S.; Li, H. Applications of Magnetic Particle Imaging in Biomedicine: Advancements and Prospects. *Front. Physiol.* **2022**, *13*, 898426. [CrossRef] [PubMed]
234. Nisticò, R.; Cesano, F.; Garello, F. Magnetic materials and systems: Domain structure visualization and other characterization techniques for the application in the materials science and biomedicine. *Inorganics* **2020**, *8*, 6. [CrossRef]
235. Du, H.; Yao, C.-Y.; Peng, H.; Jiang, B.; Li, S.-X.; Yao, J.-L.; Zheng, F.; Yang, F.; Wu, A.-G. Applications of Transition Metal-doped Iron-based Nanoparticles in Biomedicine. *Chin. J. Appl. Chem.* **2022**, *39*, 391. [CrossRef]
236. Kee, H.; Lee, H.; Park, S. Optimized Halbach array for focused magnetic drug targeting. *J. Magn. Magn. Mater.* **2020**, *514*, 167180. [CrossRef]
237. Garg, R.; Kaur, S.; Ritika Khatoon, S.; Naina Verma, H. A complete and updated review on various types of drug delivery systems. *Int. J. Appl. Pharm.* **2020**, *12*, 4. [CrossRef]
238. Das, S.S.; Bharadwaj, P.; Bilal, M.; Barani, M.; Rahdar, A.; Taboada, P.; Bungau, S.; Kyzas, G.Z. Stimuli-responsive polymeric nanocarriers for drug delivery, imaging, and theragnosis. *Polymers* **2020**, *12*, 1397. [CrossRef]
239. Al-Rawi, N.N.; Anwer, B.A.; Al-Rawi, N.H.; Uthman, A.T.; Ahmed, I.S. Magnetism in drug delivery: The marvels of iron oxides and substituted ferrites nanoparticles. *Saudi Pharm. J.* **2020**, *28*, 876–887. [CrossRef]
240. Mahmoodpour, M.; Goharkhah, M.; Ashjaee, M. Investigation on trajectories and capture of magnetic drug carrier nanoparticles after injection into a direct vessel. *J. Magn. Magn. Mater.* **2020**, *497*, 166065. [CrossRef]
241. Kiaie, N.; Emami, S.H.; Rabbani, S.; Aghdam, R.M.; Tafti, H.A. Targeted and Controlled Drug Delivery to a Rat Model of Heart Failure Through a Magnetic Nanocomposite. *Ann. Biomed. Eng.* **2020**, *48*, 709–721. [CrossRef] [PubMed]
242. Kim, D.-I.; Lee, H.; Kwon, S.-H.; Sung, Y.J.; Song, W.K.; Park, S. Bilayer Hydrogel Sheet-Type Intraocular Microrobot for Drug Delivery and Magnetic Nanoparticles Retrieval. *Adv. Healthc. Mater.* **2020**, *9*, 2000118. [CrossRef] [PubMed]
243. Nguyen, C.T.; Kim, C.R.; Le, T.H.; Koo, K.-I.; Hwang, C.H. Magnetically guided targeted delivery of erythropoietin using magnetic nanoparticles: Proof of concept. *Medicine* **2020**, *99*, e19972. [CrossRef]
244. Wang, C.H. Targeted delivery of erythropoietin hybridized with magnetic nanocarriers for the treatment of central nervous system injury: A literature review. *Int. J. Nanomed.* **2020**, *15*, 9683–9701. [CrossRef]
245. Timerbaev, A.R. Analytical methodology for developing nanomaterials designed for magnetically-guided delivery of platinum anticancer drugs. *Talanta* **2022**, *243*, 123371. [CrossRef]
246. Ferreira, B.J.M.L.; Martel, F.; Silva, C.; Santos, T.M.; Daniel-da-Silva, A.L. Nanostructured functionalized magnetic platforms for the sustained delivery of cisplatin: Synthesis, characterization and in vitro cytotoxicity evaluation. *J. Inorg. Biochem.* **2020**, *213*, 111258. [CrossRef]
247. Schroffenegger, M.; Leitner, N.S.; Morgese, G.; Ramakrishna, S.N.; Willinger, M.; Benetti, E.M.; Reimhult, E. Polymer Topology Determines the Formation of Protein Corona on Core–Shell Nanoparticles. *ACS Nano* **2020**, *14*, 12708–12718. [CrossRef]

248. Shadmani, P.; Mehrafrooz, B.; Montazeri, A.; Naghdabadi, R. Protein corona impact on nanoparticle-cell interactions: Toward an energy-based model of endocytosis. *J. Phys. Condens. Matter* **2020**, *32*, 115101. [CrossRef]
249. Costa, L.S.D.; Khan, L.U.; Franqui, L.S.; Delite, F.D.S.; Muraca, D.; Martinez, D.S.T.; Knobel, M. Hybrid magneto-luminescent iron oxide nanocubes functionalized with europium complexes: Synthesis, hemolytic properties and protein corona formation. *J. Mater. Chem. B* **2021**, *9*, 428–439. [CrossRef]
250. Nowak-Jary, J.; Machnicka, B. Pharmacokinetics of magnetic iron oxide nanoparticles for medical applications. *J. Nanobiotechnol.* **2022**, *20*, 305. [CrossRef]
251. Rezaei-Aghdam, E.; Shamel, A.; Khodadadi-Moghaddam, M.; Rajaei, G.E.; Mohajeri, S. Synthesis of TiO_2 and ZnO Nanoparticles and CTAB-Stabilized Fe3O4 nanocomposite: Kinetics and thermodynamics of adsorption. *Res. Chem. Intermed.* **2021**, *47*, 1759–1774. [CrossRef]
252. Saifullah, S.; Ali, I.; Kawish, M.; El-Shabasy, R.M.; Chen, L.; El-Seedi, H.R. Surface functionalized magnetic nanoparticles for targeted cancer therapy and diagnosis. In *Metal Nanoparticles for Drug Delivery and Diagnostic Applications*; Elsevier: Amsterdam, The Netherlands, 2020; pp. 215–236. [CrossRef]
253. Mirza, S.; Ahmad, M.S.; Shah, M.I.A.; Ateeq, M. Magnetic nanoparticles: Drug delivery and bioimaging applications. In *Metal Nanoparticles for Drug Delivery and Diagnostic Applications*; Elsevier: Amsterdam, The Netherlands, 2020; pp. 189–213. [CrossRef]
254. Patra, P.; Chattopadhyay, D. Sustainable release of nanodrugs: A new biosafe approach. In *Green Approaches in Medicinal Chemistry for Sustainable Drug Design*; Elsevier: Amsterdam, The Netherlands, 2020; pp. 603–615. [CrossRef]
255. Sun, T.; Dasgupta, A.; Zhao, Z.; Nurunnabi, M.; Mitragotri, S. Physical triggering strategies for drug delivery. *Adv. Drug Deliv. Rev.* **2020**, *158*, 36–62. [CrossRef]
256. Ahmad, M.Z.; Ahmad, J.; Warsi, M.H.; Abdel-Wahab, B.A.; Akhter, S. Metallic nanoparticulate delivery systems. In *Nanoengineered Biomaterials for Advanced Drug Delivery*; Elsevier: Amsterdam, The Netherlands, 2020; pp. 279–328. [CrossRef]
257. Jafari, R.M.; Ala, M.; Goodarzi, N.; Dehpour, A.R. Does Pharmacodynamics of Drugs Change After Presenting them as Nanoparticles Like their Pharmacokinetics? *Curr. Drug Targets* **2020**, *21*, 807–818. [CrossRef]
258. Kakaei, S.; Khameneh, E.S.; Ghasemi, E.; Aghazadeh, M. Targeted Drug Delivery of Teniposide by Magnetic Nanocarrier. *Curr. Nanosci.* **2020**, *16*, 608–616. [CrossRef]
259. Aghajanzadeh, M.; Naderi, E.; Zamani, M.; Sharafi, A.; Naseri, M.; Danafar, H. In vivo and in vitro biocompatibility study of $MnFe_2O_4$ and $Cr_2Fe_6O_{12}$ as photosensitizer for photodynamic therapy and drug delivery of anti-cancer drugs. *Drug Dev. Ind. Pharm.* **2020**, *46*, 846–851. [CrossRef]
260. Al-Musawi, S.; Albukhaty, S.; Al-Karagoly, H.; Sulaiman, G.M.; Jabir, M.S.; Naderi-Manesh, H. Dextran-coated superparamagnetic nanoparticles modified with folate for targeted drug delivery of camptothecin. *Adv. Nat. Sci. Nanosci. Nanotechnol.* **2020**, *11*, 045009. [CrossRef]
261. Gholami, A.; Mousavi, S.M.; Hashemi, S.A.; Ghasemi, Y.; Chiang, W.-H.; Parvin, N. Current trends in chemical modifications of magnetic nanoparticles for targeted drug delivery in cancer chemotherapy. *Drug Metab. Rev.* **2020**, *52*, 205–224. [CrossRef]
262. Nabipour, H.; Hu, Y. Sustainable drug delivery systems through green nanotechnology. In *Nanoengineered Biomaterials for Advanced Drug Delivery*; Mozafari, M., Ed.; Elsevier: San Diego, CA, USA, 2020; pp. 61–89. [CrossRef]
263. Sadhasivam, J.; Sugumaran, A. Magnetic nanocarriers: Emerging tool for the effective targeted treatment of lung cancer. *J. Drug Deliv. Sci. Technol.* **2020**, *55*, 101493. [CrossRef]
264. Saadat, M.; Manshadi, M.K.D.; Mohammadi, M.; Zare, M.J.; Zarei, M.; Kamali, R.; Sanati-Nezhad, A. Magnetic particle targeting for diagnosis and therapy of lung cancers. *Control. Release* **2020**, *328*, 776–791. [CrossRef]
265. Ngema, L.M.; Adeyemi, S.A.; Marimuthu, T.; Choonara, Y.E. A review on engineered magnetic nanoparticles in Non-Small-Cell lung carcinoma targeted therapy. *Int. J. Pharm.* **2021**, *606*, 120870. [CrossRef] [PubMed]
266. Rastogi, A.; Yadav, K.; Mishra, A.; Singh, M.S.; Chaudhary, S.; Manohar, R.; Parmar, A.S. Early diagnosis of lung cancer using magnetic nanoparticles-integrated systems. *Nanotechnol. Rev.* **2022**, *11*, 544–574. [CrossRef]
267. Hatami, E.; Nagesh, P.K.B.; Chauhan, N.; Jaggi, M.; Chauhan, S.C.; Yallapu, M.M. In Situ Nanoparticle Self-Assembly for Combination Delivery of Therapeutics to Non-Small Cell Lung Cancer. *ACS Appl. Bio Mater.* **2022**, *5*, 1104–1119. [CrossRef] [PubMed]
268. Li, K.; Li, P.; Wang, Y.; Han, S. Manganese-Based Targeted Nanoparticles for Postoperative Gastric Cancer Monitoring via Magnetic Resonance Imaging. *Front. Oncol.* **2020**, *10*, 601538. [CrossRef]
269. Zhan, W.; Cai, X.; Li, H.; Du, G.; Hu, H.; Wu, Y.; Wang, L. GMBP1-conjugated manganese oxide nanoplates for: In vivo monitoring of gastric cancer MDR using magnetic resonance imaging. *RSC Adv.* **2020**, *10*, 13687–13695. [CrossRef]
270. Sharif, A.P.; Habibi, K.; Bijarpas, Z.K.; Tolami, H.F.; Alkinani, T.A.; Jameh, M.; Dehkaei, A.A.; Monhaser, S.K.; Daemi, H.B.; Mahmoudi, A.; et al. Cytotoxic Effect of a Novel $GaFe_2O_4$@Ag Nanocomposite Synthesized by Scenedesmus obliquus on Gastric Cancer Cell Line and Evaluation of BAX, Bcl-2 and CASP8 Genes Expression. *J. Clust. Sci.* **2022**. [CrossRef]
271. Hajializadeh, D.; Saber, A.A.; Jameh, M.; Ahang, B.; Moafy, A.; Bijarpas, Z.K.; Masouleh, R.S.; Kia, M.B.; Mojdehi, S.R.; Salehzadeh, A. Potential of Apoptosis-Inducing by a Novel Bio-synthesized $CoFe_2O_4$@Ag Nanocomposite in Gastric Cell Line at the Cellular and Molecular Level. *J. Clust. Sci.* **2022**. [CrossRef]
272. Zou, J.; Chen, S.; Li, Y.; Zeng, L.; Lian, G.; Li, J.; Chen, S.; Huang, K.; Chen, Y. Nanoparticles modified by triple single chain antibodies for MRI examination and targeted therapy in pancreatic cancer. *Nanoscale* **2020**, *12*, 4473–4490. [CrossRef]

273. Karahaliloglu, Z.; Kilicay, E.; Hazer, B. PLinaS-g-PEG coated magnetic nanoparticles as a contrast agent for hepatocellular carcinoma diagnosis. *J. Biomater. Sci. Polym. Ed.* **2020**, *31*, 1580–1603. [CrossRef]
274. Fu, Y.; He, G.; Liu, Z.; Wang, J.; Li, M.; Zhang, Z.; Bao, Q.; Wen, J.; Zhu, X.; Zhang, C.; et al. DNA Base Pairing-Inspired Supramolecular Nanodrug Camouflaged by Cancer-Cell Membrane for Osteosarcoma Treatment. *Small* **2022**, *18*, 2202337. [CrossRef]
275. Zivarpour, P.; Hallajzadeh, J.; Asemi, Z.; Sadoughi, F.; Sharifi, M. Chitosan as possible inhibitory agents and delivery systems in leukemia. *Cancer Cell Int.* **2021**, *21*, 544. [CrossRef] [PubMed]
276. Goorbandi, R.G.; Mohammadi, M.R.; Malekzadeh, K. Synthesizing efficacious genistein in conjugation with superparamagnetic Fe_3O_4 decorated with bio-compatible carboxymethylated chitosan against acute leukemia lymphoma. *Biomater. Res.* **2020**, *24*, 9. [CrossRef] [PubMed]
277. Khutsishvili, S.S.; Aleksandrova, G.P.; Vakul'Skaya, T.I.; Sukhov, B.G. Structural and Magnetic Properties of Biocompatible-Coated Magnetite Nanoparticles for Treating Antianemia. *IEEE Trans. Magn.* **2021**, *57*, 5200309. [CrossRef]
278. Hafez, A.A.; Salimi, A.; Jamali, Z.; Shabani, M.; Sheikhghaderi, H. Overview of the application of inorganic nanomaterials in breast cancer diagnosis. In *Inorganic and Nano-Metal Chemistry*; Taylor & Francis: Abingdon, UK, 2021. [CrossRef]
279. Bai, X.; Su, G.; Zhai, S. Recent advances in nanomedicine for the diagnosis and therapy of liver fibrosis. *Nanomaterials* **2020**, *10*, 1945. [CrossRef]
280. Farid, R.M.; Gaafar, P.M.E.; Hazzah, H.A.; Helmy, M.W.; Abdallah, O.Y. Chemotherapeutic potential of L-carnosine from stimuli-responsive magnetic nanoparticles against breast cancer model. *Nanomedicine* **2020**, *15*, 891–911. [CrossRef]
281. Taheri-Ledari, R.; Zhang, W.; Radmanesh, M.; Mirmohammadi, S.S.; Maleki, A.; Cathcart, N.; Kitaev, V. Multi-Stimuli Nanocomposite Therapeutic: Docetaxel Targeted Delivery and Synergies in Treatment of Human Breast Cancer Tumor. *Small* **2020**, *16*, 2002733. [CrossRef]
282. Panda, J.; Satapathy, B.S.; Mandal, B.; Sen, R.; Mukherjee, B.; Sarkar, R.; Tudu, B. Anticancer potential of docetaxel-loaded cobalt ferrite nanocarrier: An in vitro study on MCF-7 and MDA-MB-231 cell lines. *J. Microencapsul.* **2021**, *38*, 36–46. [CrossRef]
283. Li, Z.; Wu, X.; Wang, W.; Gai, C.; Zhang, W.; Li, W.; Ding, D. Fe(II) and Tannic Acid-Cloaked MOF as Carrier of Artemisinin for Supply of Ferrous Ions to Enhance Treatment of Triple-Negative Breast Cancer. *Nanoscale Res. Lett.* **2021**, *16*, 37. [CrossRef]
284. Helmy, L.A.; Abdel-Halim, M.; Hassan, R.; Sebak, A.; Farghali, H.A.M.; Mansour, S.; Tammam, S.N. The other side to the use of active targeting ligands; the case of folic acid in the targeting of breast cancer. *Colloids Surf. B Biointerfaces* **2022**, *211*, 112289. [CrossRef]
285. Jani, K.; Kaushal, N.; Sadoqi, M.; Long, G.; Chen, Z.-S.; Squillante, E. Formulation and characterization of oleic acid magnetic PEG PLGA nanoparticles for targeting glioblastoma multiforme. *J. Magn. Magn. Mater.* **2021**, *533*, 167970. [CrossRef]
286. Gandhi, H.; Sharma, A.K.; Mahant, S.; Kapoor, D.N. Recent advancements in brain tumor targeting using magnetic nanoparticles. *Ther. Deliv.* **2020**, *11*, 97–112. [CrossRef] [PubMed]
287. Guigou, C.; Lalande, A.; Millot, N.; Belharet, K.; Grayeli, A.B. Use of super paramagnetic iron oxide nanoparticles as drug carriers in brain and ear: State of the art and challenges. *Brain Sci.* **2021**, *11*, 358. [CrossRef] [PubMed]
288. Estelrich, J.; Busquets, M.A. Magnetic Nanoparticles as Delivery Systems to Penetrate the Blood-Brain Barrier. *Neuromethods* **2021**, *157*, 173–208. [CrossRef]
289. Joshi, B.; Joshi, A. Polymeric magnetic nanoparticles: A multitargeting approach for brain tumour therapy and imaging. *Drug Deliv. Transl. Res.* **2022**, *12*, 1588–1604. [CrossRef]
290. Dhar, D.; Ghosh, S.; Das, S.; Chatterjee, J. A review of recent advances in magnetic nanoparticle-based theranostics of glioblastoma. *Nanomedicine* **2022**, *17*, 107–132. [CrossRef]
291. Yasaswi, P.S.; Shetty, K.; Yadav, K.S. Temozolomide nano enabled medicine: Promises made by the nanocarriers in glioblastoma therapy. *J. Control. Release* **2021**, *336*, 549–571. [CrossRef]
292. Chaudhary, R.; Morris, R.J.; Steinson, E. The multifactorial roles of microglia and macrophages in the maintenance and progression of glioblastoma. *J. Neuroimmunol.* **2021**, *357*, 577633. [CrossRef]
293. Gupta, R.; Kaur, T.; Chauhan, A.; Kumar, R.; Kuanr, B.K.; Sharma, D. Tailoring nanoparticles design for enhanced heating efficiency and improved magneto-chemo therapy for glioblastoma. *Biomater. Adv.* **2022**, *139*, 213021. [CrossRef]
294. Guo, L.; Yang, C.; Yang, R.; Zhao, W. Magnetically anchored antibody-coupled nanocomposite as α-Amylase inhibitor for long-time protection against glycemic variability. *Chem. Eng. J.* **2022**, *430*, 132984. [CrossRef]
295. Zhou, H.; Alici, G. A Magnetically Actuated Novel Robotic Capsule for Site-Specific Drug Delivery Inside the Gastrointestinal Tract. *IEEE Trans. Syst. Man Cybern. Syst.* **2022**, *52*, 4010–4020. [CrossRef]
296. Cicha, I.; Alexiou, C. Cardiovascular applications of magnetic particles. *J. Magn. Magn. Mater.* **2021**, *518*, 167428. [CrossRef]
297. Zhao, Y.-Z.; Chen, R.; Xue, P.-P.; Luo, L.-Z.; Zhong, B.; Tong, M.-Q.; Chen, B.; Yao, Q.; Yuan, J.-D.; Xu, H.-L. Magnetic PLGA microspheres loaded with SPIONs promoted the reconstruction of bone defects through regulating the bone mesenchymal stem cells under an external magnetic field. *Mater. Sci. Eng. C* **2021**, *122*, 111877. [CrossRef] [PubMed]
298. Modak, M.; Bobbala, S.; Lescott, C.; Liu, Y.-G.; Nandwana, V.; Dravid, V.P.; Scott, E.A. Magnetic Nanostructure-Loaded Bicontinuous Nanospheres Support Multicargo Intracellular Delivery and Oxidation-Responsive Morphological Transitions. *ACS Appl. Mater. Interfaces* **2020**, *12*, 55584–55595. [CrossRef] [PubMed]

299. Janik-Olchawa, N.; Drozdz, A.; Ryszawy, D.; Pudełek, M.; Planeta, K.; Setkowicz, Z.; Śniegocki, M.; Żądło, A.; Ostachowicz, B.; Chwiej, J. Comparison of ultrasmall IONPs and Fe salts biocompatibility and activity in multi-cellular in vitro models. *Sci. Rep.* **2020**, *10*, 15447. [CrossRef]
300. Nguyen, K.; Nuß, B.; Mühlberger, M.; Unterweger, H.; Friedrich, R.P.; Alexiou, C.; Janko, C. Superparamagnetic iron oxide nanoparticles carrying chemotherapeutics improve drug efficacy in monolayer and spheroid cell culture by enabling active accumulation. *Nanomaterials* **2020**, *10*, 1577. [CrossRef]
301. Friedrich, R.P.; Schreiber, E.; Tietze, R.; Yang, H.; Pilarsky, C.; Alexiou, C. Intracellular quantification and localization of label-free iron oxide nanoparticles by holotomographic microscopy. *Nanotechnol. Sci. Appl.* **2020**, *13*, 119–130. [CrossRef]
302. Raval, Y.S.; Samstag, A.; Taylor, C.; Huang, G.; Mefford, O.T.; Tzeng, T.-R.J. Assessing the biocompatibility of multi-anchored glycoconjugate functionalized iron oxide nanoparticles in a normal human colon cell line ccd-18co. *Nanomaterials* **2021**, *11*, 2465. [CrossRef]
303. Pardo, A.; Gómez-Florit, M.; Barbosa, S.; Taboada, P.; Domingues, R.M.A.; Gomes, M.E. Magnetic Nanocomposite Hydrogels for Tissue Engineering: Design Concepts and Remote Actuation Strategies to Control Cell Fate. *ACS Nano* **2021**, *15*, 175–209. [CrossRef]
304. Ivanova, A.V.; Nikitin, A.A.; Gabashvily, A.N.; Vishnevskiy, D.A.; Abakumov, M.A. Synthesis and intensive analysis of antibody labeled single core magnetic nanoparticles for targeted delivery to the cell membrane. *J. Magn. Magn. Mater.* **2021**, *521*, 167487. [CrossRef]
305. Hillion, A.; Hallali, N.; Clerc, P.; Lopez, S.; Lalatonne, Y.; Noûs, C.; Motte, L.; Gigoux, V.; Carrey, J. Real-Time Observation and Analysis of Magnetomechanical Actuation of Magnetic Nanoparticles in Cells. *Nano Lett.* **2022**, *22*, 1986–1991. [CrossRef]
306. Goren, K.; Neelam, N.; Yuval, J.B.; Weiss, D.J.; Kunicher, N.; Margel, S.; Mintz, Y. Targeting tumor cells using magnetic nanoparticles–A feasibility study in animal models. In *Minimally Invasive Therapy and Allied Technologies*; Taylor&Francis: Abingdon, UK, 2022. [CrossRef]
307. Ishmukhametov, I.; Batasheva, S.; Rozhina, E.; Akhatova, F.; Mingaleeva, R.; Rozhin, A.; Fakhrullin, R. DNA/Magnetic Nanoparticles Composite to Attenuate Glass Surface Nanotopography for Enhanced Mesenchymal Stem Cell Differentiation. *Polymers* **2022**, *14*, 344. [CrossRef] [PubMed]
308. Mohammadalizadeh, M.; Dabirian, S.; Akrami, M.; Hesari, Z. SPION based magnetic PLGA nanofibers for neural differentiation of mesenchymal stem cells. *Nanotechnology* **2022**, *33*, 375101. [CrossRef] [PubMed]
309. Mazloum Tabaei, M.A.; Bamoniri, A.; Mirjalili, B.B.F. One-pot Biginelli synthesis of 3,4-dihydropyrimidin-2(1H)-ones using nano-cellulose/BF3/Fe_3O_4. *J. Iran. Chem. Soc.* **2022**, *19*, 2679–2691. [CrossRef]
310. Panina, L.V.; Gurevich, A.; Beklemisheva, A.; Omelyanchik, A.; Levada, K.; Rodionova, V. Spatial Manipulation of Particles and Cells at Micro-and Nanoscale via Magnetic Forces. *Cells* **2022**, *11*, 950. [CrossRef] [PubMed]
311. Dalal, V.; Biswas, S. Nanoscience: Convergence with Biomedical and Biological Applications. In *Functional Bionanomaterials*; Springer: Berlin/Heidelberg, Germany, 2020; pp. 1–25. [CrossRef]
312. Puri, R.; Arora, V.; Kabra, A.; Dureja, H.; Hamaal, S. Magnetosomes: A Tool for Targeted Drug Delivery in the Management of Cancer. *J. Nanomater.* **2022**, *2022*, 6414585. [CrossRef]
313. Kotakadi, S.M.; Borelli, D.P.R.; Nannepaga, J.S. Therapeutic Applications of Magnetotactic Bacteria and Magnetosomes: A Review Emphasizing on the Cancer Treatment. *Front. Bioeng. Biotechnol.* **2022**, *10*, 789016. [CrossRef]
314. Ying, G.; Zhang, G.; Yang, J.; Hao, Z.; Xing, W.; Lu, D.; Zhang, S.; Yan, L. Biomineralization and biotechnological applications of bacterial magnetosomes. *Colloids Surf. B Biointerfaces* **2022**, *216*, 112556. [CrossRef]
315. Zwiener, T.; Dziuba, M.; Mickoleit, F.; Rückert, C.; Busche, T.; Kalinowski, J.; Uebe, R.; Schüler, D. Towards a 'chassis' for bacterial magnetosome biosynthesis: Genome streamlining of Magnetospirillum gryphiswaldense by multiple deletions. *Microb. Cell Factories* **2021**, *20*, 35. [CrossRef]
316. Jubran, A.S.; Al-Zamely, O.M.; Al-Ammar, M.H. A study of iron oxide nanoparticles synthesis by using bacteria. *Int. J. Pharm. Qual. Assur.* **2020**, *11*, 88–92. [CrossRef]
317. Nemati, Z.; Um, J.; Zamani Kouhpanji, M.R.; Zhou, F.; Gage, T.; Shore, D.; Makielski, K.; Donnelly, A.; Alonso, J. Magnetic Isolation of Cancer-Derived Exosomes Using Fe/Au Magnetic Nanowires. *ACS Appl. Nano Mater.* **2020**, *3*, 2058–2069. [CrossRef]
318. Talukdar, S.; Saha, P.; Mandal, K. Folate modified zinc ferrite nano-hollowspheres for drug delivery and intrinsic fluorescence. *AIP Conf. Proc.* **2020**, *2265*, 030131. [CrossRef]
319. Rani, V.; Venkatesan, J.; Prabhu, A. Nanotherapeutics in glioma management: Advances and future perspectives. *J. Drug Deliv. Sci. Technol.* **2020**, *57*, 101626. [CrossRef]
320. D'souza, U.P.; Rao, N.; Shriram, R.G.; Dubey, A. In vitro and in vivo exploration of super-magnetically modulated novel parenteral carrier: A targeted drug delivery of polymeric carboplatin nanosphere capped with the vitamin c to treat breast cancer in rats. *Indian J. Pharm. Educ. Res.* **2020**, *54*, S140–S153. [CrossRef]
321. Lim, E.-B.; Vy, T.A.; Lee, S.-W. Comparative release kinetics of small drugs (ibuprofen and acetaminophen) from multifunctional mesoporous silica nanoparticles. *J. Mater. Chem. B* **2020**, *8*, 2096–2106. [CrossRef] [PubMed]
322. Anirudhan, T.S.; Christa, J. Temperature and pH sensitive multi-functional magnetic nanocomposite for the controlled delivery of 5-fluorouracil, an anticancer drug. *J. Drug Deliv. Sci. Technol.* **2020**, *55*, 101476. [CrossRef]

323. Ayyanaar, S.; Bhaskar, R.; Esthar, S.; Vadivel, M.; Rajesh, J.; Rajagopal, G. Design and development of 5-fluorouracil loaded biodegradable magnetic microspheres as site-specific drug delivery vehicle for cancer therapy. *J. Magn. Magn. Mater.* **2022**, *546*, 168853. [CrossRef]
324. Truong, D.H.; Le, V.K.H.; Pham, T.T.; Dao, A.H.; Pham, T.P.D.; Tran, T.H. Delivery of erlotinib for enhanced cancer treatment: An update review on particulate systems. *J. Drug Deliv. Sci. Technol.* **2020**, *55*, 101348. [CrossRef]
325. Jithendra, T.; Sreekanth Reddy, O.; Subha, M.C.S.; Chowdoji Rao, K. Fabrication of drug delivery system for controlled release of curcumin, intercalated with magnetite nanoparticles through sodium alginate/polyvinylpyrrolidone-co-vinyl acetate semi ipn microbeads. *Int. J. Appl. Pharm.* **2020**, *12*, 249–257. [CrossRef]
326. de Santana, W.M.O.S.; Caetano, B.L.; de Annunzio, S.R.; Pulcinelli, S.H.; Ménager, C.; Fontana, C.R.; Santilli, C.V. Conjugation of superparamagnetic iron oxide nanoparticles and curcumin photosensitizer to assist in photodynamic therapy. *Colloids Surf. B Biointerfaces* **2020**, *196*, 111297. [CrossRef]
327. Dutta, B.; Rawoot, Y.A.; Checker, S.; Shelar, S.B.; Barick, K.C.; Kumar, S.; Somani, R.R.; Hassan, P.A. Micellar assisted aqueous stabilization of iron oxide nanoparticles for curcumin encapsulation and hyperthermia application. *Nano-Struct. Nano-Objects* **2020**, *22*, 100466. [CrossRef]
328. Santos, E.C.S.; Cunha, J.A.; Martins, M.G.; Galeano-Villar, B.M.; Caraballo-Vivas, R.J.; Leite, P.B.; Rossi, A.L.; Garcia, F.; Finotelli, P.V.; Ferraz, H.C. Curcuminoids-conjugated multicore magnetic nanoparticles: Design and characterization of a potential theranostic nanoplatform. *J. Alloys Compd.* **2021**, *879*, 160448. [CrossRef]
329. Molaei, H.; Zaaeri, F.; Sharifi, S.; Ramazani, A.; Safaei, S.; Abdolmohammadi, J.; Khoobi, M. Polyethylenimine-graft-poly (maleic anhydride-alt-1-octadecene) coated Fe_3O_4 magnetic nanoparticles: Promising targeted pH-sensitive system for curcumin delivery and MR imaging. *Int. J. Polym. Mater. Polym. Biomater.* **2021**, *70*, 1344–1353. [CrossRef]
330. Gharagozlou, M. $NiFe_2O_4$@SiO_2@HKUST-1 as Novel Magnetic Metal-Organic Framework Nanocomposites for the Curcumin Adsorption. *J. Nanostructures* **2022**, *12*, 455–473. [CrossRef]
331. Gharehaghaji, N.; Divband, B. PEGylated Magnetite/Hydroxyapatite: A Green Nanocomposite for T2-Weighted MRI and Curcumin Carrying. *Evid. Based Complementary Altern. Med.* **2022**, *2022*, 1337588. [CrossRef] [PubMed]
332. Kowalik, P.; Mikulski, J.; Borodziuk, A.; Duda, M.; Kamińska, I.; Zajdel, K.; Rybusinski, J.; Szczytko, J.; Wojciechowski, T.; Sobczak, K.; et al. Yttrium-Doped Iron Oxide Nanoparticles for Magnetic Hyperthermia Applications. *J. Phys. Chem. C* **2020**, *124*, 6871–6883. [CrossRef] [PubMed]
333. Khan, A.; Sahu, N.K. Folate encapsulation in PEG-diamine grafted mesoporous Fe_3O_4 nanoparticles for hyperthermia and in vitro assessment. *IET Nanobiotechnol.* **2020**, *14*, 881–888. [CrossRef]
334. Gahrouei, Z.E.; Imani, M.; Soltani, M.; Shafyei, A. Synthesis of iron oxide nanoparticles for hyperthermia application: Effect of ultrasonic irradiation assisted co-precipitation route. *Adv. Nat. Sci. Nanosci. Nanotechnol.* **2020**, *11*, 025001. [CrossRef]
335. Barrera, G.; Coisson, M.; Celegato, F.; Martino, L.; Tiwari, P.; Verma, R.; Kane, S.N.; Mazaleyrat, F.; Tiberto, P. Specific loss power of Co/Li/Zn-mixed ferrite powders for magnetic hyperthermia. *Sensors* **2020**, *20*, 2151. [CrossRef]
336. Salati, A.; Ramazani, A.; Kashi, M.A. Tuning hyperthermia properties of FeNiCo ternary alloy nanoparticles by morphological and magnetic characteristics. *J. Magn. Magn. Mater.* **2020**, *498*, 166172. [CrossRef]
337. Leonel, A.G.; Mansur, A.A.P.; Carvalho, S.M.; Outon, L.E.F.; Ardisson, J.D.; Krambrock, K.; Mansur, H.S. Tunable magnetothermal properties of cobalt-doped magnetite–carboxymethylcellulose ferrofluids: Smart nanoplatforms for potential magnetic hyperthermia applications in cancer therapy. *Nanoscale Adv.* **2021**, *3*, 1029. [CrossRef]
338. Derakhshankhah, H.; Jahanban-Esfahlan, R.; Vandghanooni, S.; Akbari-Nakhjavani, S.; Massoumi, B.; Haghshenas, B.; Rezaei, A.; Farnudiyan-Habibi, A.; Samadian, H.; Jaymand, M. A bio-inspired gelatin-based pH - and thermal-sensitive magnetic hydrogel for in vitro chemo/hyperthermia treatment of breast cancer cells. *J. Appl. Polym. Sci.* **2021**, *138*, 50578. [CrossRef]
339. Eivazzadeh-Keihan, R.; Asgharnasl, S.; Bani, M.S.; Radinekiyan, F.; Maleki, A.; Mahdavi, M.; Babaniamansour, P.; Bahreinizad, H.; Shalan, A.E.; Lanceros-Méndez, S. Magnetic Copper Ferrite Nanoparticles Functionalized by Aromatic Polyamide Chains for Hyperthermia Applications. *Langmuir* **2021**, *37*, 8847–8854. [CrossRef] [PubMed]
340. Das, R.; Kim, N.P.; Attanayake, S.B.; Phan, M.-H.; Srikanth, H. Role of magnetic anisotropy on the hyperthermia efficiency in spherical $Fe_{3-x}Co_xO_4$ (X = 0–1) nanoparticles. *Appl. Sci.* **2021**, *11*, 930. [CrossRef]
341. Fiorito, S.; Soni, N.; Silvestri, N.; Brescia, R.; Gavilán, H.; Conteh, J.S.; Mai, B.T.; Pellegrino, T. Fe_3O_4@Au@$Cu_{2-x}S$ Heterostructures Designed for Tri-Modal Therapy: Photo- Magnetic Hyperthermia and 64Cu Radio-Insertion. *Small* **2022**, *18*, 2200174. [CrossRef] [PubMed]
342. Islam, M.A.; Hasan, M.R.; Haque, M.M.; Rashid, R.; Syed, I.M.; Hoque, S.M. Efficacy of surface-functionalized $Mg_{1-x}Co_xFe_2O_4$ ($0 < x < 1$; $\Delta x = 0.1$) for hyperthermia and in vivo MR imaging as a contrast agent. *RSC Adv.* 2022; 12, 7835–7849. [CrossRef]
343. Benjamin, A.S.; Remya, V.; Arunai Nambi Raj, N.; Nayak, S. Evaluation of Doxorubicin Loaded Gelatin Coated Iron Oxide Nanoparticles for Drug Delivery and Magnetic Hyperthermia for Anti-Cancer Treatment. *Trends Biomater. Artif. Organs* **2022**, *36*, 3–10.
344. Kovrigina, E.; Chubarov, A.; Dmitrienko, E. High Drug Capacity Doxorubicin-Loaded Iron Oxide Nanocomposites for Cancer Therapy. *Magnetochemistry* **2022**, *8*, 54. [CrossRef]
345. Spiridonov, V.; Panova, I.; Kusaia, V.; Makarova, L.; Romodina, M.; Fedyanin, A.; Pozdnyakova, N.; Shibaeva, A.; Zezin, S.; Sybachin, A.; et al. Doxorubicin Loaded Magnetosensitive Water-Soluble Nanogel Based on NIPAM and Iron (3+) Containing Nanoparticles. *Macromol. Symp.* **2020**, *389*, 1900072. [CrossRef]

346. Obireddy, S.R.; Chintha, M.; Kashayi, C.R.; Venkata, K.R.K.S.; Subbarao, S.M.C. Gelatin-Coated Dual Cross-Linked Sodium Alginate/Magnetite Nanoparticle Microbeads for Controlled Release of Doxorubicin. *ChemistrySelect* **2020**, *5*, 10276–10284. [CrossRef]
347. Prospero, A.G.; Fidelis-De-Oliveira, P.; Soares, G.A.; Miranda, M.F.; Pinto, L.A.; Dos Santos, D.C.; Silva, V.D.S.; Zufelato, N.; Bakuzis, A.F.; Miranda, J.R.A. AC biosusceptometry and magnetic nanoparticles to assess doxorubicin-induced kidney injury in rats. *Nanomedicine* **2020**, *15*, 511–525. [CrossRef]
348. Javadian, S.; Najafi, K.; Sadrpoor, S.M.; Ektefa, F.; Dalir, N.; Nikkhah, M. Graphene quantum dots based magnetic nanoparticles as a promising delivery system for controlled doxorubicin release. *J. Mol. Liq.* **2021**, *331*, 115746. [CrossRef]
349. Fant, C.; Granzotto, A.; Mestas, J.-L.; Ngo, J.; Lafond, M.; Lafon, C.; Foray, N.; Padilla, F. DNA Double-Strand Breaks in Murine Mammary Tumor Cells Induced by Combined Treatment with Doxorubicin and Controlled Stable Cavitation. *Ultrasound Med. Biol.* **2021**, *47*, 2941–2957. [CrossRef] [PubMed]
350. Da Silva, J.V.S.; Da Silva, M.R.; Da Silva, M.A.C. Magnetic gelatin microspheres for targeted release of doxorubicin. *Mater. Res.* **2021**, *24*, e20210176. [CrossRef]
351. Ramnandan, D.; Mokhosi, S.; Daniels, A.; Singh, M. Chitosan, polyethylene glycol and polyvinyl alcohol modified $MgFe_2O_4$ ferrite magnetic nanoparticles in doxorubicin delivery: A comparative study in vitro. *Molecules* **2021**, *26*, 3893. [CrossRef] [PubMed]
352. Ehsanimehr, S.; Moghadam, P.N.; Dehaen, W.; Irannejad, V.S. PEI grafted Fe_3O_4@SiO_2@SBA-15 labeled FA as a pH-sensitive mesoporous magnetic and biocompatible nanocarrier for targeted delivery of doxorubicin to MCF-7 cell line. *Colloids Surf. A Physicochem. Eng. Asp.* **2021**, *615*, 126302. [CrossRef]
353. Obireddy, S.R.; Lai, W.-F. ROS-Generating Amine-Functionalized Magnetic Nanoparticles Coupled with Carboxymethyl Chitosan for pH-Responsive Release of Doxorubicin. *Int. J. Nanomed.* **2022**, *17*, 589–601. [CrossRef]
354. Korolkov, I.V.; Ludzik, K.; Kozlovskiy, A.L.; Fadeev, M.S.; Shumskaya, A.E.; Gorin, Y.G.; Jazdzewska, M.; Anisovich, M.; Rusakov, V.S.; Zdorovets, M.V. Immobilization of carboranes on Fe_3O_4-polymer nanocomposites for potential application in boron neutron cancer therapy. *Colloids Surfaces A: Physicochem. Eng. Asp.* **2020**, *601*, 125035. [CrossRef]
355. Rashid, Z.; Shokri, F.; Abbasi, A.; Khoobi, M.; Zarnani, A. Surface modification and bioconjugation of anti-CD4 monoclonal antibody to magnetic nanoparticles as a highly efficient affinity adsorbent for positive selection of peripheral blood T CD4+ lymphocytes. *Int. J. Biol. Macromol.* **2020**, *161*, 729–737. [CrossRef]
356. Sundar, S.; Ganesh, V. Bio-assisted preparation of efficiently architectured nanostructures of γ-Fe_2O_3 as a molecular recognition platform for simultaneous detection of biomarkers. *Sci. Rep.* **2020**, *10*, 15071. [CrossRef] [PubMed]
357. Parsian, M.; Mutlu, P.; Yalcin, S.; Gunduz, U. Characterization of gemcitabine loaded polyhydroxybutyrate coated magnetic nanoparticles for targeted drug delivery. *Anti-Cancer Agents Med. Chem.* **2020**, *20*, 1233–1240. [CrossRef]
358. Lee, X.J.; Lim, H.N.; Gowthaman, N.S.K.; Rahman, M.B.A.; Abdullah, C.A.C.; Muthoosamy, K. In-situ surface functionalization of superparamagnetic reduced graphene oxide—Fe_3O_4 nanocomposite via Ganoderma lucidum extract for targeted cancer therapy application. *Appl. Surf. Sci.* **2020**, *512*, 145738. [CrossRef]
359. Ashjari, M.; Panahandeh, F.; Niazi, Z.; Abolhasani, M.M. Synthesis of PLGA–mPEG star-like block copolymer to form micelle loaded magnetite as a nanocarrier for hydrophobic anticancer drug. *J. Drug Deliv. Sci. Technol.* **2020**, *56*, 101563. [CrossRef]
360. Khan, B.; Nawaz, M.; Price, G.J.; Hussain, R.; Baig, A.; Haq, S.; Rehman, W.; Waseem, M. In vitro sustained release of gallic acid from the size-controlled PEGylated magnetite nanoparticles. *Chem. Pap.* **2021**, *75*, 5339–5352. [CrossRef]
361. Harris, R.A. The PEGylated and non-PEGylated interaction of the anticancer drug 5-fluorouracil with paramagnetic Fe_3O_4 nanoparticles as drug carrier. *J. Mol. Liq.* **2022**, *360*, 119515. [CrossRef]
362. Fuentes-Baile, M.; Pérez-Valenciano, E.; García-Morales, P.; Romero, C.d.; Bello-Gil, D.; Barberá, V.M.; Rodríguez-Lescure, Á.; Sanz, J.M.; Alenda, C.; Saceda, M. CLytA-DAAO Chimeric Enzyme Bound to Magnetic Nanoparticles. A New Therapeutical Approach for Cancer Patients? *Int. J. Mol. Sci.* **2021**, *22*, 1477. [CrossRef]
363. Rezaei, A.; Morsali, A.; Bozorgmehr, M.R.; Nasrabadi, M. Quantum chemical analysis of 5-aminolevulinic acid anticancer drug delivery systems: Carbon nanotube, –COOH functionalized carbon nanotube and iron oxide nanoparticle. *J. Mol. Liq.* **2021**, *340*, 117182. [CrossRef]
364. Karade, V.C.; Sharma, A.; Dhavale, R.P.; Dhavale, R.P.; Shingte, S.R.; Patil, P.S.; Kim, J.H.; Zahn, D.R.T.; Chougale, A.D.; Salvan, G.; et al. APTES monolayer coverage on self-assembled magnetic nanospheres for controlled release of anticancer drug Nintedanib. *Sci. Rep.* **2021**, *11*, 5674. [CrossRef]
365. Marycz, K.; Kornicka-Garbowska, K.; Patej, A.; Sobierajska, P.; Kotela, A.; Turlej, E.; Kepska, M.; Bienko, A.; Wiglusz, R.J. Aminopropyltriethoxysilane (APTES)-Modified Nanohydroxyapatite (nHAp) Incorporated with Iron Oxide (IO) Nanoparticles Promotes Early Osteogenesis, Reduces Inflammation and Inhibits Osteoclast Activity. *Materials* **2022**, *15*, 2095. [CrossRef]
366. Dhavale, R.P.; Dhavale, R.P.; Sahoo, S.C.; Kollu, P.; Jadhav, S.U.; Patil, P.S.; Dongale, T.D.; Chougale, A.D.; Patil, P.B. Chitosan coated magnetic nanoparticles as carriers of anticancer drug Telmisartan: pH-responsive controlled drug release and cytotoxicity studies. *J. Phys. Chem. Solids* **2021**, *148*, 109749. [CrossRef]
367. Taheri-Kafrani, A.; Shirzadfar, H.; Abbasi Kajani, A.; Kudhair, B.K.; Jasim Mohammed, L.; Mohammadi, S.; Lotfi, F. Functionalized graphene oxide/Fe_3O_4 nanocomposite: A biocompatible and robust nanocarrier for targeted delivery and release of anticancer agents. *J. Biotechnol.* **2021**, *331*, 26–36. [CrossRef]

368. Al-Jameel, S.S.; Rehman, S.; Almessiere, M.A.; Khan, F.A.; Slimani, Y.; Al-Saleh, N.S.; Manikandan, A.; Al-Suhaimi, E.A.; Baykal, A. Anti-microbial and anti-cancer activities of $Mn_{0.5}Zn_{0.5}Dy_xFe_{2-x}O_4$ ($x \leq 0.1$) nanoparticles. *Artif. Cells Nanomed. Biotechnol.* **2021**, *49*, 493–499. [CrossRef]
369. Tomeh, M.A.; Hadianamrei, R.; Xu, D.; Brown, S.; Zhao, X. Peptide-functionalised magnetic silk nanoparticles produced by a swirl mixer for enhanced anticancer activity of ASC-J9. *Colloids Surf. B Biointerfaces* **2022**, *216*, 112549. [CrossRef] [PubMed]
370. Sugito, S.F.A.; Firdaus, F.; Aung, Y.; Sakti, S.C.W.; Chiu, H.-T.; Fahmi, M.Z. In situ tailoring of carbon dots-metal ferrite nanohybrid as multipurpose marker agent of HeLa cancer cells. *J. Mater. Res.* **2022**, *37*, 1941–1951. [CrossRef]
371. Ramezanpour, A.; Karami, K.; Kharaziha, M.; Bayat, P.; Jamshidian, N. Smart poly(amidoamine) dendron-functionalized magnetic graphene oxide for cancer therapy. *New J. Chem.* **2022**, *46*, 5052–5064. [CrossRef]
372. Sagir, T.; Huysal, M.; Senel, M.; Isık, S.; Burgucu, N.; Tabakoglu, O.; Zaim, M. Folic acid conjugated PAMAM-modified mesoporous silica-coated superparamagnetic iron oxide nanoparticles for potential cancer therapy. *J. Colloid Interface Sci.* **2022**, *625*, 711–721. [CrossRef]
373. Yeganeh, F.E.; Yeganeh, A.E.; Yousefi, M.; Far, B.F.; Akbarzadeh, I.; Bokov, D.O.; Raahemifar, K.; Soltani, M. Formulation and Characterization of Poly (Ethylene Glycol)-Coated Core-Shell Methionine Magnetic Nanoparticles as a Carrier for Naproxen Delivery: Growth Inhibition of Cancer Cells. *Cancers* **2022**, *14*, 1797. [CrossRef]
374. Serio, F.; Silvestri, N.; Avugadda, S.K.; Nucci, G.E.P.; Nitti, S.; Onesto, V.; Catalano, F.; D'Amone, E.; Gigli, G.; del Mercato, L.L.; et al. Co-loading of doxorubicin and iron oxide nanocubes in polycaprolactone fibers for combining Magneto-Thermal and chemotherapeutic effects on cancer cells. *J. Colloid Interface Sci.* **2022**, *607*, 34–44. [CrossRef]
375. Suhasini, A.; Kumar, K.P.V.; Sheela, A.M.; Sheenkumar, N. Electrical and Electrochemical studies of Polyurethane diol/Polycaprolactone-Iron Oxide nanocomposites. *IOP Conf. Ser. Mater. Sci. Eng.* **2020**, *983*, 012009. [CrossRef]
376. Bahjat, H.H.; Ismail, R.A.; Sulaiman, G.M.; Mohammed, H.A.; Al-Omar, M.; Mohammed, S.A.A.; Khan, R.A. Preparation of Iron Oxide and Titania-Based Composite, Core-Shell Populated, Nanoparticulates Material by Two-Step LASER Ablation in Aqueous Media as Antimicrobial and Anticancer Agents. *Bioinorg. Chem. Appl.* **2022**, *2022*, 1854473. [CrossRef] [PubMed]
377. Hosseini, S.F.; Eshaghi, Z. Synthesis of Bio-Nanomagnetite and Its Optimized Conditions for Phthalate Absorption. *Int. J. Eng. Sci. Technol.* **2020**, *4*, 3. [CrossRef]
378. Kurniawan, D.W.; Booijink, R.; Pater, L.; Wols, I.; Vrynas, A.; Storm, G.; Prakash, J.; Bansal, R. Fibroblast growth factor 2 conjugated superparamagnetic iron oxide nanoparticles (FGF2-SPIONs) ameliorate hepatic stellate cells activation in vitro and acute liver injury in vivo. *J. Control. Release* **2020**, *328*, 640–652. [CrossRef]
379. Zachanowicz, E.; Kulpa-Greszta, M.; Tomaszewska, A.; Gazińska, M.; Marędziak, M.; Marycz, K.; Pazik, R. Multifunctional properties of binary polyrhodanine manganese ferrite nanohybrids—from the energy converters to biological activity. *Polymers* **2020**, *12*, 2934. [CrossRef] [PubMed]
380. Rong, R.; Zhang, Y.; Tan, W.; Hu, T.; Wang, X.; Gui, Z.; Gong, J.; Xu, X. Evidence of Translocation of Oral Zn^{2+} Doped Magnetite Nanoparticles across the Small Intestinal Wall of Mice and Deposition in Spleen: Unique Advantage in Biomedical Applications. *ACS Appl. Bio Mater.* **2020**, *3*, 7919–7929. [CrossRef]
381. Yang, L.; Fu, L.; Li, B.; Ma, J.; Li, C.; Jin, T.; Gu, W. Fluorescence enhancement method for enrofloxacin extraction by core-shell magnetic microspheres. *Aust. J. Chem.* **2020**, *73*, 1105–1111. [CrossRef]
382. Yeganeh, F.E.; Yousefi, M.; Hekmati, M.; Bikhof, M. An experimental research on pH-responsive amino acid-coated $Ni_{(1-x)}Co_xFe_2O_4$ nanoparticles as a nano-carrier for drug delivery and biological applications. *Chem. Pap.* **2021**, *75*, 6047–6057. [CrossRef]
383. Amiri, M.A.; Aghamaali, M.R.; Parsian, H.; Tashakkorian, H. Coenzyme Q0 immobilized on magnetic nanoparticle: Synthesis and antitumoral effect on saos, MCF7 and hela cell lines. *Iran. J. Pharm. Res.* **2020**, *19*, 394–409. [CrossRef]
384. Micheletti, G.; Boga, C.; Telese, D.; Cassani, M.C.; Boanini, E.; Nitti, P.; Ballarin, B.; Ghirri, A.; Barucca, G.; Rinaldi, D. Magnetic Nanoparticles Coated with (R)-9-Acetoxystearic Acid for Biomedical Applications. *ACS Omega* **2020**, *5*, 12707–12715. [CrossRef]
385. Kawish, M.; Elhissi, A.; Jabri, T.; Iqbal, K.M.; Zahid, H.; Shah, M.R. Enhancement in oral absorption of ceftriaxone by highly functionalized magnetic iron oxide nanoparticles. *Pharmaceutics* **2020**, *12*, 492. [CrossRef]
386. Huang, J.; Guo, J.; Zou, X.; Zhu, J.; Wu, S.; Zhang, T. Bioinspired Heteromultivalent Chitosan- α -Fe_2O_3 /Gadofullerene Hybrid Composite for Enhanced Antibiotic-Resistant Bacterial Pneumonia. *J. Biomed. Nanotechnol.* **2021**, *17*, 1217–1228. [CrossRef]
387. Senthilkumar, M.; Pandimurugan, R.; Muthuvinayagam, M. Investigations on chitosan/α-Fe_2O_3 nanocomposite for efficient antibacterial activity. *Indian J. Appl. Res.* **2021**, 67–69. [CrossRef]
388. Fiejdasz, S.; Gilarska, A.; Strączek, T.; Nowakowska, M.; Kapusta, C. Magnetic Properties of Collagen–Chitosan Hybrid Materials with Immobilized Superparamagnetic Iron Oxide Nanoparticles (SPIONs). *Materials* **2021**, *14*, 7652. [CrossRef]
389. Ahmadi, M.; Pourmadadi, M.; Ghorbanian, S.A.; Yazdian, F.; Rashedi, H. Ultra pH-sensitive nanocarrier based on Fe_2O_3/chitosan/montmorillonite for quercetin delivery. *Int. J. Biol. Macromol.* **2021**, *191*, 738–745. [CrossRef]
390. Forouzan, M.M.; Ghasemzadeh, M.A.; Razavian, S.M.H. Preparation and characterization of a novel Fe_3O_4@PAA@MIL-100(Cr) metal-organic framework for the drug delivery of ciprofloxacin and investigation of its antibacterial activities. *Inorg. Nano-Metal Chem.* **2022**, *52*, 1318–1324. [CrossRef]
391. Mehrabi, F.; Shamspur, T.; Sheibani, H.; Mostafavi, A.; Mohamadi, M.; Hakimi, H.; Bahramabadi, R.; Salari, E. Silver-coated magnetic nanoparticles as an efficient delivery system for the antibiotics trimethoprim and sulfamethoxazole against *E. Coli* and *S. aureus*: Release kinetics and antimicrobial activity. *BioMetals* **2021**, *34*, 1237–1246. [CrossRef] [PubMed]

392. Casillas-Popova, S.N.; Bernad-Bernad, M.J.; Gracia-Mora, J. Modeling of adsorption and release kinetics of methotrexate from thermo/magnetic responsive $CoFe_2O_4$–$BaTiO_3$, $CoFe_2O_4$–$Bi_4Ti_3O_{12}$ and Fe_3O_4–$BaTiO_3$ core-shell magnetoelectric nanoparticles functionalized with PNIPAm. *J. Drug Deliv. Sci. Technol.* **2022**, *68*, 103121. [CrossRef]
393. Mathur, R.; Chauhan, R.P.; Singh, G.; Singh, S.; Varshney, R.; Kaul, A.; Jain, S.; Mishra, A.K. Tryptophan conjugated magnetic nanoparticles for targeting tumors overexpressing indoleamine 2,3 dioxygenase (IDO) and L-type amino acid transporter. *J. Mater. Sci. Mater. Med.* **2020**, *31*, 87. [CrossRef]
394. Li, S.; Liu, X.; Xu, J.; Wei, D.; Li, C.; Zhao, R.; Yang, L. Magnetic solid-phase extraction of norfloxacin by core-shell magnetic nanoparticles. *J. Coord. Chem.* **2022**. [CrossRef]
395. Zhong, B.; Mateu-Roldán, A.; Fanarraga, M.L.; Han, W.; Muñoz-Guerra, D.; González, J.; Tao Weng, L.; Ibarra, M.R.; Marquina, C.; Yeung, K.L. Graphene-encapsulated magnetic nanoparticles for safe and steady delivery of ferulic acid in diabetic mice. *Chem. Eng. J.* **2022**, *435*, 134466. [CrossRef]
396. Ali, T.H.; Mandal, A.M.; Heidelberg, T.; Hussen, R.S.D.; Goh, E.W. Ionic magnetic core-shell nanoparticles for DNA extraction. *RSC Adv.* **2020**, *10*, 38818–38830. [CrossRef]
397. Bilici, K.; Atac, N.; Muti, A.; Baylam, I.; Dogan, O.; Sennaroglu, A.; Can, F.; Acar, H.Y. Broad spectrum antibacterial photodynamic and photothermal therapy achieved with indocyanine green loaded SPIONs under near infrared irradiation. *Biomater. Sci.* **2020**, *8*, 4616–4625. [CrossRef]
398. Binandeh, M.; Rostamnia, S.; Karimi, F. MNPs-IHSPN nanoparticles in multi-application with absorption of bio drugs in vitro. *Biochem. Biophys. Rep.* **2021**, *28*, 101159. [CrossRef] [PubMed]
399. Gera, T.; Smausz, T.; Ajtai, T.; Kurilla, B.; Homik, Z.; Kopniczky, J.; Bozóki, Z.; Szabó-Révész, P.; Ambrus, R.; Hopp, B. Production of ibuprofen-magnetite nanocomposites by pulsed laser ablation. *J. Phys. D Appl. Phys.* **2021**, *54*, 395401. [CrossRef]
400. Avarand, S.; Morsali, A.; Heravi, M.M.; Beyramabadi, S.A. A quantum chemical study on the magnetic nanocarrier-tirapazamine drug delivery system. *Nanosyst. Phys. Chem. Math.* **2021**, *12*, 167–174. [CrossRef]
401. Parvaneh, S.; Khademi, F.; Abdi, G.; Alizadeh, A.; Mostafaie, A. Efficient conjugation of anti-HBsAg antibody to modified core-shell magnetic nanoparticles (Fe_3O_4@SiO_2/NH_2). *BioImpacts* **2021**, *11*, 237–244. [CrossRef]
402. Kawish, M.; Jabri, T.; Elhissi, A.; Zahid, H.; Iqbal, K.M.; Rao, K.; Gul, J.; Abdullah, M.; Shah, M.R. Galactosylated iron oxide nanoparticles for enhancing oral bioavailability of ceftriaxone. *Pharm. Dev. Technol.* **2021**, *26*, 291–301. [CrossRef] [PubMed]
403. Turrina, C.; Berensmeier, S.; Schwaminger, S.P. Bare iron oxide nanoparticles as drug delivery carrier for the short cationic peptide lasioglossin. *Pharmaceuticals* **2021**, *14*, 405. [CrossRef]
404. Shima, P. Damodaran, Mesoporous Magnetite Nanoclusters as Efficient Nanocarriers for Paclitaxel Delivery. *ChemistrySelect* **2020**, *5*, 9261–9268. [CrossRef]
405. Dabaghi, M.; Hilger, I. Magnetic nanoparticles behavior in biological solutions; The impact of clustering tendency on sedimentation velocity and cell uptake. *Materials* **2020**, *13*, 1644. [CrossRef]
406. Rauwel, E.; Al-Arag, S.; Salehi, H.; Amorim, C.O.; Cuisinier, F.; Guha, M.; Rosario, M.S.; Rauwel, P. Assessing cobalt metal nanoparticles uptake by cancer cells using live Raman spectroscopy. *Int. J. Nanomed.* **2020**, *15*, 7051–7062. [CrossRef]
407. Ilkhani, H.; Zhong, C.-J.; Hepel, M. Magneto-plasmonic nanoparticle grid biosensor with enhanced raman scattering and electrochemical transduction for the development of nanocarriers for targeted delivery of protected anticancer drugs. *Nanomaterials* **2021**, *11*, 1326. [CrossRef]
408. Vurro, F.; Jabalera, Y.; Mannucci, S.; Glorani, G.; Sola-Leyva, A.; Gerosa, M.; Romeo, A.; Romanelli, M.G.; Malatesta, M.; Calderan, L.; et al. Improving the cellular uptake of biomimetic magnetic nanoparticles. *Nanomaterials* **2021**, *11*, 766. [CrossRef]
409. Xiao, Z.; Zhang, Q.; Guo, X.; Villanova, J.; Hu, Y.; Külaots, I.; Garcia-Rojas, D.; Guo, W.; Colvin, V.L. Libraries of Uniform Magnetic Multicore Nanoparticles with Tunable Dimensions for Biomedical and Photonic Applications. *ACS Appl. Mater. Interfaces* **2020**, *12*, 41932–41941. [CrossRef] [PubMed]
410. Socoliuc, V.; Peddis, D.; Petrenko, V.I.; Avdeev, M.V.; Susan-Resiga, D.; Szabó, T.; Turcu, R.; Tombácz, E.; Vekas, L. Magnetic nanoparticle systems for nanomedicine–A materials science perspective. *Magnetochemistry* **2020**, *6*, 2. [CrossRef]
411. Schneider, M.G.M.; Martín, M.J.; Otarola, J.; Vakarelska, E.; Simeonov, V.; Lassalle, V.; Nedyalkova, M. Biomedical Applications of Iron Oxide Nanoparticles: Current Insights Progress and Perspectives. *Pharmaceutics* **2022**, *14*, 204. [CrossRef] [PubMed]
412. Aslam, H.; Shukrullah, S.; Naz, M.Y.; Fatima, H.; Hussain, H.; Ullah, S.; Assiri, M.A. Current and future perspectives of multifunctional magnetic nanoparticles based controlled drug delivery systems. *J. Drug Deliv. Sci. Technol.* **2022**, *67*, 102946. [CrossRef]
413. Lavorato, G.C.; Das, R.; Masa, J.A.; Phan, M.-H.; Srikanth, H. Hybrid magnetic nanoparticles as efficient nanoheaters in biomedical applications. *Nanoscale Adv.* **2021**, *3*, 867–888. [CrossRef]
414. Ovejero, J.G.; Gallo-Cordova, A.; Roca, A.G.; Morales, M.P.; Veintemillas-Verdaguer, S. Reproducibility and Scalability of Magnetic Nanoheater Synthesis. *Nanomaterials* **2021**, *11*, 2059. [CrossRef]
415. Das, R.; Witanachchi, C.; Nemati, Z.; Kalappattil, V.; Rodrigo, I.; García, J.Á.; Garaio, E.; Alonso, J.; Lam, V.D.; Le, A.; et al. Magnetic Vortex and Hyperthermia Suppression in Multigrain Iron Oxide Nanorings. *Appl. Sci.* **2020**, *10*, 787. [CrossRef]
416. Keshavarz, H.; Khavandi, A.; Alamolhoda, S.; Naimi-Jamal, M.R. PH-Sensitive magnetite mesoporous silica nanocomposites for controlled drug delivery and hyperthermia. *RSC Adv.* **2020**, *10*, 39008–39016. [CrossRef]

417. Jabalera, Y.; Oltolina, F.; Peigneux, A.; Sola-Leyva, A.; Carrasco-Jiménez, M.P.; Prat, M.; Jimenez-Lopez, C.; Iglesias, G.R. Nanoformulation design including MamC-mediated biomimetic nanoparticles allows the simultaneous application of targeted drug delivery and magnetic hyperthermia. *Polymers* **2020**, *12*, 1832. [CrossRef]
418. Gahrouei, Z.E.; Labbaf, S.; Kermanpur, A. Cobalt doped magnetite nanoparticles: Synthesis, characterization, optimization and suitability evaluations for magnetic hyperthermia applications. *Phys. E Low-Dimens. Syst. Nanostruct.* **2020**, *116*, 113759. [CrossRef]
419. Rajan, A.; Sahu, N.K. Review on magnetic nanoparticle-mediated hyperthermia for cancer therapy. *J. Nanoparticle Res.* **2020**, *22*, 319. [CrossRef]
420. Oltolina, F.; Peigneux, A.; Colangelo, D.; Clemente, N.; D'Urso, A.; Valente, G.; Iglesias, G.R.; Jiménez-Lopez, C.; Prat, M. Biomimetic Magnetite Nanoparticles as Targeted Drug Nanocarriers and Mediators of Hyperthermia in an Experimental Cancer Model. *Cancers* **2020**, *12*, 2564. [CrossRef] [PubMed]
421. Seynhaeve, A.L.B.; Amin, M.; Haemmerich, D.; van Rhoon, G.C.; ten Hagen, T.L.M. Hyperthermia and smart drug delivery systems for solid tumor therapy. *Adv. Drug Deliv. Rev.* **2020**, *163–164*, 125–144. [CrossRef]
422. Martinez-Boubeta, C.; Simeonidis, K.; Oró, J.; Makridis, A.; Serantes, D.; Balcells, L. Finding the Limits of Magnetic Hyperthermia on Core-Shell Nanoparticles Fabricated by Physical Vapor Methods. *Magnetochemistry* **2021**, *7*, 49. [CrossRef]
423. Yu, X.; Ding, S.; Yang, R.; Wu, C.; Zhang, W. Research progress on magnetic nanoparticles for magnetic induction hyperthermia of malignant tumor. *Ceram. Int.* **2021**, *47*, 5909–5917. [CrossRef]
424. Szczęch, M.; Orsi, D.; Łopuszyńska, N.; Cristofolini, L.; Jasiński, K.; Węglarz, W.Ł.P.; Albertini, F.; Kereïche, S.; Szczepanowicz, K. Magnetically responsive polycaprolactone nanocarriers for application in the biomedical field: Magnetic hyperthermia, magnetic resonance imaging, and magnetic drug delivery. *RSC Adv.* **2020**, *10*, 43607–43618. [CrossRef]
425. Didarian, R.; Vargel, I. Treatment of tumour tissue with radiofrequency hyperthermia (using antibody-carrying nanoparticles). *IET Nanobiotechnol.* **2021**, *15*, 639–653. [CrossRef]
426. Veres, T.; Voniatis, C.; Molnár, K.; Nesztor, D.; Fehér, D.; Ferencz, A.; Gresits, I.; Thuróczy, G.; Márkus, B.G.; Simon, F.; et al. An Implantable Magneto-Responsive Poly(aspartamide) Based Electrospun Scaffold for Hyperthermia Treatment. *Nanomaterials* **2022**, *12*, 1476. [CrossRef]
427. Yin, P.; Wei, C.; Jin, X.; Yu, X.; Wu, C.; Zhang, W. Magnetic polyvinyl alcohol microspheres with self-regulating temperature hyperthermia and CT/MR imaging for arterial embolization. *Polym. Bull.* **2022**. [CrossRef]
428. Ferreira, L.P.; Reis, C.P.; Robalo, T.T.; Melo Jorge, M.E.; Ferreira, P.; Gonçalves, J.; Hajalilou, A.; Cruz, M.M. Assisted Synthesis of Coated Iron Oxide Nanoparticles for Magnetic Hyperthermia. *Nanomaterials* **2022**, *12*, 1870. [CrossRef]
429. Buschmann, H.M. Critical review of heat transfer experiments in ferrohydrodynamic pipe flow utilising ferronanofluids. *Int. J. Therm. Sci.* **2020**, *157*, 106426. [CrossRef]
430. Socoliuc, V.; Avdeev, M.V.; Kuncser, V.; Turcu, R.; Tombácz, E.; Vékás, L. Ferrofluids and bio-ferrofluids: Looking back and stepping forward. *Nanoscale* **2022**, *14*, 4786–4886. [CrossRef] [PubMed]
431. Mortezaee, K.; Narmani, A.; Salehi, M.; Bagheri, H.; Farhood, B.; Haghi-Aminjan, H.; Najafi, M. Synergic effects of nanoparticles-mediated hyperthermia in radiotherapy/chemotherapy of cancer. *Life Sci.* **2021**, *269*, 119020. [CrossRef] [PubMed]
432. Maksoud, M.I.A.A.; Ghobashy, M.M.; Kodous, A.S.; Fahim, R.A.; Osman, A.I.; Al-Muhtaseb, A.H.; Rooney, D.W.; Mamdouh, M.A.; Nady, N.; Ashour, A.H. Insights on magnetic spinel ferrites for targeted drug delivery and hyperthermia applications. *Nanotechnol. Rev.* **2022**, *11*, 372–413. [CrossRef]
433. Papadopoulos, C.; Kolokithas-Ntoukas, A.; Moreno, R.; Fuentes, D.; Loudos, G.; Loukopoulos, V.C.; Kagadis, G.C. Using kinetic Monte Carlo simulations to design efficient magnetic nanoparticles for clinical hyperthermia. *Med. Phys.* **2022**, *49*, 547–567. [CrossRef]
434. Weeber, R.; Kreissl, P.; Holm, C. Magnetic field controlled behavior of magnetic gels studied using particle-based simulations. *Phys. Sci. Rev.* **2021**. [CrossRef]
435. Ilg, P.; Kroger, M. Dynamics of interacting magnetic nanoparticles: Effective behavior from competition between Brownian and Néel relaxation. *Phys. Chem. Chem. Phys.* **2020**, *22*, 22244–22259. [CrossRef]
436. Jin, D.; Kim, S.H.; Kim, H. Concentration and Magnetic Field Effects on Thermal Fluctuation of Magnetic Weight of Magnetite Nanoparticles During Agglomeration Under Magnetic Field. *Bull. Korean Chem. Soc.* **2020**, *41*, 628–633. [CrossRef]
437. Can, M.M.; Bairam, C.; Aksoy, S.; Kuruca, D.S.; Kaneko, S.; Aktaş, Z.; Öncül, M.O. Effect of Ti Atoms on Néel Relaxation Mechanism at Magnetic Heating Performance of Iron Oxide Nanoparticles. *Coatings* **2022**, *12*, 481. [CrossRef]
438. Ge, M.; Li, Y.; Zhu, C.; Liang, G.; Jahangir Alam, S.M.; Hu, G.; Gui, Y.; Rashid, M.J. Preparation of organic-modified magadiite–magnetic nanocomposite particles as an effective nanohybrid drug carrier material for cancer treatment and its properties of sustained release mechanism by Korsmeyer–Peppas kinetic model. *J. Mater. Sci.* **2021**, *56*, 14270–14286. [CrossRef]
439. Köhler, T.; Feoktystov, A.; Petracic, O.; Kentzinger, E.; Bhatnagar-Schöffmann, T.; Feygenson, M.; Nandakumaran, N.; Landers, J.; Wende, H.; Cervellino, A.; et al. Mechanism of magnetization reduction in iron oxide nanoparticles. *Nanoscale* **2021**, *13*, 6965–6976. [CrossRef] [PubMed]
440. Shreyash, N.; Sonker, M.; Bajpai, S.; Tiwary, S.K. Review of the Mechanism of Nanocarriers and Technological Developments in the Field of Nanoparticles for Applications in Cancer Theragnostics. *ACS Appl. Bio Mater.* **2021**, *4*, 2307–2334. [CrossRef] [PubMed]

441. Iacob, N.; Kuncser, A.; Comanescu, C.; Palade, P.; Kuncser, V. Optimization of magnetic fluid hyperthermia with respect to nanoparticle shape-related parameters: Case of magnetite ellipsoidal nanoparticles. *J. Nanopart. Res.* **2020**, *22*, 138. [CrossRef]
442. Stoicescu, C.S.; Culita, D.; Stanica, N.; Papa, F.; State, R.N.; Munteanu, G. Temperature programmed reduction of a core-shell synthetic magnetite: Dependence on the heating rate of the reduction mechanism. *Thermochim. Acta* **2022**, *709*, 179146. [CrossRef]
443. Liao, L.; Cen, D.; Fu, Y.; Liu, B.; Fang, C.; Wang, Y.; Cai, X.; Li, X.; Wu, H.B.; Han, G. Biodegradable MnFe-hydroxide nanocapsules to enable multi-therapeutics delivery and hypoxia-modulated tumor treatment. *J. Mater. Chem. B* **2020**, *8*, 3929–3938. [CrossRef]
444. Zhou, H.; Guo, M.; Li, J.; Qin, F.; Wang, Y.; Liu, T.; Liu, J.; Sabet, Z.F.; Wang, Y.; Liu, Y.; et al. Hypoxia-Triggered Self-Assembly of Ultrasmall Iron Oxide Nanoparticles to Amplify the Imaging Signal of a Tumor. *J. Am. Chem. Soc.* **2021**, *143*, 1846–1853. [CrossRef]
445. Farinha, P.; Coelho, J.M.P.; Reis, C.P.; Gaspar, M.M. A comprehensive updated review on magnetic nanoparticles in diagnostics. *Nanomaterials* **2021**, *11*, 3432. [CrossRef]
446. Avolio, M.; Innocenti, C.; Lascialfari, A.; Mariani, M.; Sangregorio, C. Medical Applications of Magnetic Nanoparticles. *Springer Ser. Mater. Sci.* **2021**, *308*, 327–351. [CrossRef]
447. Aisida, S.O.; Akpa, P.A.; Ahmad, I.; Zhao, T.-K.; Maaza, M.; Ezema, F.I. Bio-inspired encapsulation and functionalization of iron oxide nanoparticles for biomedical applications. *Eur. Polym. J.* **2020**, *122*, 109371. [CrossRef]
448. Kolishetti, N.; Vashist, A.; Arias, A.Y.; Atluri, V.; Dhar, S.; Nair, M. Recent advances, status, and opportunities of magneto-electric nanocarriers for biomedical applications. *Mol. Asp. Med.* **2022**, *83*, 101046. [CrossRef]
449. Singh, R.; Pal, D.; Chattopadhyay, S. Target-Specific Superparamagnetic Hydrogel with Excellent pH Sensitivity and Reversibility: A Promising Platform for Biomedical Applications. *ACS Omega* **2020**, *5*, 21768–21780. [CrossRef] [PubMed]
450. Xiao, Y.; Du, J. Superparamagnetic nanoparticles for biomedical applications. *J. Mater. Chem. B* **2020**, *8*, 354–367. [CrossRef] [PubMed]
451. Dash, P.; Raut, S.; Jena, M.; Nayak, B. Harnessing the biomedical properties of ferromagnetic α-Fe2O3 NPs with a plausible formation mechanism. *Ceram. Int.* **2020**, *46*, 26190–26204. [CrossRef]
452. Sheikhpour, M.; Arabi, M.; Kasaeian, A.; Rabei, A.R.; Taherian, Z. Role of nanofluids in drug delivery and biomedical technology: Methods and applications. *Nanotechnol. Sci. Appl.* **2020**, *13*, 47–59. [CrossRef]
453. Yang, H.Y.; Li, Y.; Lee, D.S. Functionalization of Magnetic Nanoparticles with Organic Ligands toward Biomedical Applications. *Adv. NanoBio Res.* **2021**, *1*, 2000043. [CrossRef]
454. Monteserín, M.; Larumbe, S.; Martínez, A.V.; Burgui, S.; Martín, L.F. Recent Advances in the Development of Magnetic Nanoparticles for Biomedical Applications. *J. Nanosci. Nanotechnol.* **2021**, *21*, 2705–2741. [CrossRef]
455. Baryeh, K.; Attia, M.; Ulloa, J.C.; Ye, J.Y. Magnetic nanoparticle-based hybrid materials in the biomedical field: Fundamentals and applications. In *Magnetic Nanoparticle-Based Hybrid Materials*; Woodhead Publishing: Cambridge, UK, 2021; pp. 387–423. [CrossRef]
456. Saadatmand, S.E.; Kavousi, S.M.; Alam, N.R. The investigation of conductivity of magnetic nanoparticles in the vascular network by DCC method and the effect of forces on the efficiency of targeted magnetic drug delivery. *Front. Biomed. Technol.* **2021**, *8*, 26–36. [CrossRef]
457. Canaparo, R.; Foglietta, F.; Limongi, T.; Serpe, L. Biomedical applications of reactive oxygen species generation by metal nanoparticles. *Materials* **2021**, *14*, 53. [CrossRef]
458. Almeida, A.F.; Vinhas, A.; Gonçalves, A.I.; Miranda, M.S.; Rodrigues, M.T.; Gomes, M.E. Magnetic triggers in biomedical applications—Prospects for contact free cell sensing and guidance. *J. Mater. Chem. B* **2021**, *9*, 1259–1271. [CrossRef]
459. Anik, M.I.; Hossain, M.K.; Hossain, I.; Ahmed, I.; Doha, R.M. Biomedical applications of magnetic nanoparticles. *Magn. Nanoparticle-Based Hybrid Mater. Fundam. Appl.* **2021**, 463–497. [CrossRef]
460. Jiang, K.; Zhang, L.; Bao, G. Magnetic iron oxide nanoparticles for biomedical applications. *Curr. Opin. Biomed. Eng.* **2021**, *20*, 100330. [CrossRef] [PubMed]
461. Căpraru, A.; Moacă, E.-A.; Păcurariu, C.; Ianoş, R.; Lazău, R.; Barbu-Tudoran, L. Development and characterization of magnetic iron oxide nanoparticles using microwave for the combustion reaction ignition, as possible candidates for biomedical applications. *Powder Technol.* **2021**, *394*, 1026–1038. [CrossRef]
462. Papadopoulou, S.; Kolokithas-ntoukas, A.; Salvanou, E.-A.; Gaitanis, A.; Xanthopoulos, S.; Avgoustakis, K.; Gazouli, M.; Paravatou-petsotas, M.; Tsoukalas, C.; Bakandritsos, A.; et al. Chelator-free/chelator-mediated radiolabeling of colloidally stabilized iron oxide nanoparticles for biomedical imaging. *Nanomaterials* **2021**, *11*, 1677. [CrossRef]
463. Li, D.; Luo, Y.; Onidas, D.; He, L.; Jin, M.; Gazeau, F.; Pinson, J.; Mangeney, C. Surface functionalization of nanomaterials by aryl diazonium salts for biomedical sciences. *Adv. Colloid Interface Sci.* **2021**, *294*, 102479. [CrossRef]
464. Han, W.J.; Lee, J.H.; Lee, J.; Choi, H.J. Remote-controllable, tough, ultrastretchable, and magneto-sensitive nanocomposite hydrogels with homogeneous nanoparticle dispersion as biomedical actuators, and their tuned structure, properties, and performances. *Compos. Part B Eng.* **2022**, *236*, 109802. [CrossRef]
465. Farzin, A.; Etesami, S.A.; Quint, J.; Memic, A.; Tamayol, A. Magnetic Nanoparticles in Cancer Therapy and Diagnosis. *Adv. Healthc. Mater.* **2020**, *9*. Available online: https://onlinelibrary.wiley.com/doi/10.1002/adhm.201901058 (accessed on 30 June 2022). [CrossRef]
466. Chi, X.; Liu, K.; Luo, X.; Yin, Z.; Lin, H.; Gao, J. Recent advances of nanomedicines for liver cancer therapy. *J. Mater. Chem. B* **2020**, *8*, 3747–3771. [CrossRef] [PubMed]
467. Soares, P.I.; Romão, J.; Matos, R.; Silva, J.C.; Borges, J.P. Design and engineering of magneto-responsive devices for cancer theranostics: Nano to macro perspective. *Prog. Mater. Sci.* **2020**, *116*, 100742. [CrossRef]

468. Naud, C.; Thébault, C.; Carrière, M.; Hou, Y.; Morel, R.; Berger, F.; Diény, B.; Joisten, H. Cancer treatment by magneto-mechanical effect of particles, a review. *Nanoscale Adv.* **2020**, *2*, 3632–3655. [CrossRef]
469. Indoria, S.; Singh, V.; Hsieh, M.-F. Recent advances in theranostic polymeric nanoparticles for cancer treatment: A review. *Int. J. Pharm.* **2020**, *582*, 119314. [CrossRef]
470. Gillson, J.; Ramaswamy, Y.; Singh, G.; Gorfe, A.A.; Pavlakis, N.; Samra, J.; Mittal, A.; Sahni, S. Small molecule KRAS inhibitors: The future for targeted pancreatic cancer therapy? *Cancers* **2020**, *12*, 1341. [CrossRef]
471. Magro, M.; Venerando, A.; Macone, A.; Canettieri, G.; Agostinelli, E.; Vianello, F. Nanotechnology-based strategies to develop new anticancer therapies. *Biomolecules* **2020**, *10*, 735. [CrossRef] [PubMed]
472. Bloise, N.; Massironi, A.; Della Pina, C.; Alongi, J.; Siciliani, S.; Manfredi, A.; Biggiogera, M.; Rossi, M.; Ferruti, P.; Ranucci, E.; et al. Extra-Small Gold Nanospheres Decorated with a Thiol Functionalized Biodegradable and Biocompatible Linear Polyamidoamine as Nanovectors of Anticancer Molecules. *Front. Bioeng. Biotechnol.* **2020**, *8*, 132. [CrossRef] [PubMed]
473. Do Nascimento, T.; Todeschini, A.R.; Santos-Oliveira, R.; Monteiro, M.S.S.B.; Souza, V.T.; Ricci-Júnior, E. Trends in nanomedicines for cancer treatment. *Curr. Pharm. Des.* **2020**, *26*, 3579–3600. [CrossRef] [PubMed]
474. Pandey, N.; Menon, J.U.; Takahashi, M.; Hsieh, J.-T.; Yang, J.; Nguyen, K.T.; Wadajkar, A.S. Thermo-responsive fluorescent nanoparticles for multimodal imaging and treatment of cancers. *Nanotheranostics* **2020**, *4*, 1–13. [CrossRef] [PubMed]
475. Guo, Y.-Y.; Huang, L.; Zhang, Z.-P.; Fu, D.-H. Strategies for Precise Engineering and Conjugation of Antibody Targeted-nanoparticles for Cancer Therapy. *Curr. Med. Sci.* **2020**, *40*, 463–473. [CrossRef]
476. Mukherjee, S.; Liang, L.; Veiseh, O. Recent advancements of magnetic nanomaterials in cancer therapy. *Pharmaceutics* **2020**, *12*, 147. [CrossRef] [PubMed]
477. Avval, Z.M.; Malekpour, L.; Raeisi, F.; Babapoor, A.; Mousavi, S.M.; Hashemi, S.A.; Salari, M. Introduction of magnetic and supermagnetic nanoparticles in new approach of targeting drug delivery and cancer therapy application. *Drug Metab. Rev.* **2020**, *52*, 157–184. [CrossRef]
478. Majidzadeh, H.; Araj-Khodaei, M.; Ghaffari, M.; Torbati, M.; Ezzati Nazhad Dolatabadi, J.; Hamblin, M.R. Nano-based delivery systems for berberine: A modern anti-cancer herbal medicine. *Colloids Surf. B Biointerfaces* **2020**, *194*, 111188. [CrossRef]
479. Gorbet, M.-J.; Ranjan, A. Cancer immunotherapy with immunoadjuvants, nanoparticles, and checkpoint inhibitors: Recent progress and challenges in treatment and tracking response to immunotherapy. *Pharmacol. Ther.* **2020**, *207*, 107456. [CrossRef]
480. Mukherjee, B.; Al Hoque, A.; Dutta, D.; Paul, B.; Mukherjee, A.; Mallick, S. Nanoformulated drug delivery of potential betulinic acid derivatives: A promising approach toward cancer therapy. In *Nanomedicine for Bioactives: Healthcare Applications*; Springer: Singapore, 2020; pp. 127–153. [CrossRef]
481. Cheng, H.-W.; Tsao, H.-Y.; Chiang, C.-S.; Chen, S.-Y. Advances in Magnetic Nanoparticle-Mediated Cancer Immune-Theranostics. *Adv. Healthcare Mater.* **2021**, *10*, 2001451. [CrossRef]
482. Zhang, Y.; Li, X.; Zhang, Y.; Wei, J.; Wang, W.; Dong, C.; Xue, Y.; Liu, M.; Pei, R. Engineered Fe_3O_4-based nanomaterials for diagnosis and therapy of cancer. *New J. Chem.* **2021**, *45*, 7918. [CrossRef]
483. Rahman, M.; Alam, K.; Hafeez, A.; Ilyas, R.; Beg, S. Metallic nanoparticles in drug delivery and cancer treatment. In *Nanoformulation Strategies for Cancer Treatment*; Elsevier: Amsterdam, The Netherlands, 2021; pp. 107–119. [CrossRef]
484. Jayaraman, M.; Dutta, P.; Telang, J.; Krishnan, B.B.S. Nanoparticles for Cancer Therapy. In *Nanomedicine for Cancer Diagnosis and Therapy*; Springer: Singapore, 2021; pp. 1–45. [CrossRef]
485. Nedyalkova, M.; Todorov, B.; Barazorda-Ccahuanac, H.L.; Madurga, S. Iron oxide Nanoparticles in Anticancer Drug Delivery and Imaging Diagnostics. In *Magnetic Nanoparticles in Human Health and Medicine*; Wiley: Hoboken, NJ, USA, 2021; pp. 151–163.
486. Chen, W.; Sun, Z.; Lu, L. Targeted Engineering of Medicinal Chemistry for Cancer Therapy: Recent Advances and Perspectives. *Angew. Chem. Int. Ed.* **2021**, *60*, 5626–5643. [CrossRef] [PubMed]
487. Alromi, D.A.; Madani, S.Y.; Seifalian, A. Emerging application of magnetic nanoparticles for diagnosis and treatment of cancer. *Polymers* **2021**, *13*, 4146. [CrossRef] [PubMed]
488. Lorkowski, M.E.; Atukorale, P.U.; Ghaghada, K.B.; Karathanasis, E. Stimuli-Responsive Iron Oxide Nanotheranostics: A Versatile and Powerful Approach for Cancer Therapy. *Adv. Healthc. Mater.* **2021**, *10*, 2001044. [CrossRef] [PubMed]
489. Yang, K.; Zhang, S.; He, J.; Nie, Z. Polymers and inorganic nanoparticles: A winning combination towards assembled nanostructures for cancer imaging and therapy. *Nano Today* **2021**, *36*, 101046. [CrossRef]
490. Lafuente-Gómez, N.; Milán-Rois, P.; García-Soriano, D.; Luengo, Y.; Cordani, M.; Alarcón-Iniesta, H.; Salas, G.; Somoza, Á. Smart modification on magnetic nanoparticles dramatically enhances their therapeutic properties. *Cancers* **2021**, *13*, 4095. [CrossRef]
491. Cerqueira, M.; Belmonte-Reche, E.; Gallo, J.; Baltazar, F.; Bañobre-López, M. Magnetic Solid Nanoparticles and Their Counterparts: Recent Advances towards Cancer Theranostics. *Pharmaceutics* **2022**, *14*, 506. [CrossRef]
492. Ahmed, F.; Khan, M.A.; Haider, N.; Ahmad, M.Z.; Ahmad, J. Recent Advances in Theranostic Applications of Nanomaterials in Cancer. *Curr. Pharm. Des.* **2022**, *28*, 133–150. [CrossRef]
493. Morsink, M.; Parente, L.; Silva, F.; Abrantes, A.; Ramos, A.; Primo, I.; Willemen, N.; Sanchez-Lopez, E.; Severino, P.; Souto, E.B. Nanotherapeutics and Nanotheragnostics for Cancers: Properties, Pharmacokinetics, Biopharmaceutics, and Biosafety. *Curr. Pharm. Des.* **2022**, *28*, 104–115. [CrossRef]
494. Du, H.; Akakuru, O.U.; Yao, C.; Yang, F.; Wu, A. Transition metal ion-doped ferrites nanoparticles for bioimaging and cancer therapy. *Transl. Oncol.* **2022**, *15*, 101264. [CrossRef]

495. Maffei, M.E. Magnetic Fields and Cancer: Epidemiology, Cellular Biology, and Theranostics. *Int. J. Mol. Sci.* **2022**, *23*, 1339. [CrossRef] [PubMed]
496. Boutopoulos, I.D.; Lampropoulos, D.S.; Bourantas, G.C.; Miller, K.; Loukopoulos, V.C. Two-Phase Biofluid Flow Model for Magnetic Drug Targeting. *Symmetry* **2020**, *12*, 1083. [CrossRef]
497. Majee, S.; Shit, G.C. Modeling and simulation of blood flow with magnetic nanoparticles as carrier for targeted drug delivery in the stenosed artery. *Eur. J. Mech. B/Fluids* **2020**, *83*, 42–57. [CrossRef]
498. Tabaei, A.; Sadeghi, S.; Hosseinzadeh, S.; Bidabadi, M.; Xiong, Q.; Karimi, N. A simplified mathematical study of thermochemical preparation of particle oxide under counterflow configuration for use in biomedical applications. *J. Therm. Anal. Calorim.* **2020**, *139*, 2769–2779. [CrossRef]
499. Znoyko, S.L.; Orlova, A.V.; Bragina, V.A.; Nikitin, M.P.; Nikitin, P.I. Nanomagnetic lateral flow assay for high-precision quantification of diagnostically relevant concentrations of serum TSH. *Talanta* **2020**, *216*, 120961. [CrossRef] [PubMed]
500. Lanier, O.L.; Velez, C.; Arnold, D.P.; Dobson, J. Model of Magnetic Particle Capture Under Physiological Flow Rates for Cytokine Removal During Cardiopulmonary Bypass. *IEEE Trans. Biomed. Eng.* **2021**, *68*, 1198–1207. [CrossRef]
501. Zahn, D.; Klein, K.; Radon, P.; Berkov, D.; Erokhin, S.; Nagel, E.; Eichhorn, M.; Wiekhorst, F.; Dutz, S. Investigation of magnetically driven passage of magnetic nanoparticles through eye tissues for magnetic drug targeting. *Nanotechnology* **2020**, *31*, 495101. [CrossRef]
502. Forouzandehmehr, M.; Ghoytasi, I.; Shamloo, A.; Ghosi, S. Particles in coronary circulation: A review on modelling for drug carrier design. *Mater. Des.* **2022**, *216*, 110511. [CrossRef]
503. Eslami, P.; Albino, M.; Scavone, F.; Chiellini, F.; Morelli, A.; Baldi, G.; Cappiello, L.; Doumett, S.; Lorenzi, G.; Ravagli, C.; et al. Smart Magnetic Nanocarriers for Multi-Stimuli On-Demand Drug Delivery. *Nanomaterials* **2022**, *12*, 303. [CrossRef]
504. Kuznetsova, O.V.; Timerbaev, A.R. Magnetic nanoparticles for highly robust, facile and efficient loading of metal-based drugs. *J. Inorg. Biochem.* **2022**, *227*, 111685. [CrossRef]
505. Im, G.-B.; Jung, E.; Kim, Y.H.; Kim, Y.-J.; Kim, S.-W.; Jeong, G.-J.; Lee, T.-J.; Kim, D.-I.; Kim, J.; Hyeon, T.; et al. Endosome-triggered ion-releasing nanoparticles as therapeutics to enhance the angiogenic efficacy of human mesenchymal stem cells. *J. Control. Release* **2020**, *324*, 586–597. [CrossRef]
506. Real, D.A.; Bolaños, K.; Priotti, J.; Yutronic, N.; Kogan, M.J.; Sierpe, R.; Donoso-González, O. Cyclodextrin-modified nanomaterials for drug delivery: Classification and advances in controlled release and bioavailability. *Pharmaceutics* **2021**, *13*, 2131. [CrossRef]
507. Nguyen, D.T.; Nguyen, N.-M.; Vu, D.-M.; Tran, M.-D.; Ta, V.-T. On-demand release of drug from magnetic nanoparticle-loaded alginate beads. *J. Anal. Methods Chem.* **2021**, *2021*, 5576283. [CrossRef] [PubMed]
508. de Freitas e Castro, M.; Mendonça, T.T.; da Silva, L.F.; Gomez, J.G.C.; Sanchez Rodriguez, R.J. Carriers based on poly-3-hydroxyalkanoates containing nanomagnetite to trigger hormone release. *Int. J. Biol. Macromol.* **2021**, *166*, 448–458. [CrossRef]
509. Neves, R.P.; Bronze-Uhle, E.S.; Santos, P.L.; Lisboa-Filho, P.N.; Magdalena, A.G. Salicylic acid incorporation in Fe_3O_4-BSA nanoparticles for drug release. *Quim. Nova* **2021**, *44*, 824–829. [CrossRef]
510. Lu, C.-H.; Yeh, Y.-C. Fabrication of Multiresponsive Magnetic Nanocomposite Double-Network Hydrogels for Controlled Release Applications. *Small* **2021**, *17*, 2105997. [CrossRef] [PubMed]
511. Mandić, L.; Sadžak, A.; Erceg, I.; Baranović, G.; Šegota, S. The fine-tuned release of antioxidant from superparamagnetic nanocarriers under the combination of stationary and alternating magnetic fields. *Antioxidants* **2021**, *10*, 1212. [CrossRef] [PubMed]
512. Cui, J.; Huang, J.; Yan, Y.; Chen, W.; Wen, J.; Wu, X.; Liu, J.; Liu, H.; Huang, C. Ferroferric oxide loaded near-infrared triggered photothermal microneedle patch for controlled drug release. *J. Colloid Interface Sci.* **2022**, *617*, 718–729. [CrossRef]
513. Gil, C.J.; Li, L.; Hwang, B.; Cadena, M.; Theus, A.S.; Finamore, T.A.; Bauser-Heaton, H.; Mahmoudi, M.; Roeder, R.K.; Serpooshan, V. Tissue engineered drug delivery vehicles: Methods to monitor and regulate the release behavior. *J. Control. Release* **2022**, *349*, 143–155. [CrossRef]
514. Andjelković, L.; Jeremić, D.; Milenković, M.R.; Radosavljević, J.; Vulić, P.; Pavlović, V.; Manojlović, D.; Nikolić, A.S. Synthesis, characterization and in vitro evaluation of divalent ion release from stable $NiFe_2O_4$, $ZnFe_2O_4$ and core-shell $ZnFe_2O_4$@$NiFe_2O_4$ nanoparticles. *Ceram. Int.* **2020**, *46*, 3528–3533. [CrossRef]
515. Ranjbary, A.G.; Saleh, G.K.; Azimi, M.; Karimian, F.; Mehrzad, J.; Zohdi, J. Superparamagnetic Iron Oxide Nanoparticles Induce Apoptosis in HT-29 Cells by Stimulating Oxidative Stress and Damaging DNA. *Biol. Trace Elem. Res.* **2022**. [CrossRef] [PubMed]
516. Lee, J.J.; Pua, C.H.; Misran, M.; Lee, P.F. The rotational effect of magnetic particles on cellular apoptosis based on four electromagnet feedback control system. *Biomed. Eng. Appl. Basis Commun.* **2021**, *33*, 459. [CrossRef]
517. Ferraz, F.S.; López, J.L.; Lacerda, S.M.S.N.; Procópio, M.S.; Figueiredo, A.F.A.; Martins, E.M.N.; Guimarães, P.P.G.; Ladeira, L.O.; Kitten, G.T.; Dias, F.F.; et al. Biotechnological approach to induce human fibroblast apoptosis using superparamagnetic iron oxide nanoparticles. *J. Inorg. Biochem.* **2020**, *206*, 111017. [CrossRef]
518. Yadav, S.K.; Khan, Z.A.; Mishra, B.; Bahadur, S.; Kumar, A.; Yadav, B. The Toxic Side of Nanotechnology: An Insight into Hazards to Health and the Ecosystem. *Micro Nanosyst.* **2022**, *14*, 21–33. [CrossRef]
519. Fernández-Bertólez, N.; Costa, C.; Brandão, F.; Teixeira, J.P.; Pásaro, E.; Valdiglesias, V.; Laffon, B. Toxicological Aspects of Iron Oxide Nanoparticles. *Adv. Exp. Med. Biol.* **2022**, *1357*, 303–350. [CrossRef] [PubMed]

520. Jahanban-Esfahlan, R.; Derakhshankhah, H.; Haghshenas, B.; Massoumi, B.; Abbasian, M.; Jaymand, M. A bio-inspired magnetic natural hydrogel containing gelatin and alginate as a drug delivery system for cancer chemotherapy. *Int. J. Biol. Macromol.* **2020**, *156*, 438–445. [CrossRef]
521. Liu, Z.; Liu, J.; Cui, X.; Wang, X.; Zhang, L.; Tang, P. Recent Advances on Magnetic Sensitive Hydrogels in Tissue Engineering. *Front. Chem.* **2020**, *8*, 124. [CrossRef]
522. Chen, F.; Bian, M.; Nahmou, M.; Myung, D.; Goldberg, J.L. Fusogenic liposome-enhanced cytosolic delivery of magnetic nanoparticles. *RSC Adv.* **2021**, *57*, 35796–35805. [CrossRef]
523. Nuñez-Magos, L.; Lira-Escobedo, J.; Rodríguez-López, R.; Muñoz-Navia, M.; Castillo-Rivera, F.; Viveros-Méndez, P.X.; Araujo, E.; Encinas, A.; Saucedo-Anaya, S.A.; Aranda-Espinoza, S. Effects of DC Magnetic Fields on Magnetoliposomes. *Front. Mol. Biosci.* **2021**, *8*, 703417. [CrossRef]
524. Sriwidodo Umar, A.K.; Wathoni, N.; Zothantluanga, J.H.; Das, S.; Luckanagul, J.A. Liposome-polymer complex for drug delivery system and vaccine stabilization. *Heliyon* **2022**, *8*, e08934. [CrossRef]
525. Kumar, N.; Tyeb, S.; Verma, V. Recent advances on Metal oxide-polymer systems in targeted therapy and diagnosis: Applications and toxicological perspective. *J. Drug Deliv. Sci. Technol.* **2021**, *66*, 102814. [CrossRef]
526. Ezealigo, U.S.; Ezealigo, B.N.; Aisida, S.O.; Ezema, F.I. Iron oxide nanoparticles in biological systems: Antibacterial and toxicology perspective. *JCIS Open* **2021**, *4*, 100027. [CrossRef]
527. Novak, E.V.; Pyanzina, E.S.; Gupalo, M.A.; Mauser, N.J.; Kantorovich, S.S. Structural transitions and magnetic response of supramolecular magnetic polymerlike structures with bidisperse monomers. *Phys. Rev. E* **2022**, *105*, 054601. [CrossRef]
528. Iliasov, A.R.; Nizamov, T.R.; Naumenko, V.A.; Garanina, A.S.; Vodopyanov, S.S.; Nikitin, A.A.; Pershina, A.G.; Chernysheva, A.A.; Kan, Y.; Mogilnikov, P.S.; et al. Non-magnetic shell coating of magnetic nanoparticles as key factor of toxicity for cancer cells in a low frequency alternating magnetic field. *Colloids Surf. B* **2021**, *206*, 111931. [CrossRef]
529. Malhotra, N.; Lee, J.-S.; Liman, R.A.D.; Ruallo, J.M.S.; Villaflore, O.B.; Ger, T.-R.; Hsiao, C.-D. Potential toxicity of iron oxide magnetic nanoparticles: A review. *Molecules* **2020**, *25*, 3159. [CrossRef]
530. Kefeni, K.K.; Msagati, T.A.M.; Nkambule, T.T.; Mamba, B.B. Spinel ferrite nanoparticles and nanocomposites for biomedical applications and their toxicity. *Mater. Sci. Eng. C* **2020**, *107*, 110314. [CrossRef] [PubMed]
531. Cervantes, O.; Casillas, N.; Knauth, P.; Lopez, Z.; Virgen-Ortiz, A.; Lozano, O.; Delgado-Enciso, I.; Sámano, A.H.; Rosales, S.; Martinez-Ceseña, L.; et al. An easily prepared ferrofluid with high power absorption density and low cytotoxicity for biomedical applications. *Mater. Chem. Phys.* **2020**, *245*, 122752. [CrossRef]
532. Toropova, Y.G.; Motorina, D.S.; Gorshkova, M.; Gareev, K.G.; Korolev, D.V.; Muzhikyan, A.A. The effect of intravenous administration to rats of magnetite nanoparticles with various shells on the functional state and morphology of the endothelium and on antioxidant status. *Transl. Med.* **2020**, *7*, 52–64. [CrossRef]
533. Srikanth, K.; Nutalapati, V. Copper ferrite nanoparticles induced cytotoxicity and oxidative stress in Channel catfish ovary cells. *Chemosphere* **2022**, *287*, 132166. [CrossRef]
534. Wang, X.; Zhang, Y.; Tan, W.; Nie, K.; Xu, X. Protective effect of Fe_3O_4 nanoparticles on cadmium chloride-induced toxicity in the small intestine of mice. *J. Univ. Sci. Technol. China* **2020**, *50*, 887–893. [CrossRef]
535. Garcia-Fernandez, J.; Turiel, D.; Bettmer, J.; Jakubowski, N.; Panne, U.; Rivas García, L.; Llopis, J.; Sánchez González, C.; Montes-Bayón, M. In vitro and in situ experiments to evaluate the biodistribution and cellular toxicity of ultrasmall iron oxide nanoparticles potentially used as oral iron supplements. *Nanotoxicology* **2020**, *14*, 388–403. [CrossRef] [PubMed]
536. Radeloff, K.; Radeloff, A.; Tirado, M.R.; Scherzad, A.; Hagen, R.; Kleinsasser, N.H.; Hackenberg, S. Toxicity and functional impairment in human adipose tissue-derived stromal cells (Hascs) following long-term exposure to very small iron oxide particles (vsops). *Nanomaterials* **2020**, *10*, 741. [CrossRef]
537. Radeloff, K.; Tirado, M.R.; Haddad, D.; Breuer, K.; Müller, J.; Hochmuth, S.; Hackenberg, S.; Scherzad, A.; Kleinsasser, N.; Radeloff, A. Superparamagnetic iron oxide particles (VSOPS) show genotoxic effects but no functional impact on human adipose tissue-derived stromal cells (ASCS). *Materials* **2021**, *14*, 263. [CrossRef] [PubMed]
538. Kim, K.Y.; Chang, K.-A. Therapeutic potential of magnetic nanoparticle-based human adipose-derived stem cells in a mouse model of parkinson's disease. *Int. J. Mol. Sci.* **2021**, *22*, 654. [CrossRef] [PubMed]
539. Bag, J.; Mukherjee, S.; Ghosh, S.K.; Das, A.; Mukherjee, A.; Sahoo, J.K.; Tung, K.S.; Sahoo, H.; Mishra, M. Fe_3O_4 coated guargum nanoparticles as non-genotoxic materials for biological application. *Int. J. Biol. Macromol.* **2020**, *165*, 333–345. [CrossRef] [PubMed]
540. Janßen, H.C.; Angrisani, N.; Kalies, S.; Hansmann, F.; Kietzmann, M.; Warwas, D.P.; Behrens, P.; Reifenrath, J. Biodistribution, biocompatibility and targeted accumulation of magnetic nanoporous silica nanoparticles as drug carrier in orthopedics. *J. Nanobiotechnol.* **2020**, *18*, 14. [CrossRef]
541. Zandi, M.; Zare, M.; Nazari, H.; Ashjaee, M.; Zale, A.A. Investigating the effect of injection rate on the capture efficiency of nanoparticles in different geometries of stenosed vessel. *J. Magn. Magn. Mater.* **2022**, *544*, 168665. [CrossRef]
542. Liu, J.F.; Lan, Z.; Ferrari, C.; Stein, J.M.; Higbee-Dempsey, E.; Yan, L.; Amirshaghaghi, A.; Cheng, Z.; Issadore, D.; Tsourkas, A. Use of Oppositely Polarized External Magnets to Improve the Accumulation and Penetration of Magnetic Nanocarriers into Solid Tumors. *ACS Nano* **2020**, *14*, 142–152. [CrossRef]
543. Próspero, A.G.; Soares, G.A.; Moretto, G.M.; Quini, C.C.; Bakuzis, A.F.; De Arruda Miranda, J.R. Dynamic cerebral perfusion parameters and magnetic nanoparticle accumulation assessed by AC biosusceptometry. *Biomed. Tech.* **2020**, *65*, 343–351. [CrossRef]

544. Dahaghin, A.; Emadiyanrazavi, S.; Haghpanahi, M.; Salimibani, M.; Bahreinizad, H.; Eivazzadeh-Keihan, R.; Maleki, A. A comparative study on the effects of increase in injection sites on the magnetic nanoparticles hyperthermia. *J. Drug Deliv. Sci. Technol.* **2021**, *63*, 102542. [CrossRef]
545. Carter, T.J.; Agliardi, G.; Lin, F.; Ellis, M.; Jones, C.; Robson, M.; Richard-Londt, A.; Southern, P.; Lythgoe, M.; Thin, M.Z.; et al. Potential of Magnetic Hyperthermia to Stimulate Localized Immune Activation. *Small* **2021**, *17*, 2005241. [CrossRef] [PubMed]
546. Friedrich, R.P.; Janko, C.; Unterweger, H.; Lyer, S.; Alexiou, C. SPIONs and magnetic hybrid materials: Synthesis, toxicology and biomedical applicatiodddns. *Magn. Hybrid-Mater. Multi-Scale Model. Synth. Appl.* **2021**, 739–768. [CrossRef]
547. Khoei, A.J. Evaluation of potential immunotoxic effects of iron oxide nanoparticles (IONPs) on antioxidant capacity, immune responses and tissue bioaccumulation in common carp (Cyprinus carpio). *Comp. Biochem. Physiol. Part C Toxicol. Pharmacol.* **2021**, *244*, 109005. [CrossRef] [PubMed]
548. Tangra, A.K.; Singh, G. Investigation of cytotoxicity of superparamagnetic $KFeO_2$ nanoparticles on MCF-7 cell lines for biomedical applications. *J. Mater. Sci. Mater. Electron.* **2021**, *32*, 11232–11242. [CrossRef]
549. Khan, M.S.; Buzdar, S.A.; Hussain, R.; Afzal, G.; Jabeen, G.; Javid, M.A.; Iqbal, R.; Iqbal, Z.; Mudassir, K.B.; Saeed, S.; et al. Hematobiochemical, Oxidative Stress, and Histopathological Mediated Toxicity Induced by Nickel Ferrite ($NiFe_2O_4$) Nanoparticles in Rabbits. *Oxidative Med. Cell. Longev.* **2022**, *2022*, 5066167. [CrossRef]
550. Senthilkumar, N.; Sharma, P.K.; Sood, N.; Bhalla, N. Designing magnetic nanoparticles for in vivo applications and understanding their fate inside human body. *Coord. Chem. Rev.* **2021**, *445*, 214082. [CrossRef]
551. Timerbaev, A.R. How well can we characterize human serum transformations of magnetic nanoparticles? *Analyst* **2020**, *145*, 1103–1109. [CrossRef]
552. Sheridan, E.; Vercellino, S.; Cursi, L.; Adumeau, L.; Behan, J.A.; Dawson, K.A. Understanding intracellular nanoparticle trafficking fates through spatiotemporally resolved magnetic nanoparticle recovery. *Nanoscale Adv.* **2021**, *3*, 2397–2410. [CrossRef]
553. Sun, C.; Lee, J.S.H.; Zhang, M. Magnetic nanoparticles in MR imaging and drug delivery. *Adv. Drug Deliv. Rev.* **2008**, *60*, 1252–1265. [CrossRef]